Virginia Tech
VIRGINIA POLYTECHNIC INSTITUTE
AND STATE UNIVERSITY

The Charles E. Via, Jr.
Department of Civil Engineering
Blacksburg, VA 24061

Structural Engineering

Behavior and Modeling of Partially Restrained Composite Beam-Girder Connections

by
Clinton O. Rex
Research Assistant

W. Samuel Easterling, Ph.D., P.E.
Principal Investigator

Submitted to
The American Institute of Steel Construction
The American Iron and Steel Institute
The National Science Foundation
(MSS-9222064)
Innovative Steel Research For Construction Program

Report No. CE/VPI-ST 96/17

November, 1996

Research Report

Behavior and Modeling of Partially Restrained Composite Beam-Girder Connections

by
Clinton O. Rex
Research Assistant

W. Samuel Easterling, Ph.D., P.E.
Principal Investigator

Submitted to
The American Institute of Steel Construction
The American Iron and Steel Institute
The National Science Foundation
(MSS-9222064)
Innovative Steel Research For Construction Program

Report No. CE/VPI-ST 96/17

November, 1996

Structures and Materials Research Laboratory
The Charles E. Via, J. Department of Civil and Environmental Engineering
Virginia Polytechnic Institute and State University

TABLE OF CONTENTS

LIST OF FIGURES

LIST OF TABLES

TABLE OF NOMENCLATURE

α = Bolt tension coefficient, also Angle of fracture surface in the fillet weld and satisfies

α_1, α_4, α_3 = Parametric modifiers for the curvature parameter

a = Factor for locating center of resistance (0 if weld in compression, 0.345 if weld in tension), also the distance from the weld line to the centerline of the bolts in a single plate shear connection

A_b = Area of the bolt

A_{ceff} = Effective concrete area in tension

A_{sc} = Area of the shear stud based on the nominal shear stud diameter

A_w = Effective area of weld throat

β = Steel correction factor

β_1, β_2, β_3, β_4, β_5 = Parametric terms used for determining curvature parameter

C_1 = Tension coefficient for determining slip load

COV = Coefficient of variation

δ_{slab1} = Deformation at first critical point of reinforced concrete slab behavior

d_{stud} = Nominal shear stud diameter

δ_{stud1} = Deformation at first critical point of shear stud behavior

Δ = Deformation

$\overline{\Delta}$ = Normalized deformation

Δ_f = Deformation at fracture of fillet weld

Δ_f = Failure deformation (in.)

Δ_{fu} = Deformation at which frictional resistance is considered zero

Δ_0 = maximum deformation for a weld with $\theta = 0$

Δ_s = Deformation when a major slip occurs

Δ_u = Deformation at ultimate load of fillet weld

$\overline{\Delta}_f$ = Normalized failure deformation

D = Leg size of fillet weld (in.)

D_a = Leg size of the shear plate fillet weld

D_p = Leg size of the shear plate fillet weld

d_b = Bolt diameter

d_{bar} = Reinforcing bar diameter

ε_{yr} = Strain in reinforcing steel at yield

E = Modulus of elasticity for steel, 29,000 ksi

E_c = Modulus of elasticity of concrete

ϕ_{ult} = Ultimate rotation capacity of connection

f'_c = Compressive strength of the concrete

f_c = Concrete stress

f_{cr} = Tensile cracking stress of concrete

F_{exx} = Nominal weld electrode strength

F_{exxa} = Electrode strength used for the shear plate fillet weld

F_{exxp} = Electrode strength used for the shear plate fillet weld

F_u = Ultimate tensile stress

F_{ub} = Specified ultimate stress of bolt steel

F_{usc} = Shear stud steel tensile strength

F_y = Yield stress

F_{ya} / F_{ua} = Seat angle steel yield / tensile strength

F_{yf} / F_{uf} = Beam flange steel yield / tensile strength

F_{yp} / F_{up} = Yield and Tensile strengths of the shear plate

F_{yr} / F_{ur} = Reinforcing steel yield / tensile strength

F_{yw} / F_{uw} = Yield and Tensile strengths of beam web

G = Shear modulus for steel, 11,200 ksi

h = Elastic center of rotation

h_r = Height of the deck rib

H = Web bolt load resistance in horizontal direction

H_s = Shear stud height after welding

IC = Instantaneous center of rotation

ICX = X Distance from vertical baseline to the IC

ICY = Y Distance from horizontal baseline to the IC

K = Elastic stiffness parameter for Richard Equation

K_{fi} = Frictional initial stiffness

K_{fp} = Frictional final stiffness

K_i = Initial stiffness

K_{ia} = Initial stiffness of seat angle

K_{islab} = Initial stiffness of reinforced composite slab in tension

K_{iw} = Initial stiffness of web bolt

K_p = Plastic stiffness parameter for Richard Equation, also plate stiffness

K_{pb} = Plate bending stiffness, also the plastic stiffness of web bolts

K_{pbr} = Plate bearing stiffness

K_{pi} = Plate initial stiffness

K_{pslab} = Plastic stiffness of reinforced composite slab in tension

K_{pv} = Plate shearing stiffness

L_{ah} = Horizontal length of the outstanding angle leg

L_{av} = Vertical distance between the top of the angle and the assumed point of contact between the angle and the girder web

L_e = End distance

L_{eff} = Effective length of reinforced concrete slab for deformation calculations

L_{eh} = Horizontal distance from the bolt centerline to the end of the beam

L_{w0} = Length of fillet weld that runs parallel to the load

L_{w90} = Length of fillet weld that runs transverse to the load

μ = Coefficient of friction

M_0 = Moment capacity for Richard Equation

M_{ult} = Ultimate moment capacity of connection

n = Curvature parameter for Richard Equation

N_a = Number of bolts attaching the seat angle to the beam flange

N_{bars} = Number of reinforcing bars

N_r = Number of shear studs per deck rib

N_{studs} = Number of effective shear studs

N_w = Number of bolts in the web

P_0 = Strength of weld loaded at $\theta = 0$

P_a = Horizontal bolt pitch of seat angle bolts

P_θ = Strength of weld loaded at angle θ

PR = Partially Restrained

P_{slab1} = Load resistance at first critical point of reinforced concrete slab behavior

P_{stud1} = Load resistance at first critical point of shear stud behavior

P_w = Vertical bolt pitch

θ = Connection rotation, also angle of load with respect to the longitudinal axis of a fillet weld

Q_{sol} = The strength for a single shear stud

R = Load or force

ρ = Weld deformation ratio

R_f = Slip load

R_n = Nominal strength

R_{nh} = Nominal strength of web bolt in the horizontal direction

R_{nslab} = Composite slab strength

R_{nv} = Nominal strength of web bolt in the vertical direction

S_0 = Distance from the girder centerline to the nearest shear stud on the beam

S_{bar} = Reinforcing bar spacing

SRF = Stud reduction factor used to account for metal decking

S_{stud} = Shear stud spacing parallel to the beam

t_1 = Thickness of the thinner of two plates in a lap plate connection

t_2 = Thickness of the thicker of two plates in a lap plate connection

t_a = Seat angle thickness

t_f = Bottom beam flange thickness

t_p = Plate thickness

t_p = Shear plate thickness

t_w = Beam web thickness

V = Web bolt load resistance in vertical direction

V_{ult} = Ultimate shear capacity of connection

W_a = Seat angle width

w_c = Unit weight of concrete

W_p = Shear plate width

w_r = Width of the deck rib

Ψ_1, Ψ_2, Ψ_3, Ψ_4 = Parametric ratios used for determining the curvature parameter

Y_b = Distance from the top of the seat angle to the center of the bottom bolt

Y_{con} = Total depth of composite slab

Y_j = Vertical distance from web bolt j to top of seat angle

Y_r = Vertical distance from top of seat angle to centerline of reinforcing steel

ABSTRACT

Beams in a typical steel framed floor design are assumed to have rotationally pinned supports for purposes of design. In reality, the connections between the beams and girders in a steel framed floor system are not rotationally pinned. The design bending moments and deflections of the attached beam could be reduced if the true rotational restraint provided by the beam-girder connections could be included in the design. The connection rotational restraint is characterized by the moment-rotation behavior. Consequently, a method for approximating the moment-rotation behavior of the beam-girder connection is required before the beneficial effects of the true connection rotational restraint can be considered in design.

An experimental and analytical study of the moment-rotation behavior of composite beam-girder connections is presented in this report. Eight full-scale connections (four cruciform test setups) were tested experimentally. This experimental data is used to verify a "component" model for approximating the moment-rotation behavior of the connections. The component model is then used to analyze a variety of connection parameter combinations. The results from this analysis are used to develop a simpler method of approximating the moment-rotation behavior of composite beam-girder connections.

1. Introduction

Three changes in steel design over the last 30-40 years have allowed engineers to design longer beam spans in steel framed floors. First, composite steel-concrete floor system technology has developed which allows designers to use the synergy of tying the two floor components (the beam and the concrete slab) together to span longer distances. Second, the plastic section analysis and design procedures found in the AISC Load and Resistance Factor Design Specification (*Load and* 1986) has allowed an additional increase in span length over AISC Allowable Stress Design (*Specification for* 1989) procedures. Thirdly, high strength steel, particularly A572Gr50 steel, is becoming more readily available and at a cost comparable with A36 steel.

As the beam designs become longer and shallower serviceability design criteria such as floor deflection and vibration are, in many cases, controlling the beam design (Zandonini, 1989). Currently most beams in steel framed floor systems are designed with the assumption that the beam end connections can be treated as simple supports. In reality, no connection behaves as a simple support. Each type of connection possesses some degree of rotational restraint. If this restraint could be included in the beam design then both beam moments and deflections could be reduced and an overall improvement in the design efficiency could be achieved.

Before the true rotational restraint of beam end connections can be included in the beam design there has to be a way of calculating (i.e. approximating) the connection moment-rotation behavior. This behavior would determine the degree of continuity that could be achieved in the floor system. Connections with relatively small moment resistance result in a discontinuous floor system while connections with relatively high moment resistance result in a floor system that is nearly continuous. Obviously, a continuous floor system would be the best situation; however, the connection details required to ensure the necessary moment resistance tend to be very complex and expensive. Using connections with moment resistance that lies somewhere between these two extremes would result in a partially continuous floor system. The connection details required to achieve partial continuity can be very simple and economical while still providing a significant amount of rotational restraint. This type of connection was previously termed a "semi-rigid" connection. More recently, these connections are being called "partially-restrained" (PR) connections.

As part of a larger research program, dealing with innovative floor systems, the moment-rotation behavior of composite beam-girder connections is being investigated. A composite connection is a connection that combines the strength of the steel connection with the strength of the overlying concrete floor to develop rotational restraint. This report presents experimental and analytical work which is used to develop a method of approximating composite beam-girder connection moment-rotation behavior.

The proposed details for the beam-girder connection are discussed below. This is followed by a discussion of an experimental program that was conducted to provide experimental connection moment-rotation behavior. Next, a detailed analytical model of the composite connection is described and verified against the experimental data. Finally, the detailed model is used to investigate a number of possible connection parameter combinations. The results of this study are then used to develop a simpler method of approximating the composite connection moment-rotation behavior.

1.1 Proposed Connection

The details of the proposed composite beam-girder connection are shown in Figure 1. These details can be broken into two major groups: details associated with the steel connection and details associated with the composite slab. The steel connection consists of a typical single plate shear connection and an un-stiffened seat angle connection. The reasoning behind the choice of these connection details was previously discussed in Rex and Easterling (1996(e)).

The composite slab consists of #4 Grade 60 reinforcing steel, round headed shear studs, composite steel decking, and concrete. The reinforcing steel is specifically given as #4 Grade 60 for two primary reasons:

- All experimental tests of composite connections, composite slabs, and reinforcing steel conducted at VT (in conjunction with this research) have used #4 Grade 60 bars
- The #4 bar is believed to be an effective size for reinforcing thin composite slabs

Round headed shear studs were chosen because they are the most common type of shear connector used today. Composite steel decking was included because most steel framed floor systems use a composite steel deck. The direction of the decking was chosen to be consistent with the typical direction of the steel deck with respect to filler beams.

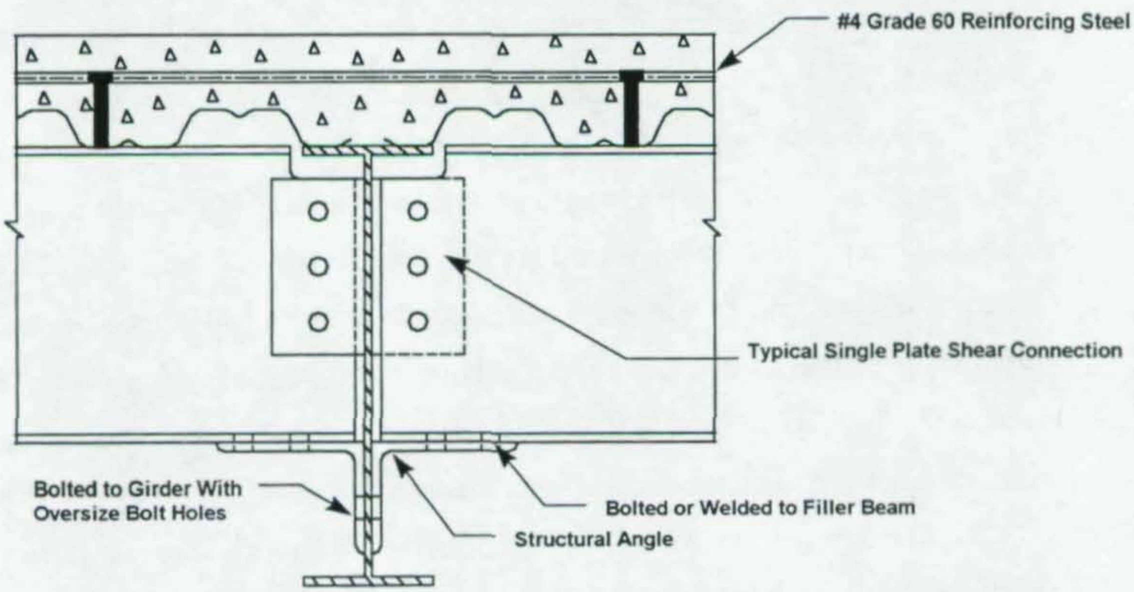

Figure 1 Details of Proposed Composite Beam-Girder Connection

1.2 Focus And Objective

The focus of this report is the moment-rotation behavior of the proposed composite beam-girder connection which was previously shown in Figure 1. With regard to the proposed composite beam-girder connection the objective of this report is to:

1. Report an experimental testing program that investigated the moment-rotation behavior
2. Determine the effect that pre-loading the steel connection has on the composite connection behavior
3. Develop a component analysis method for approximating the connection moment-rotation behavior
4. Develop a simpler analysis method for approximating the connection moment-rotation behavior by determining relationships between connection parameters and the equation parameters of the Richard Equation.

With regard to the first objective, 4 full scale cruciform test specimens (2 connections on each specimen) were tested. The complete details and results of these tests are given.

The connection details of the first two test specimens were identical. However, the first of these specimens was subjected to loading before the concrete in the composite slab could cure. Similarly the second two test specimens were also identical and the first of these was pre-loaded. The experimental results of these two pairs of connections are used to determine what if any effect the connection pre-loading has on the composite connection behavior. These effects are presented and discussed. The test results also provide a basis for evaluation of a component analysis method.

A component model of the composite connection is developed and used to approximate the moment-rotation behavior of the connection. The basic assumption upon which the model relies is that the behavior of the whole connection can be considered as the combined behavior of the connection parts. If the behavior of each connection part is understood then the behavior of the connection can be determined. Methods for approximating the behavior for each major part of the connection are presented and / or developed. These behaviors are then combined using an ultimate strength approach to approximate the moment-rotation behavior of the connection. The model is verified against the experimental data.

The component model provides a very general approach to connection analysis which is not (ideally) limited by the range of parameters that have been included in experimental test programs. However, this flexibility comes at the price of complexity. In general the component model is fairly complex to apply and requires a computer program to readily implement. Consequently, as a final step, a simpler model for approximating the composite connection moment-rotation behavior is developed. This model combines fundamental mechanics with parametric equations to provide a simpler yet less flexible model for approximating the connection moment-rotation behavior compared to the component model.

2. Experimental Investigation of Composite Beam-Girder Connections

The following sections describe the general details of the test specimens, instrumentation, test setup and test procedure. Most of this information is given in more detail in the data packs which are included in Appendix B.

2.1 Test Specimens

Four full-scale composite beam-girder cruciform specimens were experimentally tested. These were labeled #5 through #8. Connections #5 and #6 were identical to each other as were connections #7 and #8. The primary details of the connections are shown in Figure 2 and 3. The girders and beams for all the connections were W24x55 and W16x36 wide flange sections respectively and were fabricated from A572Gr50 steel. The plates and angles were fabricated from A36 steel. The beams, girder, and all connection parts were white-washed to identify yield patterns during testing.

The beam lengths were chosen to ensure that the reinforced composite slab would be long enough to allow the required number of shear studs to be installed and provide enough length beyond the last shear connector (farthest away from the girder) so that it could fully develop.

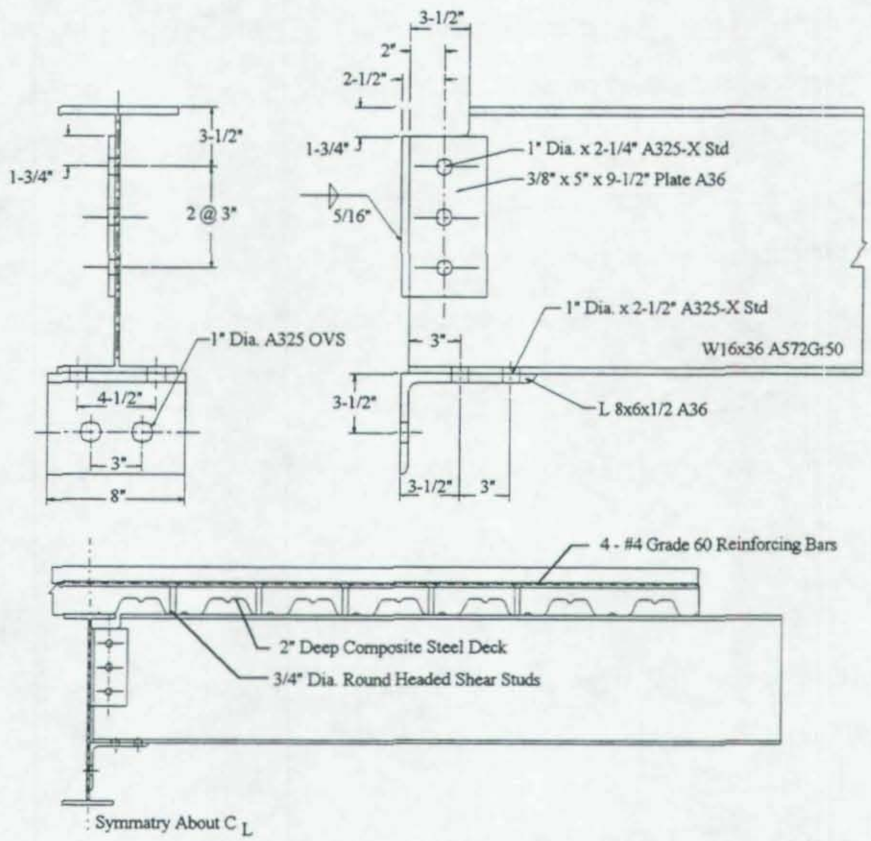

Figure 2 Details of Experimental Composite Connections #5 and #6

One-in. and ¾-in. A325-X (threads excluded from the shear plane) bolts were used with round washers under the nuts. All bolts except for bolts used to attach the seat angle to the girder were pre-tensioned using the turn-of-nut method. Bolts were first brought to a snug tight condition by tightening them with a typical spud wrench which is around 16-in. long. Bolts were tightened to snug by the writer who weighs 200 lbs and is six-ft one-in. tall with an average build. No excessive force was used while tightening any of the bolts to snug. For bolt lengths up to and including four bolt diameters, the turn-of-nut method requires 1/3 turn of the nut relative to the bolt after the nut is snug tight (Salmon and Johnson, 1990). The nuts were given the required turn from the snug condition using a socket attached to a breaker bar which was attached to a six-ft length of pipe.

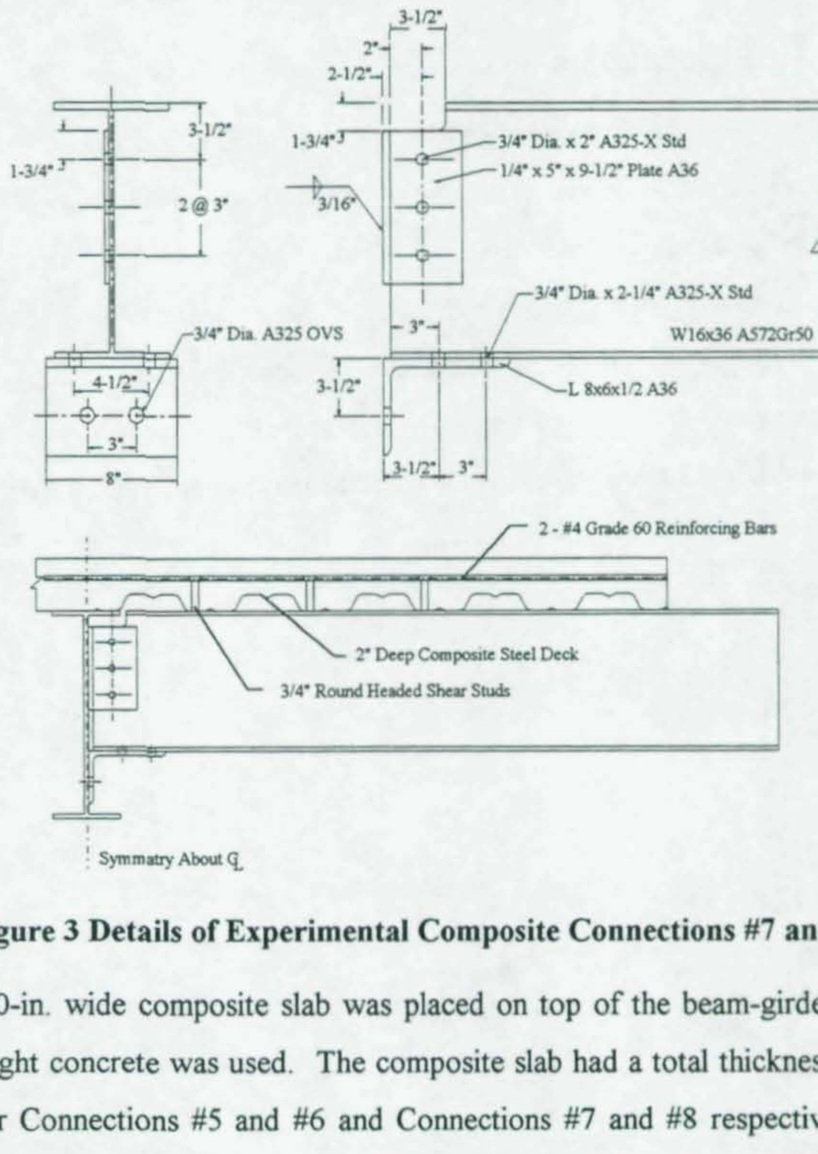

Figure 3 Details of Experimental Composite Connections #7 and #8

A 60-in. wide composite slab was placed on top of the beam-girder connection. Normal weight concrete was used. The composite slab had a total thickness of 5-in. and 5-1/2-in. for Connections #5 and #6 and Connections #7 and #8 respectively. Two-in. deep composite steel decking was used. The slabs were reinforced with WWF 6x6 - W1.4 x W1.4 mesh and #4 Grade 60 reinforcing bars. The bars and mesh were supported above the top of the composite steel decking with 3-1/2-in. high reinforcing chairs.

Four-in. high by ¾-in. diameter round headed shear studs were used to attach the composite slab to the beams and girder. The number of studs were chosen so that the reinforcing steel would fail before the shear studs. All shear studs were placed in strong deck positions

2.2 Instrumentation

The primary purpose of the test instrumentation was to measure the moment-rotation behavior of the connection. In addition, measurement of slip between the reinforced composite slab and the steel beam as well as beam and girder vertical deflections were measured. A schematic of the instrumentation used for all the connection tests is shown in Figure 4. In addition to the shown instrumentation, load cells were used to measure the load and subsequently the moment and shear applied to the connections. A PC-based data acquisition system was used to collect and record data.

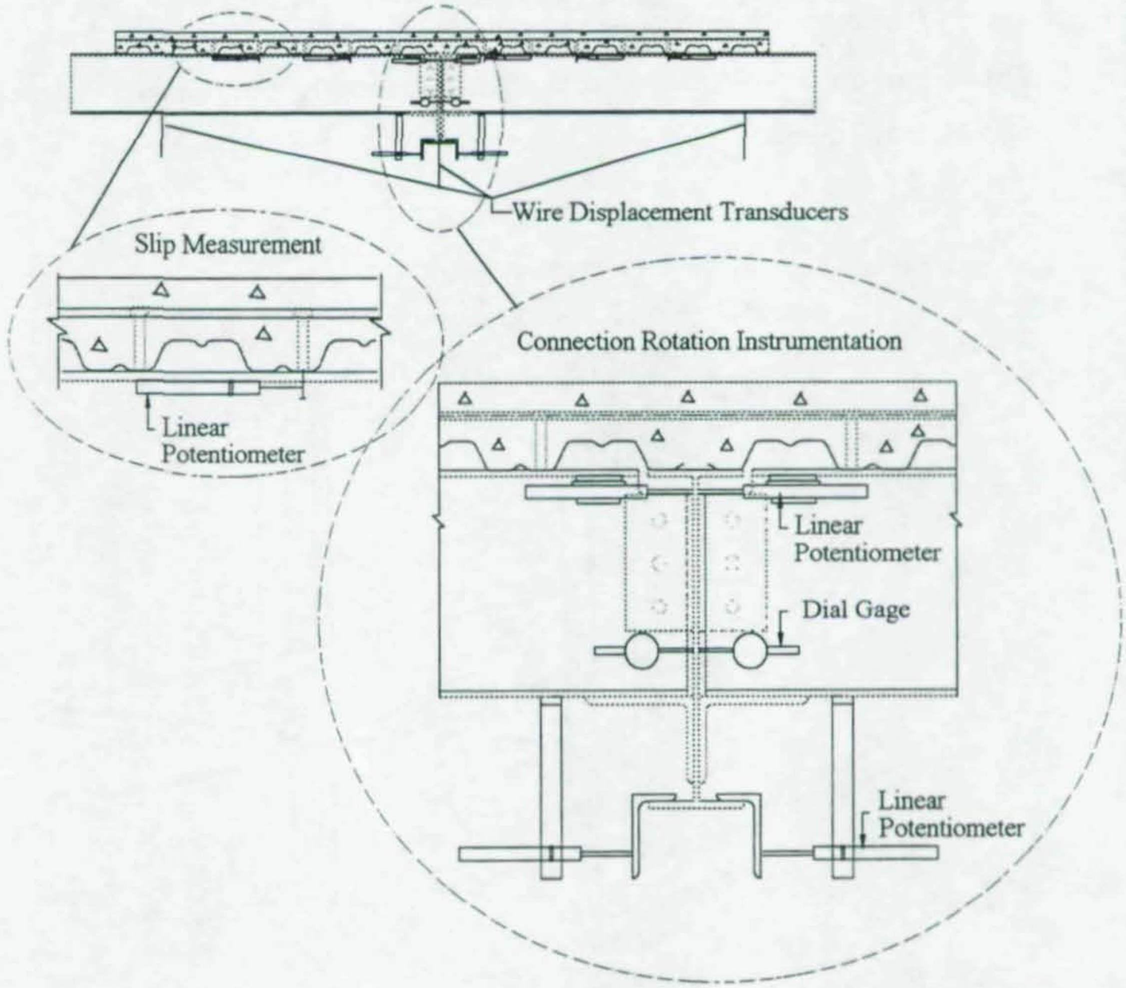

Figure 4 Instrumentation

2.3 General Test Setup And Testing Frames

The basic test setup was a cruciform type test specimen intended to represent a portion of a steel-framed composite floor system. A schematic of the test specimen setup is shown in Figure 5. The beams were attached to the girder with the connection details presented previously. The girder was then attached to two columns which were subsequently attached to a testing lab strong floor. Two different testing frames were used to load the test specimens. A dead load simulation frame was used to apply the pre-load to the connections that were loaded immediately after concrete was cast. A live load simulation frame was used to apply failure loading to the composite connections after concrete had cured.

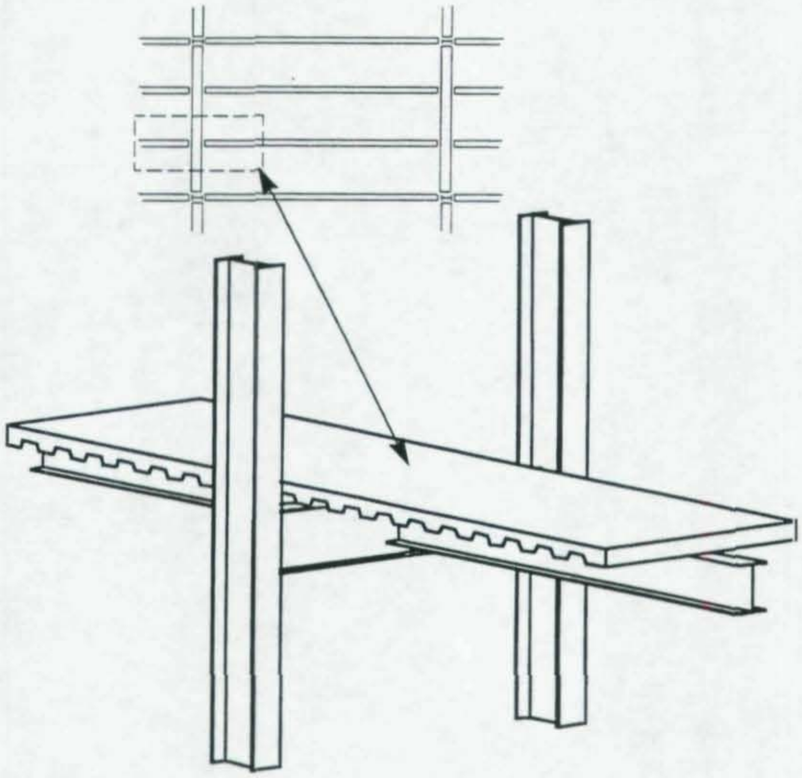

Figure 5 Test Specimen Setup

The dead load simulation frame was used apply the connection pre-load to Connections #5 and #7. The basic details of the frame are shown in Figure 6. The frame consisted of short cruciform columns that were bolted to reaction floor beams and a structural tube that spanned between the two cruciform columns. A short length of horizontal 1-1/2-in. diameter threaded rod was attached to the bottom beam flange with four U-bolts. The horizontal rod was then connected to a vertical 1-1/2-in. diameter rod with an eye nut. The top section of vertical rod was instrumented with strain gages to form a load cell transducer. The load cell was calibrated to determine a sensitivity that could be used to evaluate the applied axial load in the threaded rod. The bottom of the rod with the load cell was attached to a turnbuckle which was intern attached to another portion of threaded rod that was anchored to the tube section. The turnbuckles were tightened to apply the simulated dead load. The distance from the centerline of the connection to the applied load was either 72-in. and 48-in. for Connections #5 and #7 respectively.

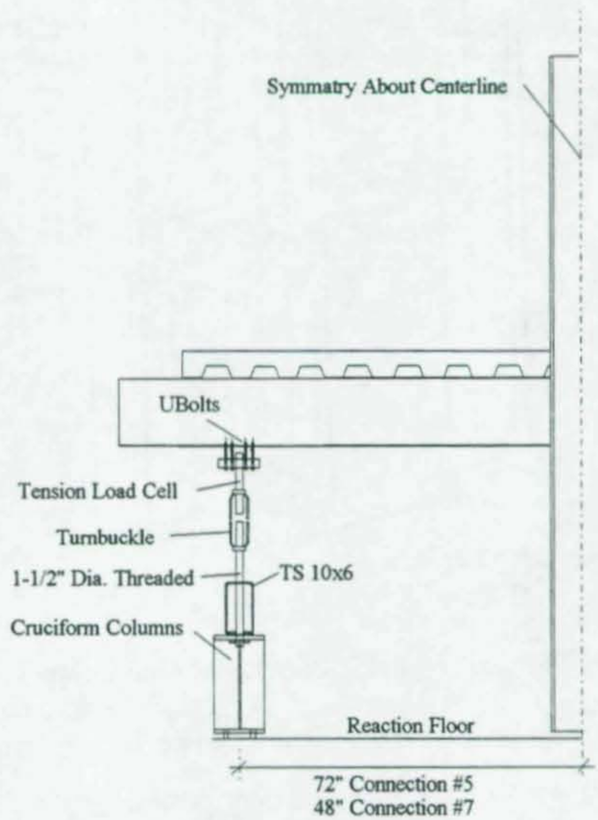

Figure 6 Dead Load Simulation Frame

The live load simulation frame was used to apply loading to the composite connections after the concrete had cured. The main details of the frame are shown in Figure 7. The frame consisted of W21x62 columns, which were attached to the reaction floor. Two C15x50 sections spanned between the columns and support a short reaction beam at their mid-span.

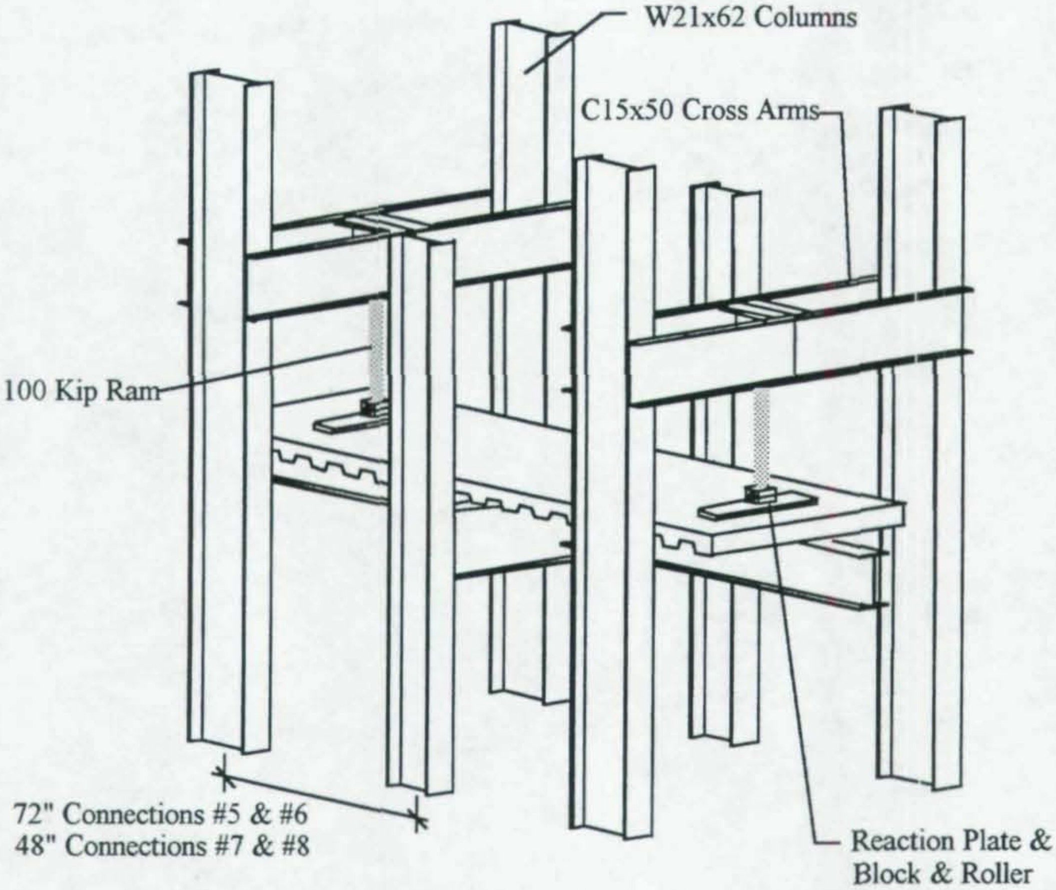

Figure 7 Live Load Simulation Frame

The test specimens were loaded with two 100 kip capacity displacement controlled hydraulic rams which were independently powered by two electric pumps. The rams reacted against the composite slab through a block and roller arrangement with the load distributed through a 36-in. long, 8-in. wide, 1-in. thick steel plate. The roller allowed rotation of the beam end while maintaining a vertical applied load. The plate allowed the load to be distributed across the end of the slab. A 500 kip capacity load cell was placed above each ram to determine ram load (except for the north ram on Connections #7 and #8 which used a 150 kip capacity load cell). The distance from the centerline of the specimen to the point of applied load was either 72-in. or 48-in. depending on the connection.

During the live load portion of the test the free end of the beam for Connections #6 through #8 was restrained against lateral movement with a lateral brace system attached to the top and bottom flange of the beam. These braces were not attached to connection #5 until near the end of the test. The lateral bracing system allows the beam end to have free vertical movement while preventing lateral movement. The brace is believed to merely provide the same lateral stability that would be provided by the rest of the beam in a real floor system.

2.4 Testing Procedure

The majority of composite beams are currently built using un-shored construction techniques. Consequently, connections associated with these beams will have tow distinct stages of behavior; before and after concrete hardens. Before the concrete hardens, the only rotational resistance of the beam-girder connection will be provided by the bare steel connection. After the concrete hardens, the composite connection will provide rotational restraint against all additionally applied load. Two test procedures were used to determine the effect the initial loading of the steel connection (i.e. before the concrete hardens) has on the moment-rotation behavior of the composite connection.

For Connections #5 and #7 the test procedure was designed to represent the loading history for un-shored construction. Immediately after placement of the concrete the dead load setup was used to simulate the connection dead load that would occur based on a hypothetical design. Loads of 11.5 and 14.6 kips were applied to Connections #5 and #7 respectively by tightening the turnbuckle of the dead load setup. The loads were based on a hypothetical design and were different because of differing slab thickness and connection behavior. In general, loading was increased in one to two kip increments until the load reached the required value of dead load or until the connection moment-rotation behavior had intersected with the beam-line associated with the beam of the hypothetical design. Connections #6 and #8 were not subjected to this pre-load immediately after casting concrete.

The simulated dead load was removed from Connections #5 and #7 within a couple of days of when the live loading test was to be applied. All instrumentation was monitored and the moment-rotation curve for the connection was plotted through all stages of the dead load removal. Once the dead load was removed the dead load setup was dismantled and the live load setup was constructed.

The live load test setup was used to apply failure loading to all the connections. Load was increased in increments believed to be reasonable for the type of connection being loaded (generally one to four kip increments). Loading was stopped when the specimen failed; i.e., the specimen was incapable of taking additional load, or the specimen was distressed to the point where violent failure was considered likely.

3. Composite Beam-Girder Connection Experimental Results

This section summarizes the experimental results from the connection tests. A more detailed presentation of the results for each connection test is given in Appendix B.

3.1 General

The principle results that are of interest for this report are the results characterizing the moment-rotation behavior. The typical characterizing values are the ultimate moment (M_{ult}), ultimate rotation (ϕ_{ult}), and the initial stiffness (K_i). These quantities along with the ultimate shear load (V_{ult}) are summarized in Table 1. In addition, comparisons of the ultimate shear load and moment to the nominal shear and moment capacity as per the AISC Specification (*Load and*, 1993) based on the measured steel properties for the bare steel beams are given. The values in Table 1 are the average values for the two sides of each connection test; in addition, K_i for the composite behavior of Connections #5 and #7 was determined by examining the moment-rotation data with moment values above the maximum moment applied during pre-load..

Table 1 Summary of Connection Results

Connection	V_{ult} (kips)	V_{ult} / V_n	M_{ult} (k-in.)	M_{ult} / M_p	ϕ_{ult} (rad)	K_i (k-in./rad)
5 Steel	N/A	N/A	N/A	N/A	N/A	245221
5 Comp	38	0.24	2618	0.74	0.096*	658486
6	34	0.22	2388	0.68	0.075	1030683
7 Steel	N/A	N/A	N/A	N/A	N/A	205270
7 Comp	33	0.21	1486	0.42	0.077	628587
8	31	0.20	1413	0.40	0.061	1070930

* Test setup limited rotation capacity

The rotation capacity of all the connections was fairly high with the lowest rotation capacity of 61 mrad for Connection #8. The rotation capacity of Connection #5 was never reached because the test was stopped before any loss in load carrying capacity occurred in the connection. Each of the other connection rotations were limited by connection failure. Connections 6 and 8 failed when one of the reinforcing bars fractured in tension.

Connection 7 also failed because of reinforcing steel tension rupture; however, in addition to the reinforcing steel rupture the shear plate ruptured immediately after the reinforcing steel ruptured. A rough sketch of the shear plate rupture is shown in Figure 8. Tension rupture of the shear plate has been seen in previous connection tests reported by Rex and Easterling (1996(e)). However, in the previous tests, rupture of the shear plate only occurred after a significant amount of plate yielding had occurred. In particular, the net section of the plate (passing through the line of bolt holes) had started to neck before the fracture had occurred in the previous tests. Connection #7 did not exhibit this ductile behavior. There was some yielding but it was primarily bearing yielding and not tensile yielding at the net section. Consequently, the plate fracture was very unexpected and it is not clear what the exact causes of the fracture were.

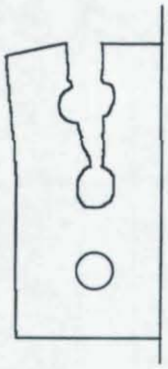

Figure 8 Shear Plate Tension Fracture For Connection #7

Connections #5 and #6 had larger bolts, a thicker shear plate, and more reinforcing steel than Connections #7 and #8. As a result of these different connection details the average moment capacity of #5 and #6 (2500 k-in.) is higher than the average moment capacity of #7 and #8 (1450 k-in.). Despite the differences in connection details the initial stiffness values associated with #5 and #6 were very similar to those determined for #7 and #8.

There are two primary reasons for the fairly small differences in the initial stiffness values despite the differences in connection details. First, the steel connection initial stiffness is primarily a function of frictional resistance. Ideally, the larger the bolt the higher the frictional resistance. However, because of the high variability in bolt tensioning and steel surface conditions the size of the bolt does not always determine the level of frictional resistance. Consequently, the size of the bolts did not have a significant effect on the initial stiffness. Second, the composite connection initial stiffness is primarily a function of the initial stiffness of the composite slab. Before cracking, the amount of reinforcing steel in the composite slab has little influence on the slab stiffness. Consequently, the amount of reinforcing steel did not have a significant effect on the initial stiffness.

3.2 Effect of Pre-loading Composite Connections

The details of Connections #5 and #7 were identical to those of Connections #6 and #8 respectively; however, #5 and #7 were loaded immediately after the concrete was cast (i.e. before the concrete could cure) while #6 and #8 were not loaded until after the concrete had cured (i.e. not loaded until over 28 days had passed since the concrete had been cast). The two stages of connection loading for Connections #5 and #7 are meant to represent the two stages of behavior that a real composite connection would exhibit (i.e. behavior before and after concrete hardens). The initial loading of #5 and #7 represented the total dead load that these connections would have been subject to if they had been part of a full steel framed composite floor system. The reason for the differing loading sequences was to determine what if any effect the pre-load had on the composite connection behavior.

To provide a visual comparison of the connections the moment-rotation behavior for all four connections has been plotted in Figure 9 and 10. The overall behavior up to 50 mrad of rotation is plotted in Figure 9 and the initial behavior of each connection is plotted in Figure 10. The moment-rotation behavior for Connections #5 and #7 have been plotted assuming that the behavior of the connections after removing the pre-load is the composite connection behavior. For comparison purposes the test data after removal of the pre-load has been shifted back to the origin.

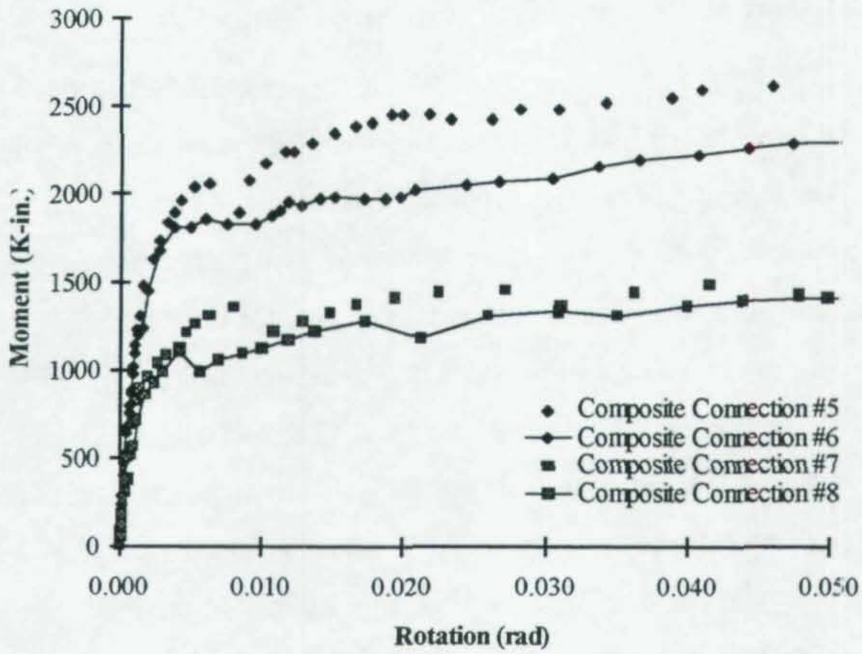

Figure 9 Overall Composite Connection Behavior For All Connections

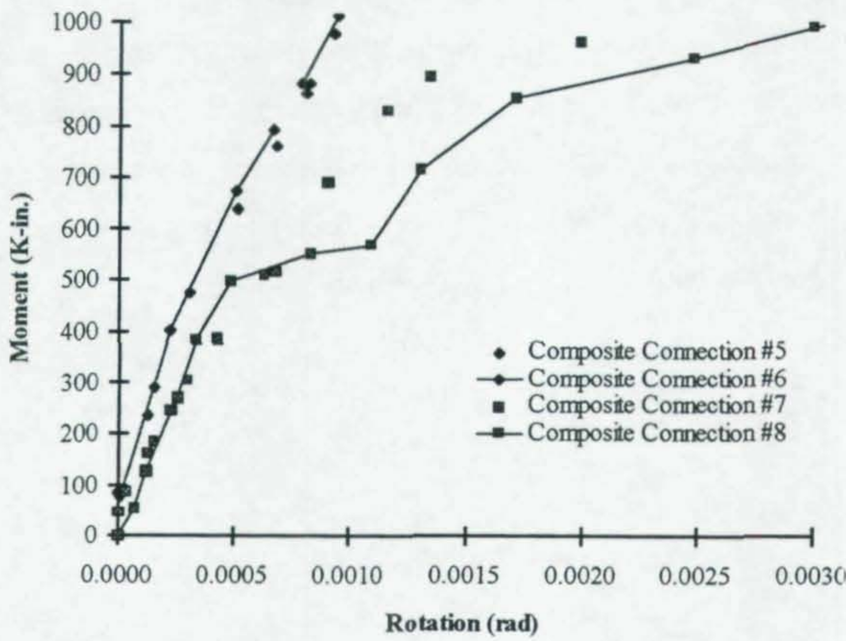

Figure 10 Initial Composite Connection Behavior For All Connections

3.2.1 General

Two general observations are clear from review of Figures 9 and 10. First, the overall moment-rotation behaviors of the connections that were pre-loaded are stiffer than the those for the connections that were not pre-loaded. This effect is explained by the difference in the composite slab forces at similar moments. Because of the pre-load on the steel connection the composite slab force is zero or in compression for moments below the pre-load moment for the connections that were pre-loaded. This would not be true for the connections that were not pre-loaded. Consequently, the moment that is associated with a slab force sufficient to crack the slab will be higher if the connection is pre-loaded. This would be true for initial and subsequent moments associated with different levels of slab cracking.

Second, there is no effect of pre-load on the initial behavior before slab cracking. The initial behavior for the pre-loaded connections is really an unloading and loading behavior while for the connections without pre-load this is only a loading behavior. The composite slabs during the initial behavior are behaving completely different yet the combined effect of the slab with the steel connection results in very similar connection behaviors.

3.2.2 Moment Capacity

Ideally, because of plastic behavior in the steel connection and composite slab the ultimate moment capacity of the connections which are pre-loaded should be very similar to those which are not pre-loaded. This is true for Connections #7 and #8 which had moment capacities of 1486 and 1413 k-in. respectively (a difference of only 5%). However, based on the test data, this does not appear to be true for Connections #5 and #6 which had moment capacities of 2618 and 2388 k-in. respectively (a difference of 9%).

The reason for the larger difference in moment capacities is believed to be attributable to the interaction of the stay in place steel forming (pour stop) used for casting the test specimens. Connection #5 was tested with forming that ran continuous over the girder. Visual observations of the test specimen clearly indicated that the forming was carrying load near the end of the test. The forming was cut on both sides of the girder top flange in Connection #6 to eliminate the possibility of the forming carrying load.

3.2.3 Rotation Capacity

In general, the connections which were pre-loaded had higher rotational capacities than the connections which were not pre-loaded. It is unclear how much higher the rotational capacity of Connection #5 is vs. #6 because #5 was not tested to failure. However, Connection #7 had an increased rotational capacity of 16 mrad compared to Connection #8. The major reason for the different rotational capacities is the difference in the elongation of the composite slab for a given rotation.

If the composite slab limits the connection ductility (as was the case for all the connections tested in this report) then the pre-loaded connections should fail at a rotation equal to the failure rotation of the connection which is not pre-loaded plus the pre-load rotation. The pre-load rotation of Connection #7 was approximately 8.5 mrad. Consequently, #7 should have failed at a rotation of 8.5 mrad greater than the failure rotation of #8. The actual increase was 16 mrad.

The most likely reason for the additional ductility beyond the pre-load rotation can be attributed to differences in cracking patterns of the two slabs. The composite slab of Connection #7 had many more cracks than the composite slab of #8. Because the ductility of the composite slab is ultimately controlled by the elongation of the reinforcing steel between the cracks the more cracks present the higher the ductility. The reason for the different cracking patterns is not known.

3.2.4 Conclusion

The primary reason it is necessary to understand the effect of pre-loading the bare steel connection is to evaluate how the behavior of the composite connection can be determined. If there is no effect, than composite connection behavior based on tests or analysis which disregards the initial loading of the steel connection can be used. However, if there is an effect of pre-loading the steel connection on the composite connection behavior (which there appears to be) then some judgment must be used when determining the composite connection behavior.

In general the composite connection behavior of the connections which were not pre-loaded was conservative compared to the composite connection behavior of the connections which were pre-loaded (i.e. the moment-rotation behavior was softer and the connection ductility was reduced). Based on this observation it appears that it would be conservative to use the composite connection behavior determined without consideration of the steel connection pre-load. This means that both test and analytical approximations of the composite stage of connection behavior do not need to consider the pre-load imposed on the steel connection. This is a very important conclusion in that the amount of pre-load (i.e. the moment and rotation) imposed on the steel connection will in general depend on the attached beams geometry and loading. If these had to be considered when determining the composite behavior of the connection the complexity of determining the behavior would increase significantly.

It should be noted that the above conclusion makes one very important assumption. It is assumed that failure of the connection occurs in the composite slab. If the connection capacity (both moment and rotation) is limited by an element of the steel connection then using a composite connection behavior which is based on an analysis or test that ignores steel connection pre-load will most likely be unconservative.

Recommending connection details which ensure the composite slab will limit the connection capacity should eliminate this problem as a major concern.

4. Component Modeling

A component model is a model in which the overall behavior of the connection is determined by combining the individual behaviors of the connection pieces or "components." The basic concept is very simple and is shown schematically in Figure 11; however, the implementation of the concept is much more difficult. First, the connection components that will have the most influence on the behavior have to be determined. Next, behavior models of these components are needed. Last, an appropriate method of combining the component behaviors must be determined.

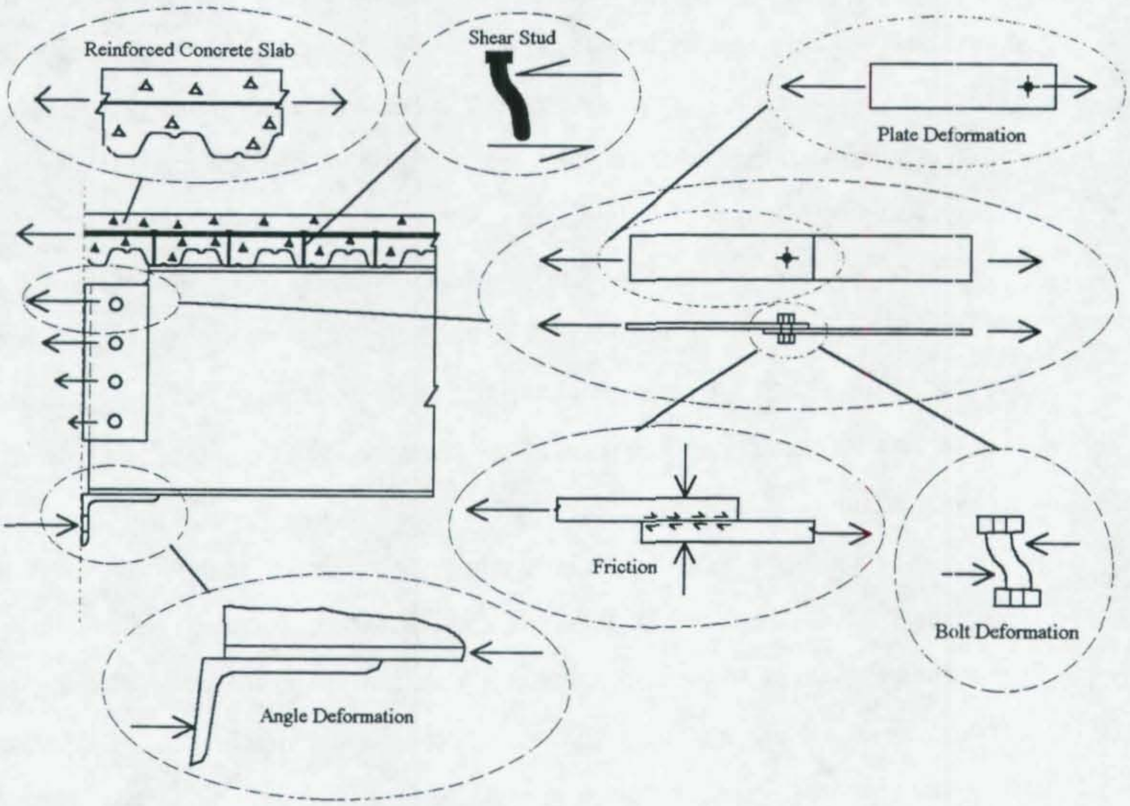

Figure 11 Primary Components of Proposed Beam-Girder Connection

This section of the report describes each of the connection components that are believed to have the most influence on the connection moment-rotation behavior. Behavior models for each of the components are presented and/or developed. Next, a method for combining the component behaviors to determine the connection moment-rotation behavior is described. This is followed by a description of how the model was calibrated and verified against the experimental test data.

4.1 Connection Component Behavior Models

4.1.1 Behavior Models For Composite Slab Components

This part of the report describes the primary composite slab components and presents and or develops behavior models for each component. These include:

- Concrete In Tension
- Reinforcing Steel
- Shear Studs

Each behavior model is based on simple mechanics or previous research by the writer or other investigators.

4.1.1.1 Reinforced Concrete Slab In Tension

The reinforced concrete that passes continuously over the girder is in tension for typical beam load and span combinations (Rex, 1994). Consequently, the behavior of the reinforced concrete in tension is needed. This will be comprised of the behavior of the reinforcing steel and the tension stiffening effects that the concrete has on the reinforcing steel.

The following sections describe a method for approximating the stress-strain behavior of the reinforcing as well as a method for considering the tension stiffening effects that the concrete has on the reinforcing. To determine loads and deformations based on the stress-strain behavior effective areas and effective lengths are also presented and / or developed.

4.1.1.1.1 Reinforcing Steel

Previous research (Rex and Easterling, 1996(a)) developed a normalized stress-strain behavior for #4 Grade 60 reinforcing steel which is shown in Figure 12. This is the most common grade and size of reinforcing steel used in composite floor slabs currently.

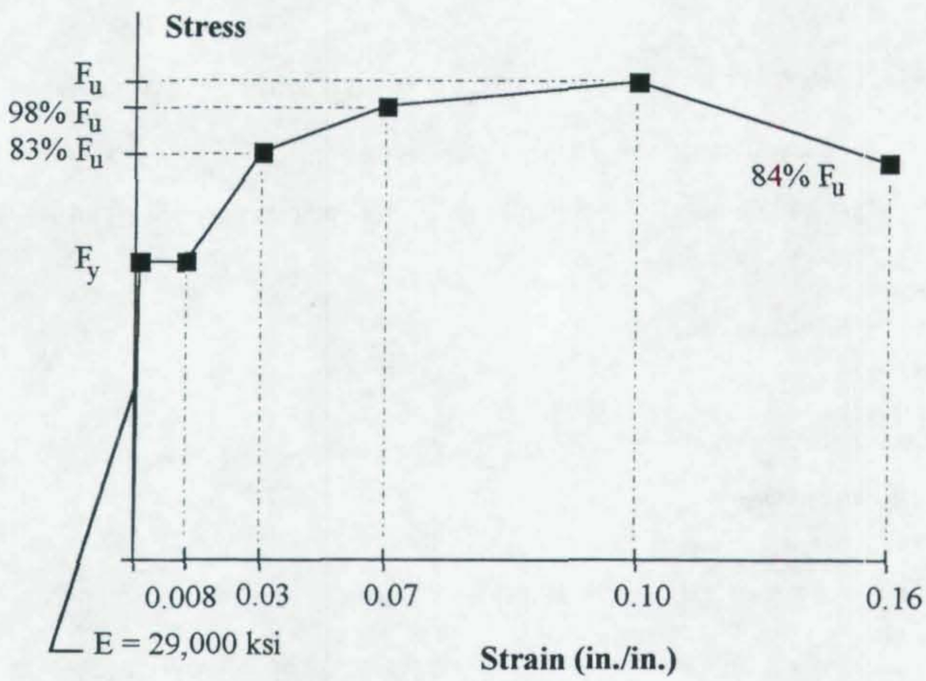

Figure 12 Multi-Linear Approximation For Reinforcing Steel Stress-Strain Behavior

Mean values of F_y and F_u were determined to be 71 ksi and 111 ksi respectively based on a mill survey of reinforcing steel. These mean values can be used when the actual yield and ultimate strengths are unknown.

The load in the reinforcing steel is simply determined by multiplying the stress by the area of reinforcing steel (A_r).

4.1.1.1.2 Concrete Tension Stiffening

The concrete in a composite beam-girder connection is typically going to be in tension. This concrete is normally assumed to have no strength. In reality, the concrete has significant strength before cracking and after cracking it has a stiffening effect on the reinforcing steel.

After cracking, the concrete cannot carry load across the cracks. This load has to be carried by the reinforcing steel. However, between cracks the concrete can carry load. This reduces the load in the reinforcing steel and consequently reduces the axial deformations in the reinforcing steel. This effect on the reinforcing steel is called concrete tension stiffening.

One way to account for the stiffening effect the concrete has on the reinforcing steel is to model the concrete as an axially loaded member acting in parallel with the reinforcing steel. The concrete is given a special stress-strain behavior and the strain in the concrete is assumed to be the same as the strain in the reinforcing steel (i.e., no slip between the reinforcing steel and the concrete surrounding it). By combining the load resisted by the reinforcing steel with the load resisted by the fictitious concrete element the real effect of concrete tension stiffening is satisfactorily represented.

Methods of modeling the tension stress-strain behavior were presented and discussed in Rex and Easterling (1996(b)). A multi-linear representation of the stress-strain behavior was recommended and is given in Table 2.

Table 2 Recommended Concrete Tension Stiffening Stress-Strain Behavior

Strain	Stress
f_{cr} / E_c	f_{cr}
0.001	$0.6\ f_{cr}$
0.002	$0.4\ f_{cr}$
0.008	$0.3\ f_{cr}$
0.1	0

Where f_{cr} is the tension cracking stress of the concrete which was given by Collins and Mitchell (1991) as:

$$f_{cr} = \frac{4\sqrt{1000\, f'_c}}{1000} \qquad \text{(Eq 1)}$$

Where:

f'_c = Concrete compressive strength (ksi)

The load in the concrete is determined by multiplying the stress by the effective area of concrete (A_{ceff}). Before cracking A_{ceff} is the gross area (i.e. the effective width of the slab times the depth of the slab minus the height of the steel decking). After concrete cracking the area is taken as a block of concrete around each reinforcing bar with a height and width of 15 times the bar diameter (Collins and Mitchell, 1991). The writer assumes that if the full effective concrete area is not available (as would be the case for thin composite slabs or close reinforcing spacing) that the portion of this area that is available would be used instead. This can be put into equation form as

$$A_{ceff} = \left\{ {}_{\min} \begin{vmatrix} 15\, d_{bar} \\ Y_{con} - h_r \end{vmatrix} \right\} \left\{ {}_{\min} \begin{vmatrix} 15\, d_{bar} \\ S_{bar} \end{vmatrix} \right\} \qquad \text{(Eq 2)}$$

Where:

d_{bar} = Reinforcing bar diameter

Y_{con} = Total depth of the composite slab from bottom of deck to top of slab

h_r = Depth of the composite steel decking

S_{bar} = Reinforcing bar spacing

Rather than dealing with two distinct effective areas (one before cracking and one after cracking) a conservative assumption of using A_{ceff} as defined in Equation 2 was made for analysis purposes.

4.1.1.1.3 Effective Length of Reinforced Concrete Slab

The two previous sections presented stress-strain models for the reinforcing steel and concrete in tension. In addition, methods for determining the load carried by the reinforcing steel and concrete were described. However, a method for determining the deformation associated with the reinforced concrete slab for a given strain level is still needed before a load-deformation behavior can be determined for the reinforced concrete slab. One method for determining the deformation which uses the concept of an effective length of slab was developed by Rex and Easterling (1996(b)). The deformation for the slab is assumed to be the strain multiplied by the effective length. Two effective length values were recommended: one before the reinforcing steel has yielded and one after.

4.1.1.1.3.1 Elastic Effective Length

Before the reinforcing steel yields the length of reinforced concrete slab that has significant contributions to the slab deformation is believed to be the entire length of slab which is in tension. In general this would be the length of slab between the centerline of the girder and the inflection point of the filler beam. However, because the tension load in the slab is transferred out of the slab and into the beam by the shear studs, the tension load in the slab is reduced at each shear stud location (i.e. the full length of the slab in tension does not carry the same tension load). Because it is desirable to use one length of slab for determining the slab deformation an effective length which is less than the full length of the slab in tension is used instead. By assuming shear studs of equal strength and by assuming equal shear stud spacing parallel to the beam this effective length can be derived as

$$L_{eff} = S_0 + S_{studs} \frac{\sum_{i=1}^{N_{studs}-1} N_{studs} - i}{N_{studs}} \qquad \text{(Eq 3)}$$

Where

N_{studs} = Number of effective shear studs (in the tension region)

S_0 = Distance from the girder centerline to the nearest shear stud on the beam

S_{stud} = Shear stud spacing parallel to the beam

Because the inflection point will generally move closer to the beam end as the connection softens the length of the slab in tension will also change. The above effective length has only been proven to work for experimental tests in which the length of the slab in tension was constant from the beginning to the end of the test. An analytical study showing what effect the changing inflection point has on the slab behavior and consequently the connection behavior should be conducted.

4.1.1.1.3.2 Plastic Effective Length

When the reinforcing steel starts to yield it will primarily yield over the length between the center of the girder and the location of the first shear stud on the beam. Consequently the length used to determine reinforced slab deformations after the reinforcing steel yields is assumed to be S_0 or in equation form

$$L_{eff} = S_0 \qquad \text{(Eq 4)}$$

4.1.1.2 Shear Studs

Shear studs are used to attach the reinforced concrete slab to the filler beam. The degree to which the reinforced concrete slab influences the connection behavior will be controlled by the shear stud behavior. Both the shear stud strength and load-deformation behavior are needed to evaluate the influence of the composite slab on the connection moment-rotation behavior. The following methods for approximating the strength and load-deformation behavior are based on the recommendations made by Rex and Easterling (1996(b)).

An estimate of the shear stud strength can be determined using the current AISC Specification (*Load and*, 1993) equations with a couple of modifications.

$$Q_{sol} = SRF\ 0.5\ A_{sc}\ (f'_c\ E_c)^{0.5} \leq 0.8\ A_{sc}\ F_{usc} \qquad \text{(Eq 5)}$$

Where

Q_{sol} = The strength for a single shear stud (kips)

A_{sc} = Area of the shear stud based on the nominal shear stud diameter (in^2)

f'_c = Compressive strength of the concrete (ksi)

F_{usc} = Shear stud steel tensile strength (typically taken as 60 ksi)

E_c = Modulus of elasticity of concrete = $w_c^{1.5}\ \sqrt{f'_c}$ (*Load and*, 1993) (ksi)

w_c = Unit weight of concrete (pcf)

SRF = Stud reduction factor which is given by

$$SRF = \frac{0.85}{\sqrt{N_r}}(w_r/h_r)[(H_s/h_r) - 1.0] \leq \begin{matrix} 0.75 \text{ For Strong Position Studs} \\ 0.5 \text{ For Weak Position Studs} \end{matrix} \qquad \text{(Eq 6)}$$

Where

N_r = Number of shear studs per deck rib

H_s = Shear stud height after welding

h_r = Height of the deck rib

w_r = Width of the deck rib

The modifications are the 0.8 in the upper limit on the shear stud strength given in Equation 5 and the upper limits of 0.75 and 0.5 for the SRF given in Equation 6.

It was shown that the weak position shear stud strength was influenced by the steel deck gage. To account for this a modification factor for the shear stud strength was determined for four typical deck gages. This modification factor is given in Table 3. The revised weak position shear stud strength is determined by adding the value determined in Equation 5 and the modification factor. Note that it is conservative to ignore the modification factor and the modification factor does not apply if the shear stud strength determined in Equation 5 is based on the upper bound of stud shearing ($0.8\ A_{sc}\ F_{usc}$).

Table 3 Weak Position Shear Stud Strength Modification Factors

Deck Gage	Modification Factor (kips)
22	0.00
20	0.82
18	3.25
16	4.70

The load-deformation behavior of shear studs is given by an analytical expression developed by Ollgaard et al (1971).

$$Q = Q_{sol}\left[1 - e^{-18\delta}\right]^{2/5} \qquad \text{(Eq 7)}$$

Occasionally it is convenient to rearrange it so that the deformation can be determined for a given load. This is given as

$$\delta = -\frac{1}{18}\ln\left[1 - \left(\frac{Q}{Q_{sol}}\right)^{2.5}\right] \qquad \text{(Eq 8)}$$

4.1.2 Behavior Models For Steel Connection Components

This part of the report describes the primary steel connection components and presents and / or develops behavior models for each component. These component behaviors include:

- Plate bearing
- Bolt bending, bearing, and shearing
- Friction between plates
- Bolt hole gaps
- Fillet welds
- Axial shortening of the seat angle
- Seat angle bending resulting from angle gaps
- Axial elongation of the shear plate at the gross and net sections

- Axial elongation of the beam web at the gross and net sections

Each component behavior is based on simple mechanics or previous research by the writer or other investigators.

4.1.2.1 High Strength Bolt In Single Shear

High strength bolts are the most commonly used fastener for connections in steel structures. As indicated previously in Figure 1, the proposed beam-girder connection uses high strength bolts to attach the single shear plate to the web of the beam. High strength bolts may also be used to attach the seat angle to the bottom flange of the beam if fillet welds are not used. Finally, high strength bolts are used to attach the seat angle to the girder web. The behavior of the bolts attaching the shear plate and the seat angle to the beam are of primary interest. The behavior of the bolts attaching the seat angle to the support are not expected to have a significant influence on the connection behavior and are consequently not of interest.

The bolts attaching the shear plate and seat angle to the beam are in single shear and can be either fully tensioned or only tensioned to the snug tight condition. It is assumed that the bolt behavior in either the shear plate or seat angle is similar to the behavior of a single bolt lap plate connection. This assumption was previously illustrated in Figure 11. The behavior of single bolt lap plate connections with both fully tightened and snug tight bolts was previously investigated and reported by Rex and Easterling (1996(d)). This investigation showed that single bolt lap plate connection behavior could be considered as two separate behaviors; friction and plate-bolt-plate bearing. The behavior models developed by Rex and Easterling (1996(d)) are summarized below.

4.1.2.1.1 Frictional Behavior

If the bolts are fully tensioned then friction forces which develop between the two plates help resist the movement of one plate relative to the other. Ideally, there should be no plate motion of one plate relative to the other plate until the slipping load is attained.

However, it was shown that there is slipping between the two plates prior to the major slipping event that we typically associate with the slipping load. After the slipping load is reached the frictional resistance was shown to slowly degrade until there was little to no significant load resistance that could be attributed to friction. This behavior was simplified and quantified and is shown schematically in Figure 13.

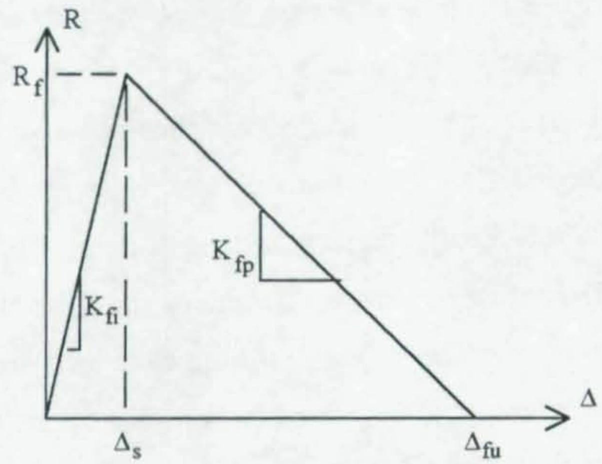

Figure 13 Bi-Linear Representation of Friction Load-Deformation Behavior

The slipping load "R_f" is based on a combination of the AISC Specification (*Load and*, 1993) requirements for bolt tightening and recommended slip coefficients given by Fisher et al (1978).

$$R_f = \alpha\ (0.7\ F_{ub})\ (0.75\ A_b)\ \mu \qquad \text{(Eq 9)}$$

Where

α = 1.0 for A325 bolts and 0.88 for A490 bolts

μ = Friction coefficient (0.33 for clean mill scale surfaces)

F_{ub} = Minimum specified tensile strength of the bolt

A_b = The area associated with the nominal diameter of the bolt

The deformation at which slip occurs "Δ_s" was empirically determined to be about 0.0076-in. with a COV of 45% based on the results of the single bolt lap plate connection tests. However, a value of 0.015-in. was recommended based on calibrations between the component model and experimental connection results (Rex and Easterling 1996(e)). The initial frictional stiffness "K_{fi}" is assumed to be the slipping load divided by the slipping deformation. The deformation at which the frictional resistance is assumed to be zero "Δ_{fu}" is given by a tri-linear prediction model which depends on the thickness of the two plates.

$$\Delta_{fu}\left|\begin{array}{ll} (t_1 + t_2) < 0.5" & \Delta_{fu} = 0.4" \\ .0.5" \le (t_1 + t_2) \le 1.5" & \Delta_{fu} = 0.4" - (t_1 + t_2 - 0.5)\, 0.3 \\ 1.5" < (t_1 + t_2) & \Delta_{fu} = 0.1" \end{array}\right. \qquad \text{(Eq 10)}$$

Where

t_1 = Thickness of the thinner of the two plates connected (in.)

t_2 = Thickness of the thicker of the two plates connected (in.)

The final frictional stiffness "K_{fp}" is assumed to be slipping load divided by the difference between Δ_s and Δ_{fu}.

4.1.2.1.2 Plate-Bolt-Plate Bearing Behavior

As the plates in the connection start to move relative to each other bearing forces are developed by contact between the bolt hole in one plate against the bolt and in turn by contact between the bolt and the bolt hole of the second plate. If the two plates and the bolt are initially in contact then these bearing forces start to develop as soon as the plates start to move relative to each other. However, in many instances, when a connection is assembled there will be gaps between the sides of the bolt and the bolt holes in the two plates. In this case, the plates must move relative to each other enough to close these gaps before bearing forces can be developed.

Once the plates and bolt are in contact (either initially or after some relative movement) then the load-deformation behavior is a complex combination of the localized load-deformation behavior in each plate and the load-deformation behavior of the bolt.

These load-deformation behaviors have been idealized and quantified and are summarized below.

4.1.2.1.2.1 Local Plate Load-Deformation Behavior

The load-deformation behavior of plates in the local vicinity of a bolt was the topic of a separate report on single bolt single plate behavior (Rex and Easterling, 1996(c)). In this report both experimental and analytical methods were used to develop an approximation to the plate load-deformation behavior. The Richard Equation using normalized parameters was used to represent the non-linear behavior.

$$\frac{R}{R_n} = \frac{1.74\,\overline{\Delta}}{\left(1 + \overline{\Delta}^{0.5}\right)^2} - 0.009\,\overline{\Delta} \qquad \text{(Eq 11)}$$

Where

R = Plate load

R_n = Nominal bearing / tearout strength as per the AISC Specification (*Load and*, 1993)

$\overline{\Delta}$ = Normalized deformation = $\Delta\,\beta\,K_{pi}/R_n$

Δ = Local plate deformation

β = Steel correction factor = 30% / %Elongation

For typical steels β is taken as one.

K_{pi} = Initial plate stiffness given by

$$K_{pi} = \frac{1}{\dfrac{1}{K_{pbr}} + \dfrac{1}{K_{pb}} + \dfrac{1}{K_{pv}}} \qquad \text{(Eq 12)}$$

K_{pbr} = Plate bearing stiffness = $120\,F_y\,t_p\,d_b^{0.8}$ (units are kips and inches)

K_{pb} = Plate bending stiffness = $32\,E\,t_p\,(L_e/d_b - 0.5)^3$

K_{pv} = Plate shearing stiffness = $6.67\,G\,t_p\,(L_e/d_b - 0.5)$

t_p = Thickness of plate being considered

d_b = Nominal diameter of bolt

F_y = Yield strength of plate being considered

F_u = Tensile strength of plate being considered

L_e = End distance of plate being considered

$\overline{\Delta}_f = 22.87$, normalized deformation at assumed plate failure

All of the terms in the above expressions except L_e can be directly interpreted from the context of the single bolt lap plate connection (for which they were developed) to the proposed beam-girder connection. The end distance "L_e" depends on the location of the bolt and the assumed direction of bolt deformation.

For the bolts that attach the shear plate to the web of the beam there are four end distance values considered: two for the shear plate and two for the beam web. Two values of the end distance are needed for both the web and plate because of the two-dimensional load-deformation behavior of these bolts. As will be discussed later, the two dimensional behavior is treated as a combination of vertical and horizontal deformations. Consequently, a vertical end distance and a horizontal end distance are needed.

The vertical end distance is assumed to be the vertical bolt pitch minus one-half of a bolt diameter. This is consistent with recommendations given in the AISC Specification (*Load and*, 1993) for determining bolt bearing strength with the exception of the top hole in the beam web and the bottom hole in the shear plate. For these holes the end distance should be the vertical distance from the bolt centerline to the bottom of the beam cope or the bottom of the shear plate respectively. For purposes of the model behavior, this refinement is not considered necessary and all bolts are assumed to have the same vertical end distance. It is further assumed that vertical end distance will be sufficient to develop the full bearing strength of the bolt (i.e. $L_e \geq 2.4\ d_b$). This assumption is based on typical bolt pitches used in practice and the likelihood that none of the bolts will be subject to strictly vertical deformations. It is more likely that all bolts will deform at some angle to the vertical witch results in more steel being between the front of the bolt and the edge of the plate (or web) toward which the bolt is deforming. The horizontal end distance is assumed to be the horizontal distance from the centerline of the bolt hole to the edge of the plate or beam web when determining the plate and the web behavior respectively.

For the bolts attaching the seat angle to the bottom flange L_e is assumed to be the bolt pitch minus ½ d_b. This assumed end distance has not been verified by any testing but it believed to be conservative. The assumed horizontal end distances for the bolts in the web and seat angle are shown schematically in Figure 14 below.

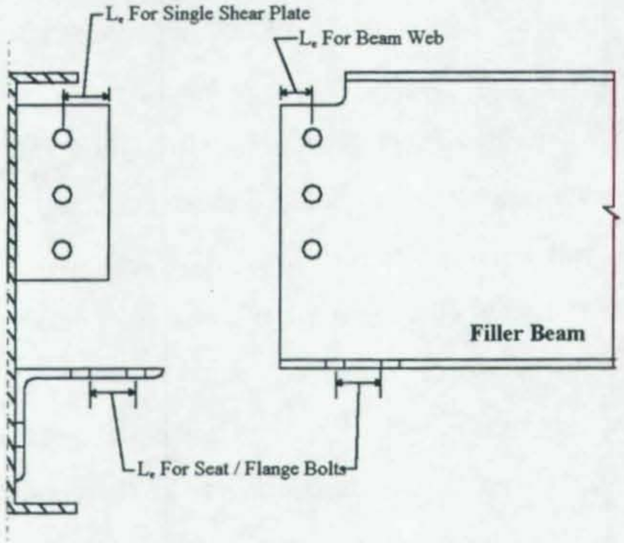

Figure 14 Assumed End Distances For Plate Strength and Stiffness

4.1.2.1.2.2 Load-Deformation Behavior of Bolt

Based on an analysis of test data reported by Wallaert and Fisher (1965), Sarkar and Wallace (1992), and Karsu (1995) along with recommendations given in EC3 Annex J (1994) a simplified approximation of the combined bearing, bending, and shearing deformations associated with a bolt in single shear was developed (Rex and Easterling, 1996(d)). This is given as

$$\frac{R}{R_n} = 1 - e^{-6.25\,[\text{illegible}]} \qquad \text{(Eq 13)}$$

Where

R = Bolt load

R_n = Nominal bolt shear strength as per the AISC Specification (*Load and*, 1986)

$\overline{\Delta} = \Delta / \Delta_f$

Δ = Combined bolt bearing, bending, and shearing deformations

Δ_f = 1/8-in., assumed deformation at shear failure of bolt

4.1.2.2 Fillet Weld

Fillet welds are probably the second most commonly used fastener for connections in steel structures. In the proposed beam-girder connection fillet welds are used to attach the shear plate to the girder web and to attach the seat angle to the beam bottom flange (if bolts are not used). The strength and load deformation behavior of fillet welds are needed for the component modeling of the beam-girder connection.

An evaluation of available methods for predicting the strength and load-deformation behavior of fillet welds was given in Rex and Easterling (1996(e)). Based on this evaluation the method given in the AISC Specification (*Load and*, 1993) was recommended. This method is a modification of the method developed by Miazga and Kennedy (1989) and Lesik and Kennedy (1990). The weld strength is given by:

$$\frac{P_\theta}{P_0} = 1 + 0.5\ \mathrm{Sin}^{1.5}\theta \qquad \text{(Eq 14)}$$

Where

P_θ = Strength of weld loaded at angle θ

$P_0 = 0.6\ F_{exx}\ A_w$ = Strength of weld loaded at $\theta = 0$

F_{exx} = Nominal weld electrode strength

A_w = Effective area of weld throat

The weld load deformation behavior is given by:

$$\frac{P}{P_\theta} = [\rho(1.9 - 0.9\,\rho)]^{0.3} \tag{Eq 15}$$

Where:

$\rho = \Delta/\Delta_u$

$\Delta_u = 0.209(\theta+2)^{-0.32}D$ = Deformation at ultimate load of fillet weld

$\Delta_f = 1.087(\theta+6)^{-0.65}D$ = Deformation at fracture of fillet weld

D = Leg size of fillet weld (in.)

4.1.2.3 Seat Angle

The seat angle in the proposed beam-girder connection is essentially designed to resist axial loads passing from the bottom flange of the beam to the seat angle and then to the girder web as shown in Figure 15. There are two primary sources of flexibility: axial shortening of the outstanding leg of the angle and flexural bending of the leg which is adjacent to the girder web. The flexural bending occurs only if there is a gap between the heel of the seat angle and the web of the girder and then only until this gap is closed. Two simple mechanical models for approximating these flexibility's are also shown in Figure 15.

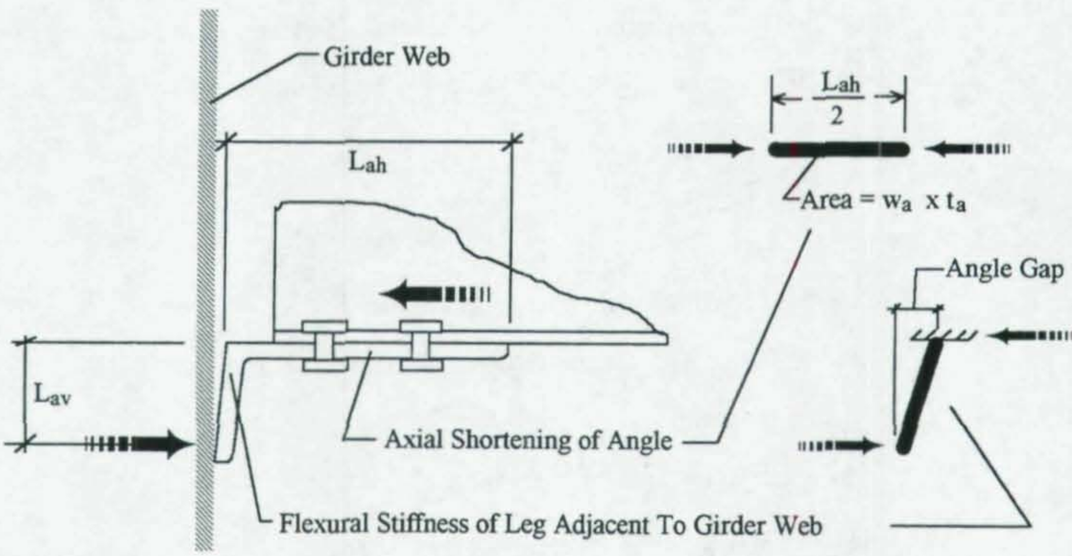

Figure 15 Modeling Seat Angle Flexibility

The axial shortening is modeled as a truss element where the area is equal to the cross-sectional area of the angle and the length is equal to the outstanding leg length (L_{ah}) divided by two. Holes in the angle leg are ignored as they would typically be filled with a bolt which would act to carry the compression load across the hole. The truss element is assumed to behave according to the constitutive behavior based on the typical stress-strain model of mild steel (Rex and Easterling, 1996(a)).

The flexural stiffness is modeled as a cantilevered beam where the moment of inertia is based on the angle cross-sectional properties and the length is assumed to be the vertical distance from the top of the angle to the location where the bolts attach the angle to the girder web (L_{av}). The flexural stiffness is assumed to increase many orders of magnitude when the angle gap closes. A reasonable estimate of the increased stiffness can be given by the axial stiffness of the girder web located between the heels of two seat angles on opposite sides of the web. This leads to a bi-linear behavior model of the flexural behavior. The flexural stiffness is assumed to remain elastic until the angle gap closes.

4.1.2.4 Shear Plate & Beam Web

As will be discussed later, the bolt deformations in the web and shear plate will be treated as a combination of vertical and horizontal deformations. The vertical deformations put the steel in the web and plate in vertical shear while the horizontal deformations typically put the steel in the web and plate in horizontal tension (occasionally compression). The flexibility of the shear plate and beam web in shear has been assumed to be small and ignored for modeling. However, the flexibility of the shear plate and beam web in tension are believed to be significant particularly around the bolt hole. Consequently, the horizontal tension behavior has been included in the model.

As shown in Figure 16, two truss elements for both the web and plate are used to model the gross and net section horizontal tension behavior. The first element (gross section) is assumed to have a length of either the "a" distance minus $d_b/2$ for the shear plate or 2.0 d_b for the beam web. The second element (net section) is assumed to have a length of d_b. The first element has a width equal to the bolt pitch while the second has a width equal to the bolt pitch minus d_b. The thickness of the first and second elements are the same as the shear plate or beam web. The truss element is assumed to behave according to the constitutive behavior based on the typical stress-strain model of mild steel (Rex and Easterling, 1996(a)).

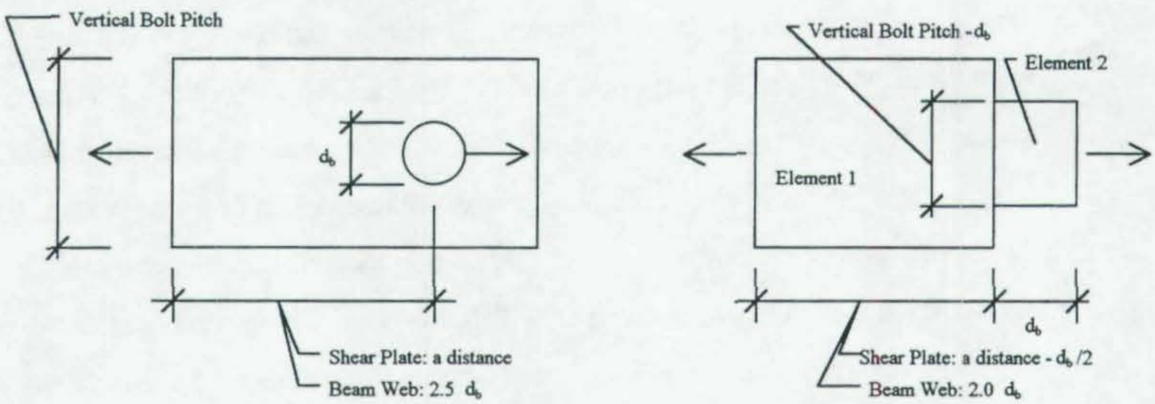

Figure 16 Modeling Shear Plate And Beam Web Flexibility

4.2 Combining Connection Component Behaviors

Behavior models for each key component of the proposed steel beam-girder connection were presented and or developed in the previous sections. The next step is to combine the behavior of each of the components to determine the moment-rotation behavior of the overall connection. This combination of behaviors is done in two major steps. First the individual component behaviors are combined in series or parallel as appropriate to create combination elements at each critical level of the connection. The critical levels being the level of the seat angle, the level of the composite slab, and the level of each of the bolts in the web. Second, the combination elements are combined in an ultimate strength model of the connection to determine the moment-rotation behavior.

4.2.1 Combination Elements

The first step in combining the connection component behaviors to determine the connection moment-rotation behavior is to create combination elements. Combination elements are the combined behavior of each connection component for a given critical level in the connection and/or direction of deformation. As will be discussed later, an ultimate strength analysis of the connection will use the combination element behaviors to determine the connection behavior. It should be noted that the individual component behaviors could be combined during the ultimate strength analysis rather than prior to the analysis. There are three primary reasons for doing the combination prior to the ultimate strength analysis. First, the speed of the ultimate strength analysis is greatly improved. Second, programming the ultimate strength analysis becomes much simpler and less prone to errors. Third, convergence difficulties tend to increase if the behaviors are not combined before the ultimate strength analysis.

For the proposed composite beam-girder connection there are essentially four combination element behaviors: horizontal web bolt behavior, vertical web bolt behavior, horizontal seat angle behavior, and composite slab behavior. Schematics of these combination elements and the components of each element are shown in Figure 17.

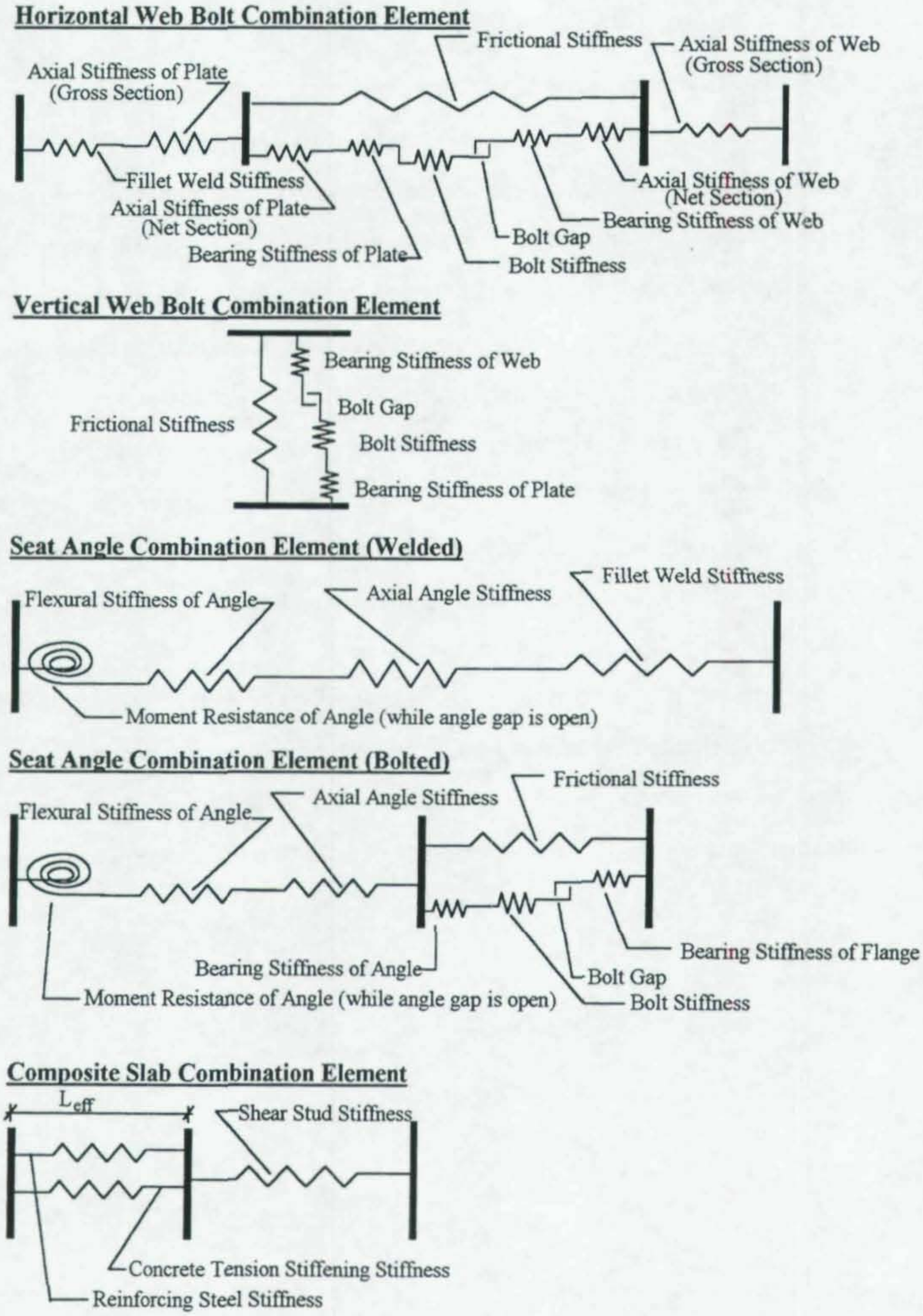

Figure 17 Combination Elements

First, at the level of each bolt in the beam web, the behavior of the fillet weld attaching the shear plate to the girder web, the shear plate and beam web axial stiffness, and the high strength bolt stiffness are combined to create a single Horizontal Web Bolt load-deformation behavior. In addition, the friction behavior, plate bearing, web bearing, and bolt behavior are combined to create a single Vertical Web Bolt load-deformation behavior. Each web bolt behavior will be identical except for differences in initial assumed bolt gap. The bolt gap represents the amount of slip that has to occur prior to the plates and bolts developing direct bearing loads.

Second, at the level of the seat angle the behavior of the angle in flexure, the angle under axial compression, and the beam flange to seat angle connection (fillet welds or high strength bolts) are combined to create a single Seat Angle load-deformation behavior and moment-deformation behavior. The moment-deformation behavior is needed because the ultimate strength analysis of the overall connection (described in the next section) assumes that the angle resistance is located at the top of the seat angle. However, before the angle gap closes the actual resistance is located at a distance L_{av} below the top of the seat angle. The moment-deformation behavior accounts for this discrepancy. The moment is equal to the value of the load for a given deformation multiplied by L_{av} until the gap closes. Once the gap closes the moment is assumed to be zero.

Third, at the level of the composite slab the behavior of the reinforced concrete slab and the shear studs are combined. The reinforced concrete slab behavior is assumed to be the parallel combination of the reinforcing steel and concrete tension stiffening behavior. The concrete slab is then combined with the shear stud behavior; where, the shear stud behavior is assumed to be a parallel combination of all the shear studs in the negative moment region.

Each combination element is represented by a single multi-linear load-deformation behavior which from the initial behavior to failure. The failure deformation and load associated with a combination element is assumed to be limited by the component in the element that fails. For example, if bolt shear failure occurs then the failure load is the bolt shear strength and the failure deformation is the bolt shear failure deformation combined with the deformations of the other components that occur at the failure load.

4.2.2 Using Ultimate Strength Analysis To Combine Combination Elements

Now that the individual connection components have been combined into combination elements the next step is to combine the combination elements to determine the moment-rotation behavior of the overall connection. The method used to combine the combination element behaviors is similar to the ultimate strength method for determining the load capacity of an eccentrically loaded bolt group. This method is fully described in the AISC Manual Vol. II (*Manual of*, 1993); however, a brief description of the fundamental ideas is given below. This is followed by a description of how the basic method is modified and used to determine the connection moment-rotation behavior.

4.2.2.1 Ultimate Strength Method

The ultimate strength method for analyzing eccentrically loaded bolt groups assumes that the connection rotates about an instantaneous center (IC). The deformation of each bolt in the bolt group is assumed to be linearly proportional to the distance between the bolt and the IC. In addition, the bolt force is assumed to act in a direction perpendicular to a line connecting the bolt to the IC. The force in each bolt is determined using a non-linear load-deformation behavior for the bolt. The bolt farthest away from the IC is assumed to fail first and it is assumed that this bolt will fail at some ultimate deformation limit (currently 0.34-in. is used). A schematic showing these concepts is presented in Figure 18.

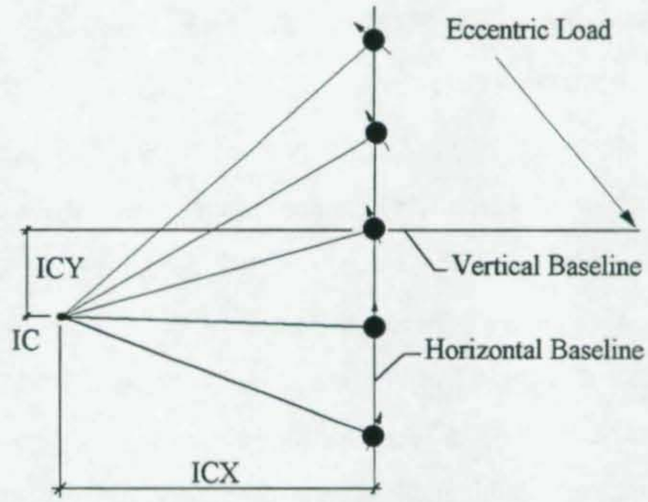

Figure 18 Ultimate Strength Analysis of Eccentrically Loaded Bolt Groups

The analysis is carried out in the following step by step procedure:

1. Assume a location for the IC.
2. Determine the distance from each bolt to the IC.
3. Assume the bolt farthest away from IC has deformed to the failure deformation.
4. Determine remaining bolt deformations based on the ratio of the distance between the bolt and the IC and the distance between the IC and the bolt farthest away from the IC.
5. Determine the force in each bolt using the bolt deformation just determined and the non-linear load-deformation behavior.
6. Break the bolt forces and applied force into x and y components.
7. Sum forces in the x and y direction and moments about the IC.
8. If forces in the x and y direction and moments about the IC do not sum to zero then revise location of IC and return to step 2.
9. When forces in the x and y direction and moments about the IC do sum to zero then the appropriate IC location has been determined and the maximum applied load can be determined.

The procedure is obviously iterative and many methods for assuming a location for the IC and revising this location have been developed.

4.2.2.2 Modification of Ultimate Strength Method For Analysis of Partially Restrained Connections

The basic ultimate strength method is modified slightly so that the moment-rotation behavior of partially restrained connections can be determined. The physical connection and the resulting ultimate strength model are shown in Figure 19. There are two primary differences between the basic ultimate strength analysis and the modified analysis. First, the single non-linear load-deformation behavior of the bolt is replaced by the Horizontal and Vertical Web Bolt combination element behaviors. Second, the seat angle and composite slab combination elements are added to the analysis. The seat angle and composite slab are assumed to only resist load in the x direction and deformations are assumed to be the x component of the total deformation at the angle or slab based on the same analysis technique used to determine the total deformation at each bolt location.

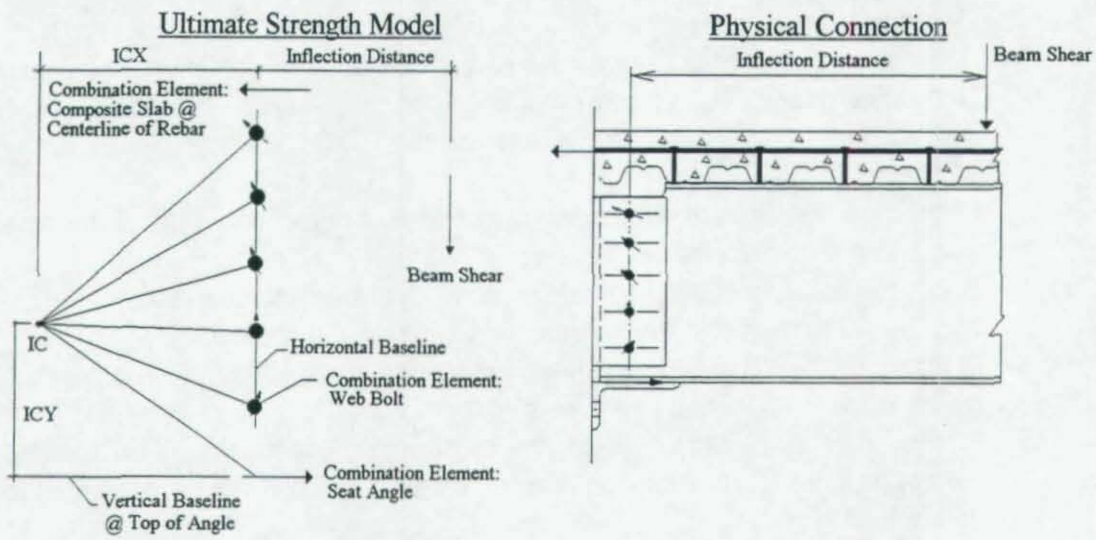

Figure 19 Modified Ultimate Strength Method

The analysis is carried out using a slightly modified step-by-step procedure:

1. Choose a deformation limit for the combination element farthest from the IC.
2. Assume a location for the IC.
3. Determine the distance from each combination element to the IC.

4. Assume the combination element farthest away from IC has deformed to the limiting deformation chosen in step 1.
5. Determine remaining combination element deformations based on the ratio of the distance between the combination element and the IC over the distance between the IC and the combination element farthest away from the IC.
6. Determine the x component of the total angle and slab combination element deformations and the corresponding combination element loads.
7. Using the deformations determined in steps 4 and 5 and the geometry based on the assumed IC determine the vertical and horizontal forces at each web bolt (Note: this procedure is expanded on in the following section).
8. Sum forces in the x and y direction and moments about the IC.
9. If forces in the x and y direction and moments about the IC do not sum to zero then revise location of IC and return to step 2.
10. When forces in the x and y direction and moments about the IC do sum to zero then the appropriate IC location has been determined and the maximum beam shear can be determined. The beam shear multiplied by the inflection distance (i.e. the connection eccentricity) gives the connection moment. The x component of the total seat angle deformation divided by the ICY distance gives the connection rotation.
11. Return to step 1 and increase the limiting deformation and repeat steps 2 through 13. Keep returning to step 1 until one of the combination elements attains a deformation equal to its failure deformation. By increasing the limiting deformation, the connection rotation will increase and consequently the connection moment. The rotation capacity of the connection is determined by stopping the analysis when a combination element failure deformation is reached.

There are three particularly nice features of this analysis process. First, it provides a method for considering the influence of the moment to shear ratio which is controlled by the inflection point distance. Second, if the ultimate deformation at failure of the combination elements is known then the ultimate moment and rotation at connection failure can be determined. Third, the analysis can be easily programmed so that a general purpose finite element program is not required.

4.2.2.3 Interaction of Horizontal and Vertical Web Bolt Combination Elements

In the typical ultimate strength analysis of an eccentrically loaded bolt group each bolt is represented by a single load-deformation relationship that is independent of the direction of loading. However, the web bolts in the modified ultimate strength analysis are represented by two different load-deformation relationships because of the different behavior in the horizontal direction compared to the vertical direction. If the bolt deformations are strictly horizontal then the horizontal load-deformation relationship would apply; and, if the deformations are strictly vertical then the vertical load-deformation relationship would apply. However, generally the web bolt deformations are not strictly horizontal or vertical but instead they are at some angle to the horizontal or vertical. Consequently, it is necessary to develop a method of estimating how the vertical and horizontal behaviors interact so that the behavior of a bolt deforming at some angle to the horizontal or vertical may be determined.

One method of accounting for the interaction between the vertical and horizontal behaviors is to treat them independently of each other. The easiest way of doing this is to break the total bolt deformation into vertical and horizontal components and then determine the vertical and horizontal resistance based on the vertical and horizontal load-deformation relationships. The problem with treating the behaviors independently of each other is that they are not independent. To illustrate this consider a bolt deforming at approximately 45 degrees from the horizontal (and from the vertical). The deformations in both the horizontal and vertical directions will be equal and if the load-deformation relationships are similar in the vertical and horizontal directions then the loads will be approximately equal in the two directions. Consider now that the web bolt strength is limited by the bolt shear capacity. Eventually the force in both the horizontal and vertical directions will equal the bolt shear capacity and the connection the model would indicate the connection failed. However, the true load on the bolt would be the vector sum of the two forces; in this case, the bolt load would be 1.41 times the bolt shear capacity. This type of treatment would clearly be inappropriate.

From the above illustration it is clear that an interaction relationship between the vertical and horizontal behaviors must be used to ensure that the total resistance attributed to the bolt cannot exceed the limiting capacity of the bolt. An elliptical interaction has been assumed for the current model. This interaction curve is shown in Figure 23. The nomenclature in Figure 20 is defined as follows:

R_{nv} = Maximum resistance in the vertical direction

R_{nh} = Maximum resistance in the horizontal direction

V = Load resistance in the vertical direction

H = Load resistance in the horizontal direction

R_n = Maximum resistance in the direction of deformation

θ = Angle of deformation with respect to the horizontal

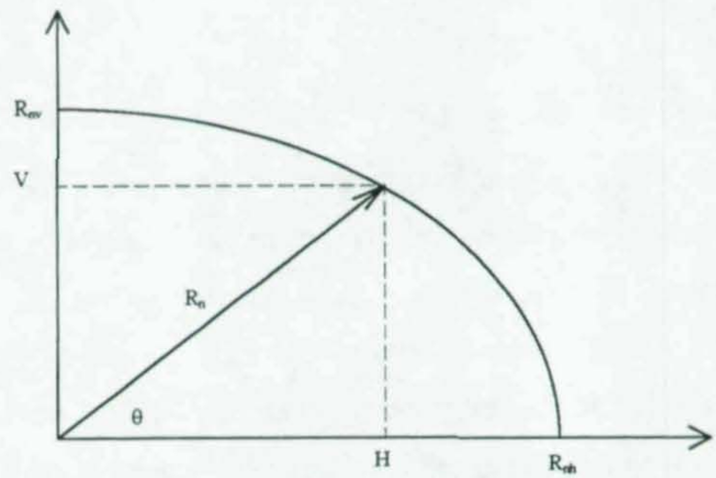

Figure 20 Elliptical Interaction Between Horizontal and Vertical Web Bolt Behavior

In the ultimate strength analysis the load resistance must be determined based on the total deformation and the angle of deformation. A two step process is used to determine the load resistance. First, using the value of the total deformation with the vertical and horizontal load-deformation relationships the maximum load resistance in the vertical and horizontal directions respectively (R_{nv} and R_{nh}) are determined. These two values define the boundaries of the ellipse (i.e. the ellipse expands as the deformation increases up to the limiting load capacity in each direction). Second, R_n is determined from the angle of deformation.

$$R_n = \frac{1}{\sqrt{\left(\frac{\text{Cos}\,\theta}{R_{nh}}\right)^2 + \left(\frac{\text{Sin}\,\theta}{R_{nv}}\right)^2}} \qquad \text{(Eq 16)}$$

There is no general proof that the interaction between vertical and horizontal behavior is elliptical; however, it can be shown that the interaction is elliptical if the vertical and horizontal behaviors are limited by the bolt shearing strength. In this case, no matter what direction the deformation occurs in the limiting strength is the bolt shear strength. This results in an elliptical interaction surface in which both legs of the ellipse are equal (i.e. a circle).

4.2.2.4 Limitation Of The Modified Ultimate Strength Analysis

The method of combining the combination elements in an ultimate strength analysis as just described has one important shortcoming: compatibility with the attached beam is not considered. In the analysis a constant inflection point is assumed. However, in reality the inflection point would vary along the beam because of the non-linear behavior of the connection. The farther away the inflection point is from the connection the better the connection moment resistance. The closer the inflection point the worse the moment resistance because of the increased influence of shear. The location of the inflection point will depend on the beam properties and loading.

Initially, it was believed to be conservative to assume the closest inflection point (i.e. the highest shear to moment ratio) that would occur given real beam and loading conditions. However, in some cases if the inflection point is chosen too close to the connection the connection may fail in shear rather than in moment. A connection fails in shear when the deformation limit of one of the vertical web bolt combination elements is reached during the analysis. A connection fails in moment when the deformation limit of one of the horizontal web bolt combination elements, the composite slab combination element, or the seat angle combination element is reached.

Connections can, in reality, fail in shear and that alone is not a problem. The problem is that the ultimate strength analysis assumes that increased shear on the connection reduces the moment capacity and the rotation capacity of the connection. In the extreme the connection could fail in shear without any connection rotation if the inflection point was chosen at the location of the connection centerline. The problem with this is that the beam end must rotate and if the beam end rotates then the connection has to develop moment resistance which then will decrease the shear capacity of the connection. In situations where the connection is failing in shear, the only way to do a proper analysis is to include the beam properties and loading; however, if designing with PR connections, the beam cannot be chosen without an estimate of the connection behavior. Consequently, the design could become very iterative.

To avoid this problem with the connection analysis one very simple rule can be applied. The maximum shear on the connection must be "small" compared to the connection shear strength to ensure that the connection fails in moment before it fails in shear.

To determine what connection shear values could be considered "small" a brief parametric study was conducted. Fifty variations of the steel connection and composite slab parameters were considered. For each of these parameter combinations the inflection point was varied to determine what value of connection shear would cause the connection to fail in shear. This value was then compared to the ultimate shear capacity of the connection assuming no eccentricity (basic shear capacity) of the load (i.e. no connection moment resistance). The component model was used to perform the connection analysis.

Based on this study it was determined that composite connections would fail in shear if the applied shear on the connection exceeded 82% of the basic shear capacity on average. The actual ratios ranged from 76% to 88% of the basic shear capacity with a COV of 3.8%. A conservative value of 75% of the basic shear capacity is recommended as a maximum applied shear to ensure that shear failure will not occur in the connection.

4.3 Programming the Component Method

A computer program that implements the component model was developed. The program was written in Visual Basic and uses batch input and output files. The basic flow of the program is as follows:

- Get input: connection geometry material properties
- Determine behavior for each connection component
- Determine combination element behavior
- Determine moment-rotation behavior using ultimate strength approach
- Write output

The program was first used to evaluate the component model against the experimental connection results. This is discussed in the following section. After the program (and component method) was evaluated against the experimental data the program was used to develop a second (somewhat simpler) method for approximating the connection moment-rotation behavior. This is discussed later in the report.

4.4 Evaluation of Component Method

The predicted moment-rotation behavior is compared to the test data in each of the experimental connection moment-rotation plots which are found in Appendix B. In addition, the primary moment-rotation behavior characteristic values (M_{ult}, ϕ_{ult}, K_i) are summarized and compared in Table 4 below. In general there was very good agreement between the predicted and the experimental behavior; however, there were some discrepancies.

There are two primary differences between the component model results and the test results. First, the test behavior of the steel connection for #7 was stiffer than the component model behavior. However, the differences only occur in the later stages of behavior. The reason for this difference is that it was over two hours between when the concrete was cast and when the pre-loading was finished. Undoubtedly some concrete setting occurred during this time which could have caused some load to be carried by the reinforcing steel. Even a small load developed in the reinforcing steel multiplied by the moment arm between the reinforcing steel and the seat angle would cause the test connection moment resistance to increase noticeably.

Second, initial stiffness values from the component model were much smaller than the initial stiffness values of the composite connection behaviors. The primary reason for this is that the component model only uses the effective area of concrete around each reinforcing bar to determine the tension resistance of the concrete. However, before the concrete cracks the actual area of concrete resisting tension forces is much larger than the effective area around each bar. Consequently, the tension forces carried by the concrete would be much higher in the experimental test than in the component model resulting in an increased connection stiffness.

Table 4 Model Vs. Test Results For Primary Moment-Rotation Characteristics

Connection	Model M_{ult} (k-in.)	Model ϕ_{ult} (mrad)	Model K_i (k-in./rad)	Model / Test M_{ult}	Model / Test ϕ_{ult}	Model / Test K_i
5 Steel	N/A	N/A	220147	N/A	N/A	0.90
5 Comp	2482	92	351335	0.95	0.96	0.53
6	2472	72	675443	1.04	0.96	0.66
7 Steel	N/A	N/A	142333	N/A	N/A	0.69
7 Comp	1417	78	295665	0.95	1.01	0.47
8	1398	62	429200	0.99	1.02	0.40
Statistics			Mean	0.98	0.99	0.61
			COV	0.04	0.03	0.29
			Max	1.04	1.02	0.90
			Min	0.95	0.96	0.40

5. Simplified Method For Approximating Composite Beam-Girder Connection Moment-Rotation Behavior

In the previous section it was shown that the component method is able to provide moment-rotation approximations that agree well with experimental results. However, the complexity of the model does not lend itself to hand or even spreadsheet calculations. Consequently, it was decided to develop a simpler method of providing moment-rotation approximations.

When a complex model is reduced to a simpler one there are simplifying assumptions involved. In the following development, the primary assumption is that the moment-rotation behavior can be represented by a single continuous analytical expression. It is also assumed that the Richard Equation is the analytical expression most capable of representing the moment-rotation behavior for the following reasons:

- The equation is continuous and easy to use
- The equation is able to accurately represent the moment-rotation behavior for most connections
- Three of the four connection parameters relate very well to definable moment-rotation characteristics such as K, K_p, and M_{ult} which are the initial stiffness, final stiffness, and moment capacity of the connection respectively

The Richard Equation, definition of equation parameters, and a graphical interpretation of the equation parameters is presented in Figure 21. The parameter notation has been modified from the original notation for use with moment-rotation behavior.

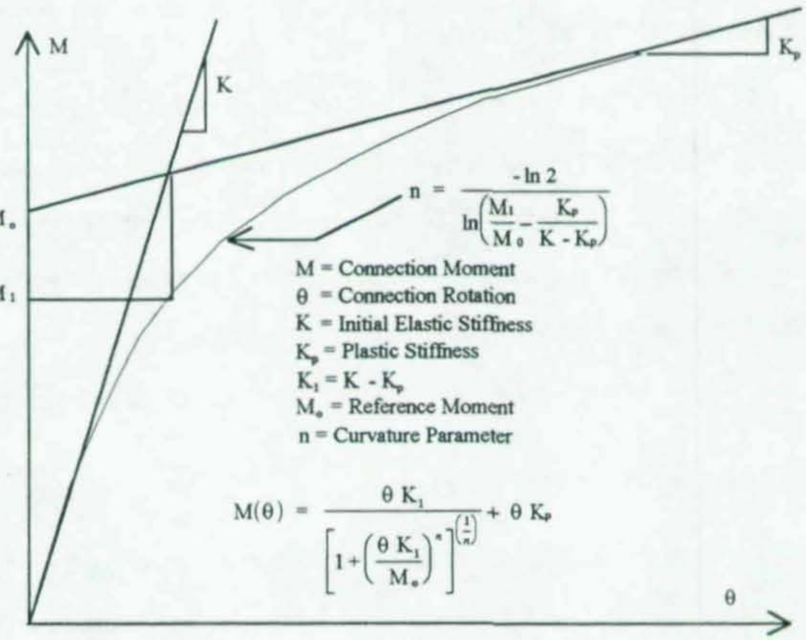

Figure 21 The Richard Equation

If the Richard Equation is used to represent the moment-rotation behavior then the next step in developing a simplified method is to determine how the connection parameters are related to the Richard Equation parameters. This is done in the following three sections. First, the connection parameters are identified and in some cases assigned simplifying notation. Second, to reduce the number of parameters that influence the moment-rotation behavior certain assumptions are made about the connection. Third, using a combination of basic mechanics and parametric analysis, relationships between the connection parameters and the Richard Equation parameters are developed.

The following development only considers composite connection behavior. A simplified method for approximating the steel connection behavior (i.e. the behavior of the connection before the concrete hardens) was developed in a separate report (Rex and Easterling, 1996(e)).

5.1 Connection Parameters

This section identifies the fundamental connection parameters that can influence the moment-rotation behavior. These include both independent and dependent parameters. The independent parameters are those which are not influenced by nor influence another independent parameter. The dependent parameters are those which are determined from the independent parameters. Some of the following parameters have been previously defined; however, they are repeated for completeness.

5.1.1 Independent Parameters

There are a number of connection material and geometric parameters that can be varied independently of each other. For clarity these parameters have been sorted into three major groups: general connection parameters, composite slab parameters, web bolt parameters, and seat angle parameters.

5.1.1.1 General Connection Parameters

General connection parameters are the parameters that influence the connection behavior but do not influence the web bolt, composite slab or seat angle combination element behaviors (these combination elements were described previously under the component method). These include:

- Distance-to-Inflection Point or V_{ult}
- Y_b = Distance from the top of the seat angle to the center of the bottom bolt
- N_w = Number of bolts in the web
- Y_r = Distance from the top of the seat angle to the center of the reinforcing steel

These parameters are illustrated in Figure 22 and 23. The reason that the Distance-to-Inflection Point and V_{ult} are not listed separately is because they are related to each other. For a given connection as V_{ult} increases the Distance-to-Inflection Point decreases and visa versa. Consequently, only one or the other value can be chosen.

5.1.1.2 Composite Slab Parameters

The composite slab parameters are the parameters that influence the composite slab combination element behavior. These parameters are illustrated in Figure 22 and include:

- f'_c = Compressive strength of concrete
- w_c = Unit weight of concrete
- Y_{con} = Total depth of composite slab
- d_{stud} = Nominal shear stud diameter
- N_{studs} = Number of effective shear studs
- S_0 = Distance from the girder centerline to the nearest shear stud on the beam
- S_{stud} = Shear stud spacing parallel to the beam
- S_{bar} = Reinforcing bar spacing
- N_r = Number of shear studs per deck rib
- H_s = Shear stud height after welding
- h_r = Height of the deck rib
- w_r = Width of the deck rib
- N_{bars} = Number of reinforcing bars
- d_{bar} = Reinforcing bar diameter
- F_{yr} / F_{ur} = Reinforcing steel yield / tensile strength

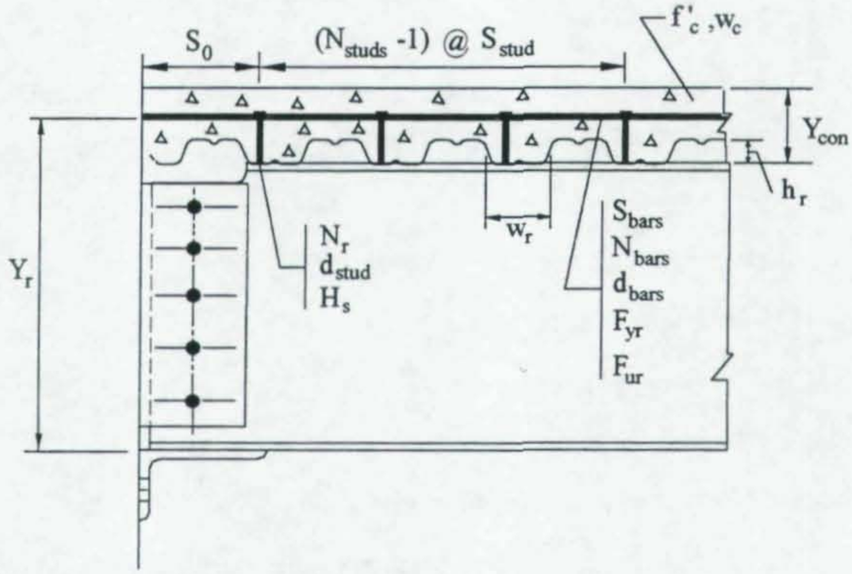

Figure 22 Composite Slab Parameters

The yield and tensile strengths of the reinforcing steel are not considered to be independent of each other. Although, there is not a constant relationship between these two values they are very much related to each other.

5.1.1.3 Web Bolt Parameters

The web bolt parameters are the connection parameters that influence the vertical and horizontal web bolt combination element behaviors. These parameters are illustrated in Figure 23 and include:

- t_w = Beam web thickness
- F_{yw} / F_{uw} = Yield and Tensile strengths of beam web
- L_{eh} = Horizontal distance from the bolt centerline to the end of the beam
- W_p = Shear plate width
- t_p = Shear plate thickness
- F_{yp} / F_{up} = Yield and Tensile strengths of the shear plate
- a Distance = Horizontal distance from shear plate weld to the centerline of the bolts

- Bolt Tension either snug or fully tightened
- Bolt threads in (N) or excluded (X) from shear plane
- d_b = Bolt diameter
- Bolt Gap
- F_{ub} = Tensile strength of bolt
- F_{exxp} = Electrode strength used for the shear plate fillet weld
- D_p = Leg size of the shear plate fillet weld
- P_w = Vertical bolt pitch

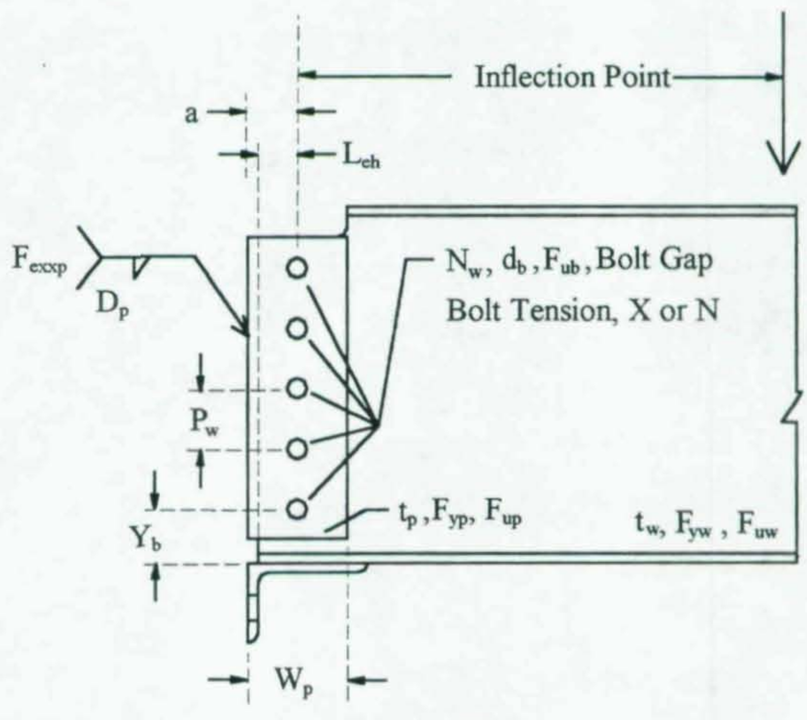

Figure 23 Web Bolt And General Connection Parameters

The yield and tensile strengths of the steel are not considered to be independent of each other. Although, there is not a constant relationship between these two values they are very much related to each other.

5.1.1.4 Seat Angle Parameters

The seat angle parameters are the connection parameters that influence the seat angle combination element behavior. These parameters are illustrated in Figure 24 and include:

- t_a = Seat angle thickness
- W_a = Seat angle width
- F_{ya} / F_{ua} = Seat angle steel yield / tensile strength
- L_{ah} = Horizontal length of the outstanding angle leg

If there is an angle gap then the following parameters must be defined

- Angle Gap Size
- L_{av} = Vertical distance between the top of the angle and the assumed point of contact between the angle and the girder web

If the angle is bolted to flange then the following parameters must be defined

- t_f = Bottom beam flange thickness
- F_{yf} / F_{uf} = Beam flange steel yield / tensile strength
- Bolt Tension either snug or fully tightened
- Bolt threads in (N) or excluded (X) from shear plane
- d_b = Bolt diameter
- Bolt Gap
- F_{ub} = Tensile strength of bolt
- N_a = Number of bolts attaching the seat angle to the beam flange
- P_a = Horizontal bolt pitch of seat angle bolts

If the angle is welded to flange then the following parameters must be defined

- F_{exxa} = Electrode strength used for the seat angle fillet weld
- D_a = Leg size of the seat angle fillet weld
- L_{w0} = Length of seat angle fillet weld that runs parallel to the beam

- L_{w90} = Length of seat angle fillet weld that runs transverse to the beam (typically equal to the width of the beam flange, b_f)

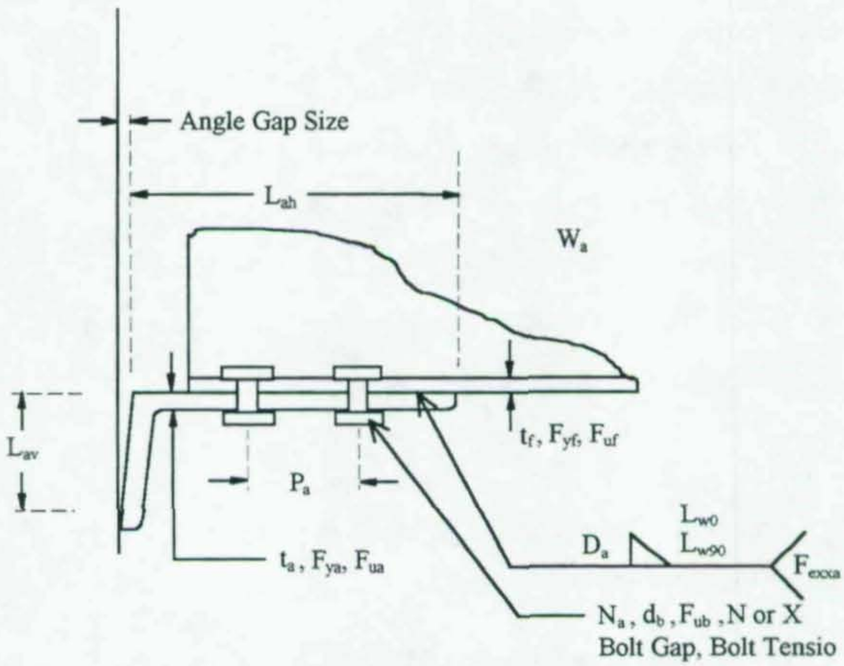

Figure 24 Seat Angle Parameters

5.1.2 Dependent Parameters

Dependent parameters are connection parameters that are derived from the independent parameters. The following dependent parameters are believed to have the most influence on the connection moment-rotation behavior.

5.1.2.1 Web Bolt Parameters

For determining the influence of the web bolts on the moment capacity and initial stiffness of the composite connection the following dependent variables need to be defined.

$$\text{Horizontal Bearing Strength of Web} = \min \left| \begin{array}{l} L_{eh}\, t_w\, F_{uw} \\ 2.4\, d_b\, t_w\, F_{uw} \end{array} \right.$$

$$\text{Horizontal Bearing Strength of Plate} = \min \begin{vmatrix} (W_p - a)\, t_p\, F_{up} \\ 2.4\, d_b\, t_p\, F_{up} \end{vmatrix}$$

Vertical Bearing Strength of Web = $2.4\ d_b\ t_w\ F_{uw}$

Vertical Bearing Strength of Plate = $2.4\ d_b\ t_p\ F_{up}$

Horizontal Net Tension Strength of Web = $(P_w - d_b)\ t_w\ F_{uw}$

Horizontal Net Tension Strength of Plate = $(P_w - d_b)\ t_p\ F_{up}$

Bolt Shear Strength = $0.6\ F_{ub}\ A_b$ (1.0 for X, 0.75 for N)

$R_f = C_1\ A_b / 5.77$

$$R_{nh} = \min \begin{vmatrix} \text{Horizontal Bearing Strength of Web} \\ \text{Horizontal Bearing Strength of Plate} \\ \text{Horizontal Net Tension Strength of Web} \\ \text{Horizontal New Tension Strength of Plate} \\ \text{Bolt Shear Strength} \end{vmatrix}$$

$$R_{nv} = \min \begin{vmatrix} \text{Vertical Bearing Strength of Web} \\ \text{Vertical Bearing Strength of Plate} \\ \text{Bolt Shear Strength} \end{vmatrix}$$

Where

C_1 = 120 for A325 bolts and 132 for A490 bolts

A_b = Area of bolt based on nominal bolt diameter

5.1.2.2 Composite Slab Parameters

For determining the influence of the composite slab on the moment capacity and initial stiffness of the composite connection the following dependent variables need to be defined. First the upper limit on the increase in moment capacity will be based on the axial load capacity of the composite slab which is expressed as the minimum of the shear stud capacity of reinforcing steel capacity.

$$R_{nslab} = \min \begin{vmatrix} A_r F_{ur} \\ N_{studs} Q_{sol} \end{vmatrix}$$

Where A_r is the area of reinforcing steel and Q_{sol} is the single stud strength determined using the rules presented in Section 4.1.1.2.

Next, to determine the influence of the composite slab on the initial stiffness of the composite connection terms that will determine the initial stiffness of the slab need defined. These terms define the first critical load deformation points of the reinforced slab behavior and shear stud behavior.

$P_{slab1} = A_{ceff} f_c + A_r F_{yr}/2$

$\delta_{slab1} = L_{eff} \varepsilon_{yr}/2$

$P_{stud1} = 0.5 N_{studs} Q_{sol}$

$\delta_{stud1} = 0.0108$

Where

f_c = Equivalent tension stiffening stress = $2.4 \dfrac{\sqrt{1000 f'_c}}{1000}$

A_{ceff} = Effective concrete area given in Section 4.1.1.1.2

L_{eff} = Elastic effective slab length given in Section 4.1.1.1.3.1

ε_{yr} = Yield strain of reinforcing steel = F_{yr}/E

5.2 Simplifying Assumptions

To limit the number of connection parameters that have to be considered in the development of a simplified method for approximating the moment-rotation behavior there are a variety of assumptions and / or simplifications made:

1. **The seat angle itself or the connection between the seat angle and the bottom flange will not fail.** To ensure this, the angle area and the connection (welds or bolts) should be designed so that angle yielding or connection failure do not occur. The load used to design these elements should be the maximum horizontal force developed by

all of the bolts in the beam web and the composite slab. This value will in general depend on the shear force that the connection must carry. However an upper bound on this value can be obtained by using a load equal to R_{nh} N_w plus R_{nslab}. To guard against over strength of the web bolts it is suggested that the load used for designing the angle and connection be 117% of the upper bound load. This percentage increase is based on the ratio of mean tensile strengths over nominal tensile strengths for A36 and A572Gr50 steels (Rex and Easterling, 1996(a)).

2. **All bolts are fully tensioned.** Fully tensioning the bolts provides an increase in the initial stiffness of the moment-rotation behavior compared to connections with snug tight bolts. This increase in the initial stiffness can have a significant impact on how much beam deflections are reduced by including connection behavior.
3. **The friction resistance will not be considered in determining the moment capacity of the connection.** Because of friction, the moment resistance of a connection can sometimes be higher in the initial stages of behavior than the final moment capacity. A single analytical expression is unable to represent this type of behavior. Consequently, it was decided that any moment resistance above the final moment capacity would be ignored in the simplified method. This can result in a somewhat conservative estimate of the moment-rotation behavior during the initial stages. However, including the increase in moment resistance resulting from friction would result in an un-conservative estimate in the later stages of the moment-rotation behavior.
4. **All bolts have 1/16-in. bolt gap.** Recall that the bolt gap represents the amount of deformation that has to occur before the plate-bolt-plate combination carries any load in bearing. For standard holes this value is somewhere between 0 and 1/8-in. The 1/16-in. bolt gap was simply assumed as an average value which is believed to be somewhat on the conservative side. Studies of the slip associated with multiple bolt connections (Kulak et al, 1987) showed that in laboratory tests slips were usually

about ½ of a hole clearance (i.e. ½ of 1/16-in.). Measured values in the field were shown to be even smaller.

5. **The weld attaching the shear plate to the girder web will not fail.** This can be ensured by following the guidelines for the design of single plate shear connections given in the AISC Manual Volume II (*Manual of*, 1993). These guidelines suggest using a weld leg equal to 75% of the shear plate thickness and using 70 ksi weld electrodes.
6. **There is no angle gap.** There are three primary reasons for this assumption. First, the cantilever beam model assumed to represent the angle flexural behavior has no real experimental or detailed analytical basis. Second, the abrupt change in angle stiffness and distance to the location of resistance (i.e. from open to closed gap and from a distance of L_{av} to 0) creates a somewhat unrealistic angle behavior. It can also result in artificially high moment resistance before the angle gap closes, particularly for very short connections. Third, angle gaps have not been reported by any other researchers working on partially restrained connections.
7. **The connection will not fail in shear.** As previously discussed, there are concerns about how valid the ultimate strength analysis (which is used to implement the component method) is when the connection fails in shear. To ensure that this possible limitation on the ultimate strength analysis is not a problem the maximum shear on the connection is limited to 75% of the basic connection shear capacity. This limitation on the applied shear was based on a brief parametric study which was previously discussed. Note that this limitation does not preclude the possibility that the applied shear will affect the moment-rotation behavior.
8. **The seat angle is welded to the beam bottom flange.** It was previously assumed that all bolts in the connection would be fully tensioned. Typically it would be very difficult to fully tension the bolts in the bottom flange during construction. In addition, because of bolt tightening clearances the number of bolts that can be used to connect

the angle to the beam flange is generally limited to an absolute maximum of six and in most cases the number of bolts would be limited to four. The limited number of bolts can severely limit the moment capacity of the connection if they are to be designed so they don't fail (as was previously assumed).

9. **Only #4 Grade 60 reinforcing steel is used.** The research on the stress-strain behavior and the average yield and tensile strengths of reinforcing steel (Rex and Easterling, 1996(a)) only considered #4 Grade 60 reinforcing bars. In addition, all experimental work involving a reinforced composite slab (conducted at VT in conjunction with the current research) used #4 Grade 60 reinforcing steel.
10. **Only strong position studs are used, there is only one stud per deck rib, and shear stud spacing is constant along beam.** Because of the severe reduction in stud strength associated with weak position studs (Rex and Easterling, 1996(b)) it is desirable to only use strong position shear studs. This usually limits the number of studs in a deck rib to one. If one strong position stud is used per deck rib then the stud spacing is most likely constant. For typical deck, the spacing would be 12-in.
11. **Only ¾-in. diameter shear studs are used.** The most commonly used shear stud diameter is ¾-in.; in addition, all experimental work involving a reinforced composite slab (conducted at VT in conjunction with the current research) used ¾-in. diameter shear studs.
12. **S_0 is at least 12-in.** This helps ensure sufficient ductility in the composite slab.
13. **The composite slab strength is always limited by the strength of the reinforcing steel.** This helps ensure sufficient ductility in the composite slab and makes economic sense. It would not make sense to use more reinforcing steel than the shear studs could carry because any additional steel would have no impact on the moment-resistance of the connection.

5.3 Parameter Relationships

The following sections develop and present methods for relating the connection parameters to the Richard Equation parameters. Relationships for M_0, K, and K_p are based on a combination of basic mechanics and assumptions about the connection behavior. Relationships for the curvature parameter "n" are based on series of parametric studies.

5.3.1 Moment Capacity, M_0

There are two simplifying assumptions made that help in developing a method for estimating M_0. First, no more than 75% of the basic connection shear strength is applied to the connection. This ensures that the connection fails in moment. Second, the seat angle and the connection between the seat angle and beam bottom flange are designed strong enough such that all other components in the connection will fail before them. This allows the connection strength to be determined without regard to the seat angle strength. In addition, it forces the center of connection rotation to be close to the seat angle.

Using these assumptions and the resulting implications a three stage method of determining the connection moment capacity has been developed. First, the shear carried by each bolt in the web is determined. Next, the remaining bolt capacity in the horizontal direction is determined for each web bolt. Finally, the connection moment is determined.

5.3.1.1 Distribution of Connection Shear To Bolts

Based on observations from the experimental connection tests and the ultimate strength analysis of the connections it is clear that the bolts closest to the center of connection rotation carry more shear than the bolts far away from the center of connection rotation. Based on the assumption about the seat angle strength it can be assumed that the center of connection rotation will be close to the bottom of the beam when the connection is near failure. Consequently, it has been assumed that the shear load carried by each bolt

(V) in the beam web will be inversely proportional to the vertical distance between the bolt and the bottom of the beam. In general for bolt j of N_w bolts this is given by:

$$V_j = \left\{ \frac{\frac{1}{Y_j}}{\sum_{i=1}^{N_w} \frac{1}{Y_i}} \right\} V_{ult} \leq R_{nv} \qquad \text{(Eq 17)}$$

Where

V_{ult} = The ultimate shear applied to the connection and

Y_j = The vertical distance from bolt j to the top of the seat angle

The upper limit of R_{nv} is imposed to ensure that the calculated shear load on the bolt does not exceed the vertical load carrying capacity of the bolt. If the calculated shear load does exceed the vertical load capacity then it is necessary to revise the vertical distances Y_j until the shear is redistributed such that no single bolt shear load exceeds the bolt vertical load capacity. This can be done by assigning an imaginary value to Y_b that is greater than the true value. By increasing the value of Y_b and using the same bolt pitch the values of Y_j for all the other bolts also increase. As Y_j for all the bolts increases the shear becomes more evenly distributed among the bolts. The final value of Y_b should be chosen such that the calculated shear for the bottom most bolt is approximately equal to R_{nv} for this bolt. This method of modifying Y_b is based on the same premise behind the ultimate strength analysis; which is, the shear load on the more heavily loaded bolts will redistribute to the less heavily loaded bolts through inelastic deformations associated with the bolts.

5.3.1.2 Determine Remaining Horizontal Capacity of Each Bolt

Once the shear load on each bolt is determined the horizontal load capacity (H) of each bolt can be determined. Based on the vertical horizontal interaction developed in Section 4.2.2.3 the remaining horizontal capacity is given by:

$$H_j = \frac{R_{nh}}{R_{nv}}\sqrt{R_{nv}^2 - V_j^2} \qquad \text{(Eq 18)}$$

5.3.1.3 Determine Connection Moment Capacity

The moment capacity (M_0) is determined by summing the products of H for each web bolt and the composite slab by the vertical distance from the bolt or slab to the top of the seat angle. This is given by:

$$M_0 = \sum_{j=1}^{N_{w+1}} H_j Y_j \qquad \text{(Eq 19)}$$

Where H_j is each of the bolt horizontal capacities for j equal 1 to N_w and H_j is the composite slab load capacity (R_{nslab}) for j equal to N_{w+1}. The inflection point when the connection attains its ultimate moment capacity is simply given by M_{ult} divided by V_{ult}.

It is important to note that the values of Y_j used to determine the moment capacity must be the real values of Y_j and not the imaginary ones used to determine the distribution of the shear load in the connection.

5.3.1.4 Comparison of Simplified Moment Capacity To Experimental Moment Capacity

The above method was used to estimate the moment capacity of each of the experimental connections. The ultimate shear applied during the test was used as V_{ult} for determining the moment capacity. The results are given in Table 5. In general, the method provided good estimates of the moment capacity.

Table 5 Comparison of Simplified Moment Capacity to Experimental Moment Capacity

Connection	M_0 (k-in)	M_{ult} (k-in)	M_0/M_{ult}
5	2618	2517	1.04
6	2388	2517	0.95
7	1486	1429	1.04
8	1413	1429	0.99
		Average	1.00
		COV	0.04

In addition to comparing M_0 to the moment capacity of the experimental connections it was also compared to the moment capacity determined by the component method. As will be described later, a parameter analysis was used to determine the relationship between connection parameters and the curvature parameter in the Richard Equation. A comparison between the moment capacity determined using the component method and M_0 determined as outlined above was made for 971 of the connections included in the parameter analysis. The ratio of M_0 over the moment capacity determined by the component method was considered. The average for the 971 connections was 1.03 with a COV of 2.9%. The minimum ratio was 0.95 and the maximum ratio was 1.11. All of the connections considered did not fail in shear.

5.3.2 Initial Stiffness, K

The initial stiffness of the connection (K) can be approximated by an elastic combination of the major connection element initial stiffness values. For the composite connection these are the composite slab, seat angle, and each of the web bolts.

The initial stiffness of the composite slab behavior can be approximated by determining the first critical point in the composite slab load deformation behavior and assuming that the behavior up to this point is essentially linear. Previously four dependent parameters were presented which defined the first critical load-deformation points for the reinforced slab and shear stud behaviors. Using these values the initial stiffness of the slab can be approximated. If $P_{slab1} < P_{stud1}$ then:

$$K_{islab} = \frac{P_{slab1}}{\delta_{slab1} - \dfrac{\ln\left\{1 - \left(\dfrac{P_{slab1}}{Q_{sol}}\right)^{2.5}\right\}}{18}}$$

Otherwise:

$$K_{islab} = \frac{P_{stud1}}{0.0108 + \delta_{slab1}\dfrac{P_{stud1}}{P_{slab1}}}$$

If there is no seat angle gap then the initial stiffness of the seat angle can be approximated by the initial stiffness of the welds or bolts that are used to attach the seat angle to the bottom flange. If the seat angle is welded then the initial stiffness is given by

$$K_{ia} = F_{exxa}\,(20.9\,L_{w0} + 106.6\,L_{w90}) \qquad \text{(Eq 20)}$$

If the seat angle is bolted then the initial stiffness is given by

$$K_{ia} = N_a\,R_f / 0.015 \qquad \text{(Eq 21)}$$

The weld stiffness is derived from the weld load-deformation model given in the AISC Specification (*Load and*, 1993) with the exception that f(p) is assumed to be 8.234 Δ/Δ_{max} as given in the original paper by Lesik and Kennedy (1990). The bolt stiffness is based on the frictional stiffness model developed by Rex and Easterling (1996(d)) with the exception that the slipping deformation Δ_s is assumed to be 0.015-in. rather than the average value of 0.0075-in. determined from single bolt lap plate connection tests. This assumes some initial bolt gap. The initial stiffness of the web bolts is given by a similar equation.

$$K_{iw} = R_f / 0.015 \qquad \text{(Eq 22)}$$

Because the initial stiffness of each of the elements is essentially elastic an elastic combination of the element stiffness is appropriate. This can be expressed in equation form as:

$$K = \sum_{j=0}^{N_w} K_j \left(h + Y_j\right)^2 \qquad \text{(Eq 23)}$$

Where h is the elastic center of rotation given by:

$$h = -\frac{\sum_{j=0}^{N_w} K_j Y_j}{\sum_{j=0}^{N_w} K_j} \qquad \text{(Eq 24)}$$

K_j and Y_j are the estimated initial stiffness and location of each of the major connection elements.

5.3.3 Final Stiffness, K_p

When the connection is near the ultimate moment strength the center of rotation is assumed to be near the top of the seat angle. With this assumption the final stiffness of the connection near ultimate can be determined by the sum of the products of the web bolt final stiffness values by the square to the distance from the bolt to the seat angle.

$$K_p = \sum_{j=1}^{N_{w+1}} K_{pj} Y_j^2 \qquad \text{(Eq 25)}$$

Where K_{pj} is the bolt plastic stiffness (K_{pb}) for j from 1 to N_w and is K_{pslab} for j equal to N_{w+1}.

Rex and Easterling (1996(d)) determined plastic stiffness of single bolt lap plate connections. A modified version of that expression is used here to estimate the plastic stiffness of the web bolts.

$$K_{pb} = 9\left\{\frac{\min\left|\begin{array}{c}\text{Plate or Web Horizontal Net Tension Strength}\\ \text{Plate or Web Horizontal Bearing Strength}\end{array}\right|}{\text{Bolt Shear Strength}}\right\}^{2.9} \quad \text{(Eq 26)}$$

Rex and Easterling (1996(b)) developed a method for estimating the plastic stiffness of a reinforced composite slab. The estimate depends on whether the composite slab strength is limited by the reinforcing steel or the shear studs. If the reinforcing steel limits the strength then:

$$K_{pslab} = 150\ A_r / S_0 \quad \text{(Eq 27)}$$

Otherwise:

$$K_{pslab} = 0.12\ N_{studs}\ Q_{sol} \quad \text{(Eq 28)}$$

5.3.4 Curvature Parameter, n

A parameter analysis was used to determine a relationship between the connection parameters and the curvature parameter in the Richard Equation. Rex and Easterling (1996(e)) previously determined that for bare steel connections with low shear ratios the curvature parameter could be approximated by:

$$n = (1.67\ \Psi_1^2 - 0.71\ \Psi_1 + 0.72)\ \alpha_1 \quad \text{(Eq 29)}$$

Where:

$\Psi_1 = R_f / R_{nh}$

α_1 = Correction factor accounting for number and spacing of bolts

$\alpha_1 = 1 + 0.0327\ P_w\ \beta_1\ \beta_2$

$\beta_1 = 0.35\ e^{2.09\Psi_1}$

$\beta_2 = 1.2 - 2.27 / N_w$

In addition, it was determined that all the variations in the web bolt parameters could be satisfactorily represented by Ψ_1. A group of 11 basic connections (presented in Table 6) which had varying values of Ψ_1 were assumed to adequately represent all the web bolt parameters.

Table 6 Resulting 11 Basic Web Bolt Parameter Combinations

Combination Number	t_w (in.)	F_{yw} / F_{uw} (ksi)	L_{eh} (in.)	t_p (in.)	Bolt Threads N or X	d_b (in.)	F_{ub} (ksi) (ksi)	P_w (in.)	Ψ_1
1	0.25	35 / 49	0.9375	0.25	N	0.75	120	2.0625	0.29
2	0.3125	35 / 49	0.9375	0.25	N	0.75	120	2.0625	0.40
3	0.375	35 / 49	0.9375	0.25	N	0.75	120	2.0625	0.44
4	0.5	35 / 49	0.9375	0.25	N	0.75	120	2.0625	0.50
5	0.5	35 / 49	0.9375	0.25	N	0.75	120	2.625	0.53
6	0.3125	50 / 70	1.875	0.5	N	0.75	120	2.625	0.64
7	0.25	35 / 49	1.875	0.75	N	0.75	120	2.25	0.80
8	0.25	35 / 49	1.09375	0.75	X	0.875	120	2.625	0.84
9	0.25	35 / 49	1.25	0.25	X	1	120	2.75	0.93
10	0.25	35 / 49	1.25	0.75	N	1	150	3	1.07
11	0.25	35 / 49	2.5	0.75	N	1	150	2.75	1.17

It was decided that, rather than develop all new parametric relationships between the composite connection parameters and the curvature parameter, correction factors which would modify the value of the curvature parameter based on Equation 29 would be developed instead. These correction factors were developed based on the results of a three stage parameter study. The first stage considered the effect of varying levels of composite slab strength with low values of the connection shear ratios (Ψ_2). The second stage considered the effect of varying Y_r with low values of Ψ_2. The third stage considered the effect of varying Ψ_2 from low values to values that would cause shear failure in the connection.

During each stage of the analysis the parameter combinations were analyzed using the component method computer program previously discussed. The program was modified to determine the best "n" value for each parameter combination. The best "n" value was determined using the following steps:

- The moment-rotation behavior for the given parameter combination was determined using the component method.

- M_0, K, and K_p were determined using the methods presented above.
- The first 20 mrad of the moment-rotation behavior was analyzed to determine the value of "n" which would minimize the L_2 Norm error between the Richard Equation and the moment-rotation behavior.
- The final values of M_0, K, K_p, and n were recorded along with a number of other dependent parameter values and the mode of connection failure.

The parameter combinations and the results were then entered into a database for analyzing.

5.3.4.1 Parameters With Constant Values

Based on the previously stated assumptions some of the connection parameters were constant values or were directly proportional to some value for all the parameter combinations considered in the parametric analysis. These included:

- F_{exxa}, F_{exxp} = 70 ksi
- $D_p = 0.75\ t_p$
- D_a = Designed to resist 1.17 ($R_{nh}\ N_w + R_{nslab}$)
- t_a = Designed to resist 1.17 ($R_{nh}\ N_w + R_{nslab}$)
- Bolts Fully Tensioned
- Bolt Gap = 1/16-in.
- Angle Gap = 0-in.
- Angle welded to beam
- d_{stud} = ¾-in.
- S_0 = 12-in.
- S_{stud} = 12-in.
- $N_r = 1$
- d_{bar} = 0.5-in.
- F_{yr} / F_{ur} = 71 / 111 ksi

In addition, it was decided that values of some parameters would have little influence on the connection behavior if they were varied within acceptable limits; consequently, they were also held constant for all the parameter combinations considered in the parametric analysis. These included:

- $F_{yp} / F_{up} = 45 / 63$ ksi
- $F_{ya} / F_{ua} = 45 / 63$ ksi
- $L_{w0} = 12$ in.
- $L_{w90} = 8$ in.
- $L_{ah} = 6$ in.
- $W_p = 5$-in.
- $W_a = 8$-in.
- a Distance = $W_p - 2\ d_b$
- $Y_b = 2$-in.
- $f'c = 4$ ksi
- $w_c = 150$ pcf
- $Y_{con} = 4.5$-in.
- $S_{bar} = 6$-in.
- $H_s = 3$-in.
- $h_r = 2$-in.
- $w_r = 6$-in.

5.3.4.2 Stage 1 Effect of Varying Composite Slab Strength

In Stage 1 of the parametric analysis N_w, Ψ_1, Ψ_3, and Ψ_4 were varied to develop a relationship between the curvature parameter given by Equation 29 (developed for bare steel connections) and the best value of the curvature parameter for the composite connection. Where:

$$\Psi_3 = \frac{N_{studs}\, Q_{sol}}{N_w\, R_{nh}}$$

$$\Psi_4 = \frac{A_r\, F_{ur}}{N_w\, R_{nh}}$$

Two groups of parameter combinations were considered. In the first group, values of N_w included 2, 3, 4, 6, 8, and 10. Ψ_1 was varied by including each of the 11 basic connections previously presented in Table 6. Six different combinations of Ψ_3 and Ψ_4 were used. Ψ_3 was varied from 0.5 to 1.5 in increments of 0.5. Ψ_4 was varied from 0.5 to Ψ_3 for each value of Ψ_3 in increments of 0.5. The cross-combination of each set of parameters resulted in 396 total combinations. In the second group, N_w was fixed at 5. The two extreme values of Ψ_1 were considered by using connections #1 and #11 of the basic connections presented in Table 6. One-hundred and twenty combinations of Ψ_3 and Ψ_4 were used. Ψ_4 was varied from 0.1 to 1.5 in increments of 0.1. Ψ_3 was varied from Ψ_4 to 1.5 for each value of Ψ_4 in increments of 0.1. These sets of parameters resulted in 240 total combinations. For both groups, Y_r was fixed at a value of 3-in. plus $N_w\, P_w$ and the inflection point was chosen sufficiently far from the connection to ensure that the value of Ψ_2 would be low. Based on the results of these two groups of combinations a correction factor for Equation 29 was developed:

$$\alpha_3 = \beta_4 - \beta_5\, \Psi_1 \qquad \text{(Eq 30)}$$

Where:

α_3 = Correction factor accounting for the composite slab

$\beta_4 = (-0.82 - 0.27\, \Psi_3)\, \Psi_4^2 + (0.9 + 0.75\, \Psi_3)\, \Psi_4 + 1.25$

$\beta_5 = (-0.93 - 0.15\, \Psi_3)\, \Psi_4^2 + (1.21 + 0.53\, \Psi_3)\, \Psi_4 + 0.51$

5.3.4.3 Stage 2 Effect of Varying Y_r

In Stage 2 of the parametric analysis Ψ_1, Ψ_3, Ψ_4, and Y_r were varied to determine if Y_r had any effect on the value of the curvature parameter. N_w was fixed at 5. The two extreme values of Ψ_1 were considered by using connections #1 and #11 of the basic connections presented in Table 6 with the exception that a 3-in. bolt pitch was used rather than the bolt pitch given in Table 6. Three different values of Ψ_3 were considered: 0.5, 1, and 1.5. Ψ_4 was equal to Ψ_3 for each value of Ψ_3. Finally, Y_r was varied from 19-in. to 23-in. An inflection point was chosen sufficiently far from the connection to ensure that the value of Ψ_2 would be low. The cross-combination of each set of parameters resulted in 30 total combinations. The results of these combinations showed that Y_r had a negligible influence on the value of the curvature parameter.

5.3.4.4 Stage 3 Effect of Varying Shear Ratio

In Stage 3 of the parametric analysis N_w, Ψ_1, Ψ_2, Ψ_3, and Ψ_4, were varied to determine the effect of Ψ_2 on the value of the curvature parameter. Y_r was fixed at a value of 3-in. plus $N_w P_w$. Values of N_w included 2, 5 and 10. Ψ_1 was varied by including each of the 11 basic connections previously presented in Table 6. Ψ_2 was varied by changing the inflection point from 0.02 Y_r to 3 Y_r in 10 increasing steps. Three different combinations of Ψ_3 and Ψ_4 were used. Ψ_3 was varied from 0.5 to 1.5 in increments of 1.5. Ψ_4 was varied from 0.5 to Ψ_3 for each value of Ψ_3 in increments of 1.5. The cross-combination of each set of parameters resulted in 990 total combinations. Based on the results of these combinations a correction factor for Equation 29 was developed:

$$\alpha_4 = \frac{\Psi_2^{0.022}\ \Psi_3^{0.003}\ \Psi_4^{0.232}}{N_w^{\ 0.02}\ \Psi_1^{0.217}} \qquad \text{(Eq 31)}$$

Where:

α_4 = Correction factor accounting for shear ratio

For $\Psi_2 < 0.3$, α_4 should be taken as 1.0

5.4 Evaluation of Parameter Relationships

The parameter relations developed in the previous section were used to estimate the moment-rotation behavior of the experimental connections that had fully tensioned bolts. The simplified estimate is plotted on the moment-rotation plots included in each connection data pack. Review of these figures will shows that the method provided a conservative estimate of the behavior up to around 30 mrad. Beyond this rotation, the estimate typically became unconservative. The estimate is initially conservative because the parameter equations were developed assuming a 1/16-in. bolt gap. It is believed that the bolt gaps for the experimental tests were much smaller than this value. The estimate becomes unconservative in the later stages because the value of n was calibrated for rotations up 20 mrad. If approximations of the moment-rotation behavior are required beyond 20 mrad then the value of n should be increased and the plastic slope should be assumed as zero.

When the simplified method is compared to component model results that are consistent with the assumptions made in the development of the simplified method there is generally good correlation between the two. To illustrate this point the component model and simplified method were used to determine the moment-rotation behavior for four different connections which had a wide range of connection parameters. The resulting moment-rotation approximations are shown in Figure 25. There is generally good agreement between the component model and simplified method.

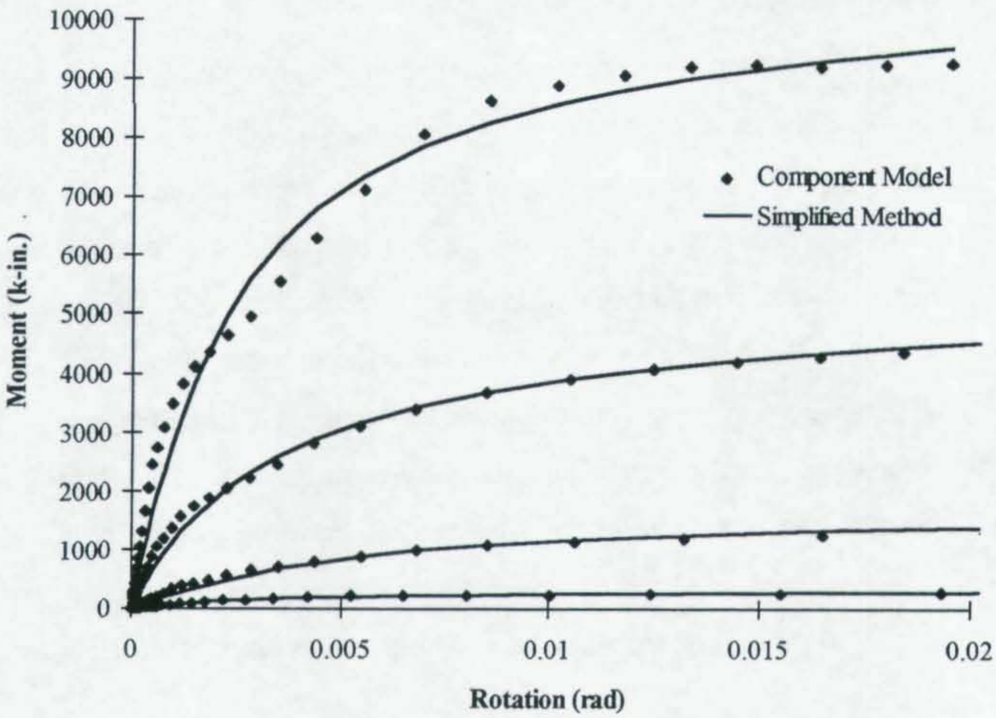

Figure 25 Comparison of Component and Simplified Model

6. Summary, Conclusions, and Recommendations

6.1 Summary and Conclusions

First, the overall moment-rotation behaviors of the connections that were pre-loaded are stiffer than the those for the connections that were not pre-loaded.

Second, there is no effect of pre-load on the initial behavior before slab cracking.

In general, the connections which were pre-loaded had higher rotational capacities than the connections which were not pre-loaded.

Based on this observation it appears that it would be conservative to use the composite connection behavior determined without consideration of the steel connection pre-load.

6.2 Recommendations

The above effective length has only been proven to work for experimental tests in which the length of the slab in tension was constant from the beginning to the end of the test. An analytical study showing what effect the changing inflection point has on the slab behavior and consequently the connection behavior should be conducted.

Because the inflection point will generally move closer to the beam end as the connection softens the length of the slab in tension will also change. The above effective length has only been proven to work for experimental tests in which the length of the slab in tension was constant from the beginning to the end of the test. An analytical study showing what effect the changing inflection point has on the slab behavior and consequently the connection behavior should be conducted.

ACKNOWLEDGEMENTS

The writers would like to thank **steel deck supplier** for donating the deck used for the connection tests.

REFERENCES

Collins, M. P. and Mitchell, D. (1991). *Prestressed Concrete Structures*, Prentice Hall, 142-154.

Eurocode 3: Design of Steel Structures, Part 1.1 Revised Annex J Joints and Building Frames (1994) Commission of The European Communities.

Fisher, J. W., Galambos, T. V., Kulak, G. L., and Ravindra, M. K. (1978) "Load and Resistance Factor Design Criteria For Connectors," *Journal of Structural Division*, **104**(ST9), 1427-1441.

Karsu, B. (1995) "The Load Deformation Response of Single Bolt Connections," M. S. Thesis Virginia Polytechnic Institute and State University.

Kulak, G. L., Fisher, J. W., and Struik, J. H. A. (1987). *Guide to Design For Bolted and Riveted Joints*, 2nd Edition, John Wiley & Sons, New York, NY, 1987.

Lesik, D. F. and Kennedy, D. J. L. (1990). "Ultimate Strength of Fillet Welded Connections Loaded in Plane," *Canadian Journal of Civil Engineering*, **17**(1), 55-67.

Load and Resistance Factor Design Specification for Structural Steel Buildings (1986). American Institute of Steel Construction, Chicago, Illinois.

Load and Resistance Factor Design Specification for Structural Steel Buildings, (1993). American Institute of Steel Construction, Chicago, Illinois.

Manual of Steel Construction Volume I and II Load and Resistance Factor Design (1993). American Institute of Steel Construction, Chicago, Illinois.

Miazga, G. S. and Kennedy, D. J. L. (1989). "Behavior of Fillet Welds As A Function Of The Angle Of Loading," *Canadian Journal of Civil Engineering*, **16**(), 583-599.

Ollgaard, J. G., Slutter, R. G., and Fisher, J. W. (1971). "Shear Strength of Stud Connectors in Lightweight and Normal Weight Concrete." *AISC Engineering Journal*, **8**(2), 55-64.

Rex, C. O. and Easterling, W. S. (1996(a)). "Behavior and Modeling of Mild and Reinforcing Steel," Report CE/VPI-ST 96/12, Virginia Polytechnic Institute and State University, Blacksburg, VA.

Rex, C. O. and Easterling, W. S. (1996(b)). "Behavior and Modeling of a Reinforced Composite Slab as Part of a Partially Restrained Composite Beam-Girder Connection," Report CE/VPI-ST 96/13, Virginia Polytechnic Institute and State University, Blacksburg, VA.

Rex, C. O. and Easterling, W. S. (1996(c)). "Behavior and Modeling Of A Single Plate Bearing On A Single Bolt," Report CE/VPI-ST 96/14, Virginia Polytechnic Institute and State University, Blacksburg, VA.

Rex, C. O. and Easterling, W. S. (1996(d)). "Behavior and Modeling of Single Bolt Lap Plate Connections," Report CE/VPI-ST 96/15, Virginia Polytechnic Institute and State University, Blacksburg, VA.

Rex, C. O. and Easterling, W. S. (1996(e)). "Behavior and Modeling of Partially Restrained Steel Beam-Girder Connections," Report CE/VPI-ST 96/16, Virginia Polytechnic Institute and State University, Blacksburg, VA.

Rex, C.O. (1994). "Behavior of Composite Semi-Rigid Beam-to-Girder Connections," Master Thesis, Virginia Polytechnic Institute and State University, Blacksburg, VA.

Salmon, C. G. and Johnson, J. E. (1990). *Steel Structures: Design and Behavior*, Third Edition, Harper and Row, New York.

Sarkar, D. and Wallace, B. (1992). *Design of Single Plate Framing Connections*, Report No. FSEL/AISC 92-01, Fears Structural Engineering Laboratory, University of Oklahoma.

Specification for Structural Steel Buildings Allowable Stress Design and Plastic Design (1989). American Institute of Steel Construction, Chicago, Illinois.

Wallaert, J. J. and Fisher, J. W. (1965). "The Shear Strength of High-Strength Bolts," *Journal of the Structural Division*, **91**(ST3), 99-125.

Zandonini, R. (1989). "Semi-Rigid Composite Joints," Strength and Stability Series, Vol. 8, *Connections*, ed. R. Narayanan, Elsevier, London, 63-120.

Appendix A

Material Properties

Steel Properties

Coupon	Average Thickness / Diameter (in.)	% Elongation (in./in.)	**Yield** Stress 2% Offset (ksi)	Average (ksi)	**Ultimate** Stress (ksi)	Average (ksi)
BW-1	0.290	25%	56.9	55.6	75.0	74.4
BW-2	0.291	24%	54.2		73.7	
BF-1	0.435	25%	53.5	54.3	72.9	73.2
BF-2	0.427	21%	55.0		73.5	
GW-1	0.397	29%	40.4	41.0	69.4	69.8
GW-2	0.397	28%	41.6		70.1	
GF-1	0.455	27%	39.7	41.3	67.4	67.7
GF-2	0.460	27%	42.8		68.0	
A-1	0.504	29%	43.5	43.5	68.8	68.8
A-2	0.506	30%	43.5		68.7	
P57-1	0.247	29%	46.4	46.3	65.4	65.4
P57-2	0.245	29%	46.2		65.4	
P58-1	0.371	29%	44.9	45.0	67.0	67.0
P58-2	0.371	28%	45.0		67.0	
1-1	0.342	0.26	60.8	58.8	90.1	88.0
1-2	0.331	*	56.8		86.0	
2-1	0.351	0.268	56.3	56.8	85.6	86.2
2-2	0.348	*	57.3		86.7	
3-1	0.349	0.25	56.6	57.2	86.4	86.4
3-2	0.351	0.257	57.8		86.5	
4-1	0.350	*	57.7	57.8	86.8	86.7
4-2	0.348	0.25	57.8		86.7	
5-1	0.346	0.27	58.6	58.9	88.3	88.5
5-2	0.347	0.28	59.3		88.8	
6-1	0.348	0.25	58.4	58.2	88.0	88.4
6-2	0.346	0.26	58.0		88.7	
7-1	0.347	0.26	59.4	58.5	88.2	87.9
7-2	0.347	0.28	57.7		87.6	
8-1	0.346	0.26	58.4	58.3	88.6	88.2
8-2	0.348	0.26	58.2		87.8	
9-1	0.350	0.26	58.3	57.8	87.3	87.2
9-2	0.349	0.26	57.4		87.1	
10-1	0.348	0.29	58.6	58.3	87.3	86.9
10-2	0.350	0.28	58.1		86.6	
11-1	0.350	0.3	57.6	57.0	86.3	86.1
11-2	0.347	*	56.4		85.8	
12-1	0.345	0.29	57.9	57.7	87.8	87.0
12-2	0.351	0.27	57.4		86.3	

* Specimen broke outside of marked gage.

Concrete Properties

Coupon	Diameter (in.)	Ultimate Stress (ksi)	Average (ksi)
5 & 6 Cylinder 1	4	5.1	5.2
5 & 6 Cylinder 2	4	5.1	
5 & 6 Cylinder 3	4	5.1	
5 & 6 Cylinder 4	4	5.3	
5 & 6 Cylinder 5	4	5.3	
7 & 8 Cylinder 1	4	5.3	5.1
7 & 8 Cylinder 2	4	5.3	
7 & 8 Cylinder 3	4	5.1	
7 & 8 Cylinder 4	4	4.8	
7 & 8 Cylinder 5	4	5.3	

Steel & Concrete Specimen Notation

Coupon	Description	Specimen	Notes
BW	Filler Beam Web	Flat	
BF	Filler Beam Flange	Flat	
GW	Girder Web	Flat	
GF	Girder Flange	Flat	
A	Seat Angle	Flat	
P57	1/4-in. Shear Plate	Flat	
P58	3/8-in. Shear Plate	Flat	
1-1 to 12-2	Reinforcing Steel	Round	Bars were milled down to the diameter indicated.
5 & 6 Cylinder 1 - 5	Concrete For Connection Tests 5 & 6	Round	All cylinders were tested within one or two days of connection
7 & 8 Cylinder 1 - 5	Concrete For Connection Tests 7 & 8	Round	All cylinders were tested within one or two days of connection

00893

Appendix B

Experimental Data Packs

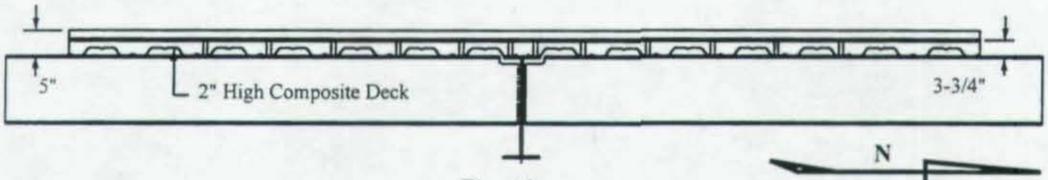

Elevation

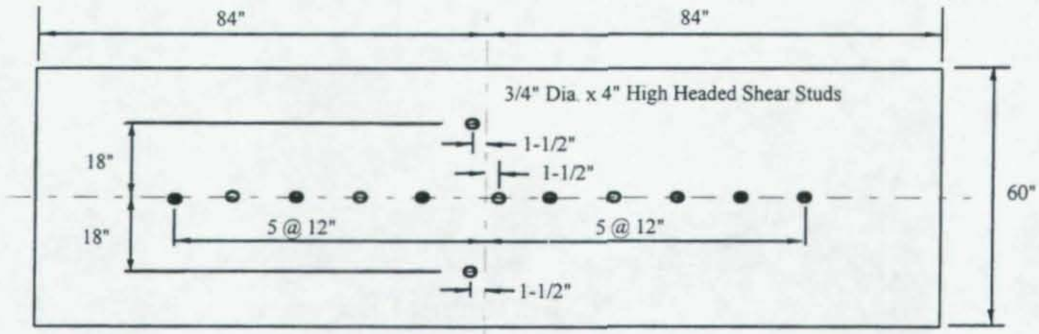

Shear Stud Layout

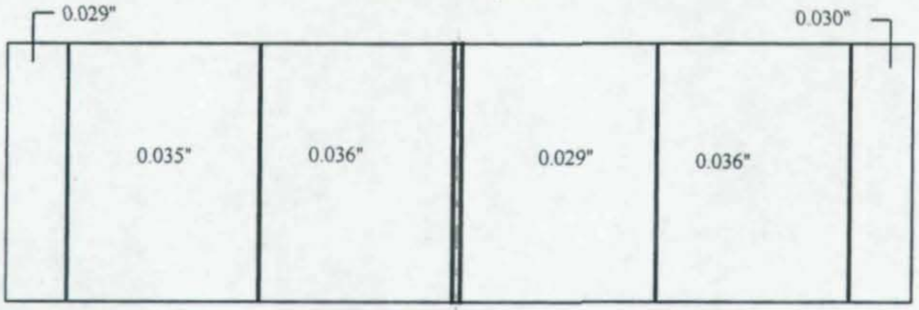

Deck Layout & Thickness

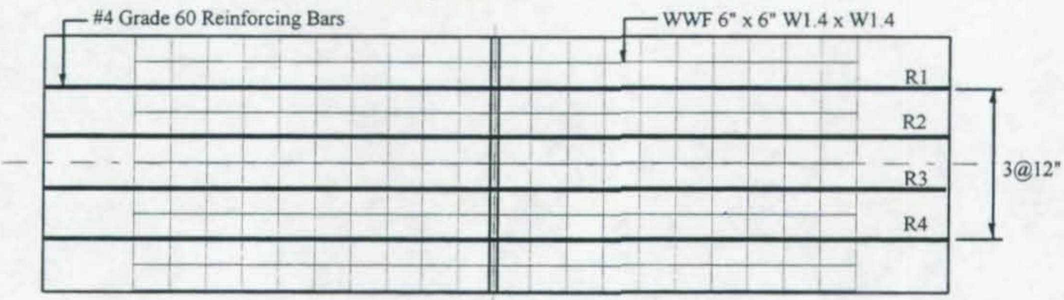

Reinforcing Identification & Layout

Reinforced Composite Deck Information

00894

Description of Instrumentation

Channel	Sense of Extension	Description of Measurement	Load Stage	Gage Type	Sensitivity	Full Scale
0	Compression (-)	North Load Ram	Dead	Load Cell	0.7135	20,000 lbs
1	Compression (-)	South Load Ram	Dead	Load Cell	0.731	20,000 lbs
0	Compression (-)	North Load Ram	Live	Load Cell	1.99	500 kips
1	Compression (-)	South Load Ram	Live	Load Cell	1.95	500 kips
80	-**	Connection Rotation	Dead/Live	POT		6"
83	-**	Connection Rotation	Dead/Live	POT		6"
84	-**	Connection Rotation	Dead/Live	POT		6"
85	-**	Connection Rotation	Dead/Live	POT		6"
86	-**	Connection Rotation	Dead/Live	POT		6"
87	-**	Connection Rotation	Dead/Live	POT		6"
88	-**	Connection Rotation	Dead/Live	POT		6"
89	-**	Connection Rotation	Dead/Live	POT		6"
90	-**	Stud Slip	Live	POT		6"
91	-**	Stud Slip	Live	POT		6"
92	-**	Stud Slip	Live	POT		6"
93	-**	Stud Slip	Live	POT		6"
94	-**	Stud Slip	Live	POT		6"
95	-**	Stud Slip	Live	POT		6"
96	-**	Stud Slip	Live	POT		6"
97	-**	Stud Slip	Live	POT		6"
98	-**	Stud Slip	Live	POT		6"
99	-**	Stud Slip	Live	POT		6"
104	-**	Girder Deflection	Live	DCDT 7	0.95	20"
105	+	Girder Deflection	Live	DCDT 8	0.949	10"
106	+	Girder Deflection	Live	DCDT 11	0.943	10"
107	+	Filler Beam Deflection	Dead/Live	DCDT 9	0.942	20"
108	+	Filler Beam Deflection	Dead/Live	DCDT 4	0.948	20"
DG1	-**	Connection Rotation	Live	Dial Gage		1"
DG2	-**	Connection Rotation	Live	Dial Gage		1"
DG3	-**	Connection Rotation	Live	Dial Gage		1"
DG4	-**	Connection Rotation	Live	Dial Gage		1"

** All data has been modified so that (+) readings indicate extension.

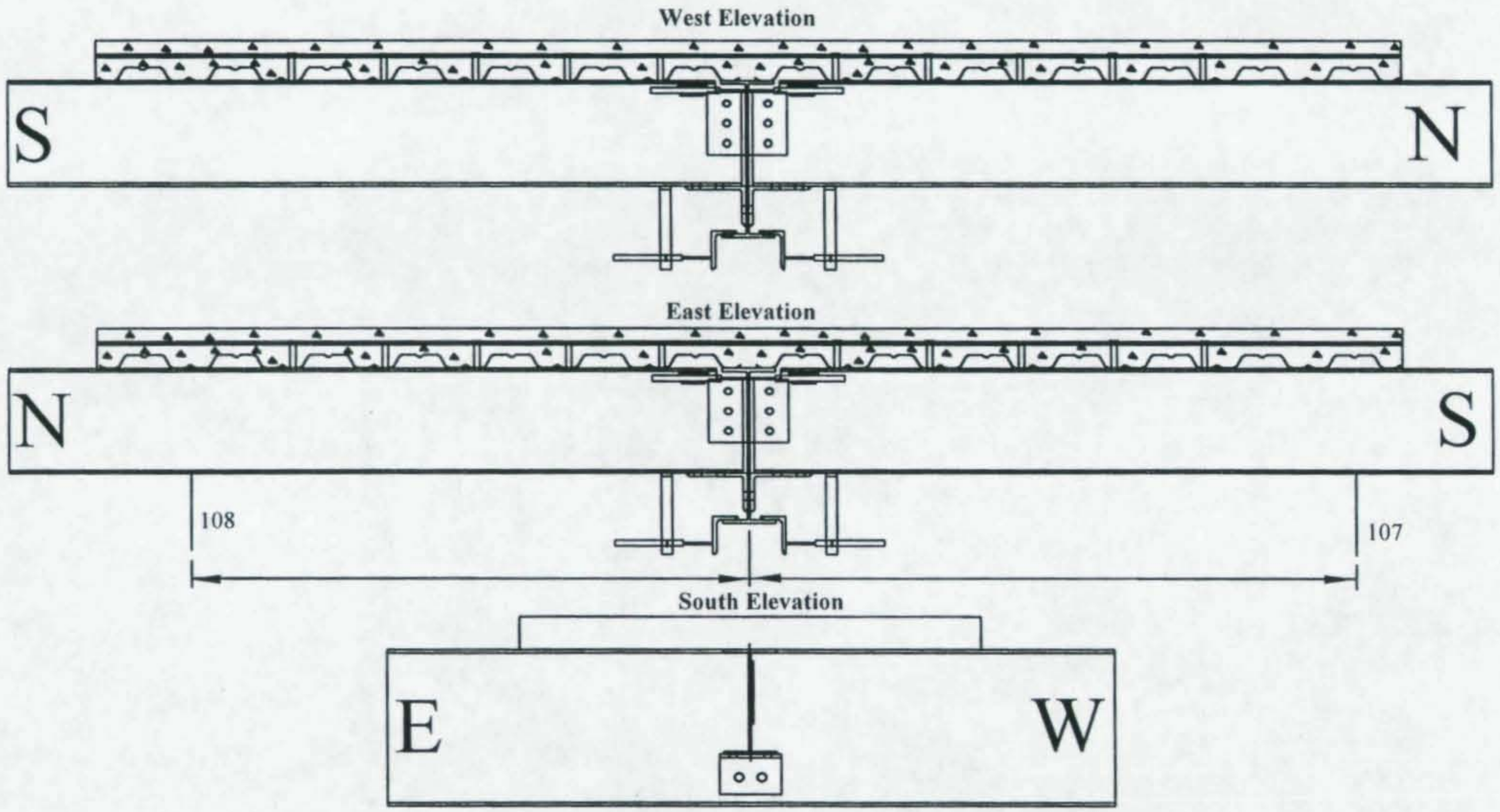

Stud Slip & Beam Deflection Instrumentation Dead Loading Stage

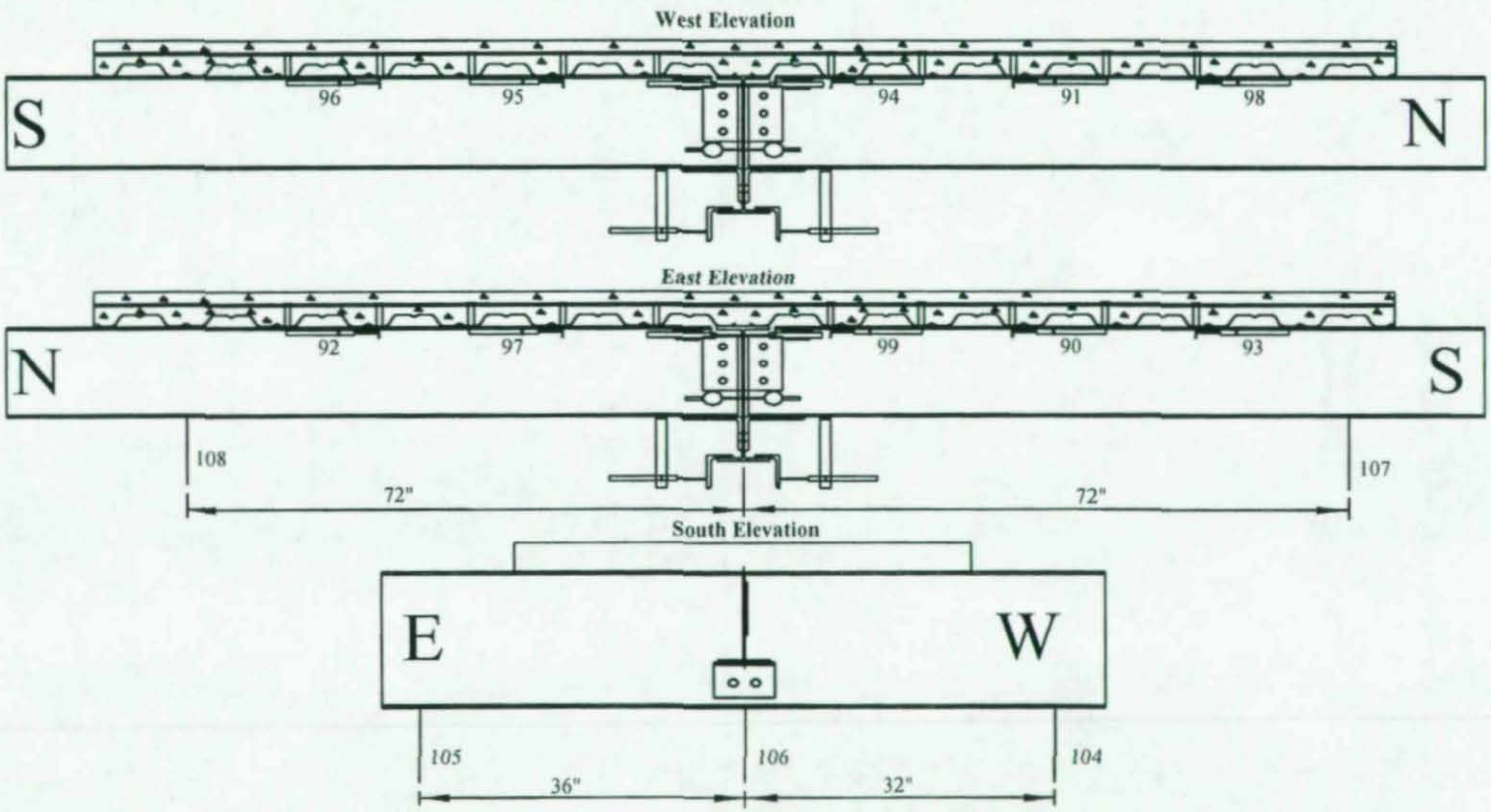

Stud Slip & Beam Deflection Instrumentation Live Loading Stage

West Elevation

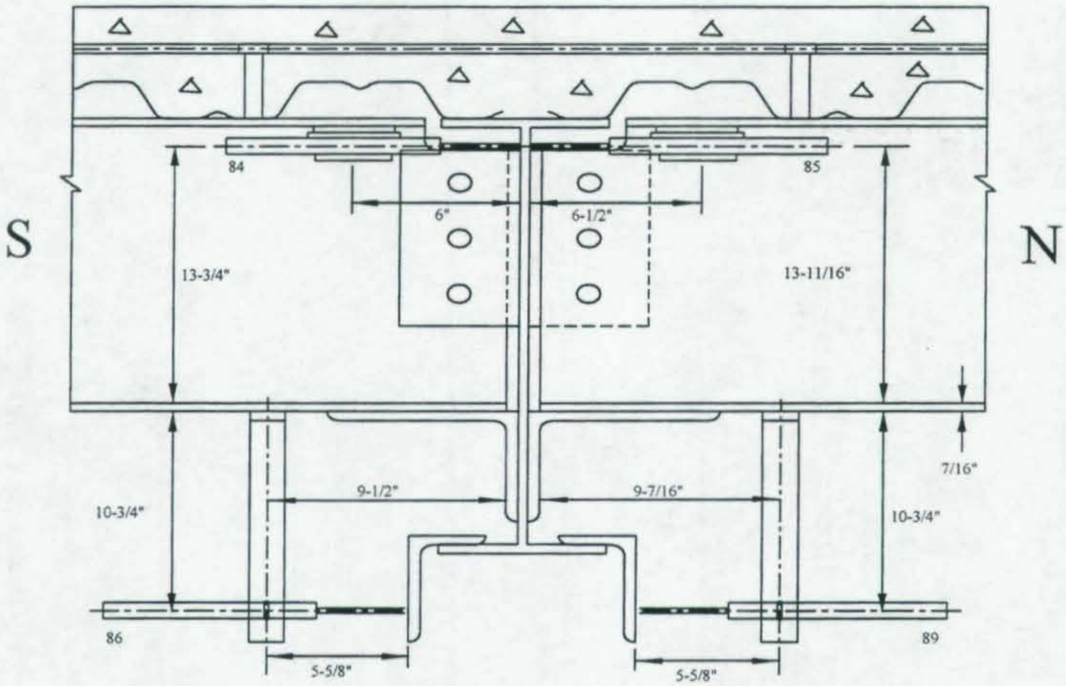

East Elevation

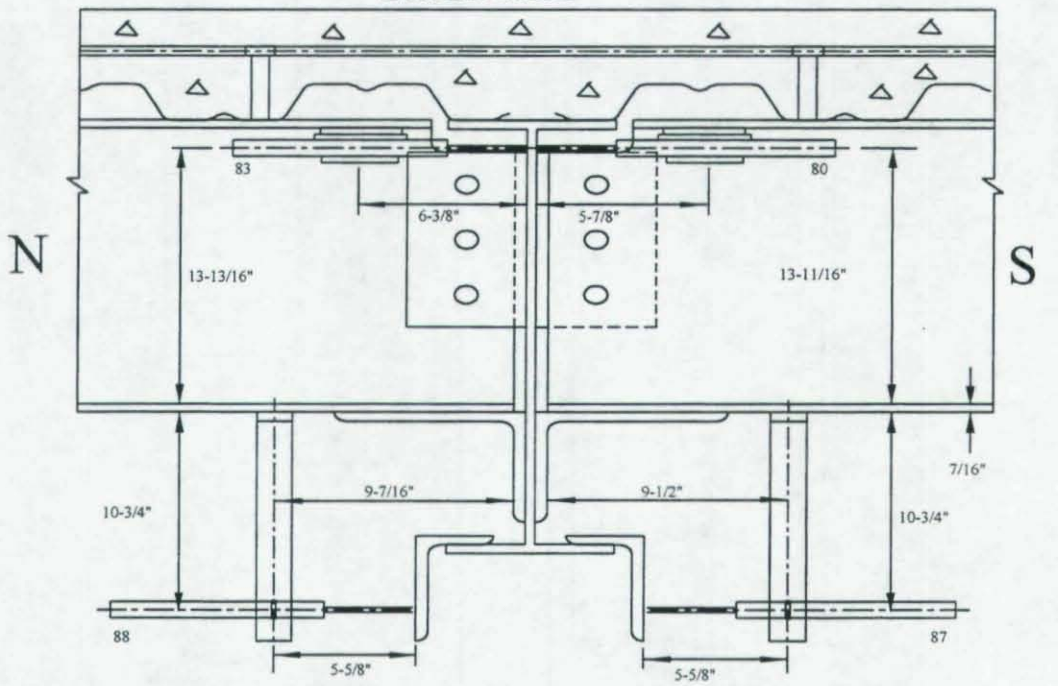

Rotation Instrumentation Dead Loading Stage

West Elevation

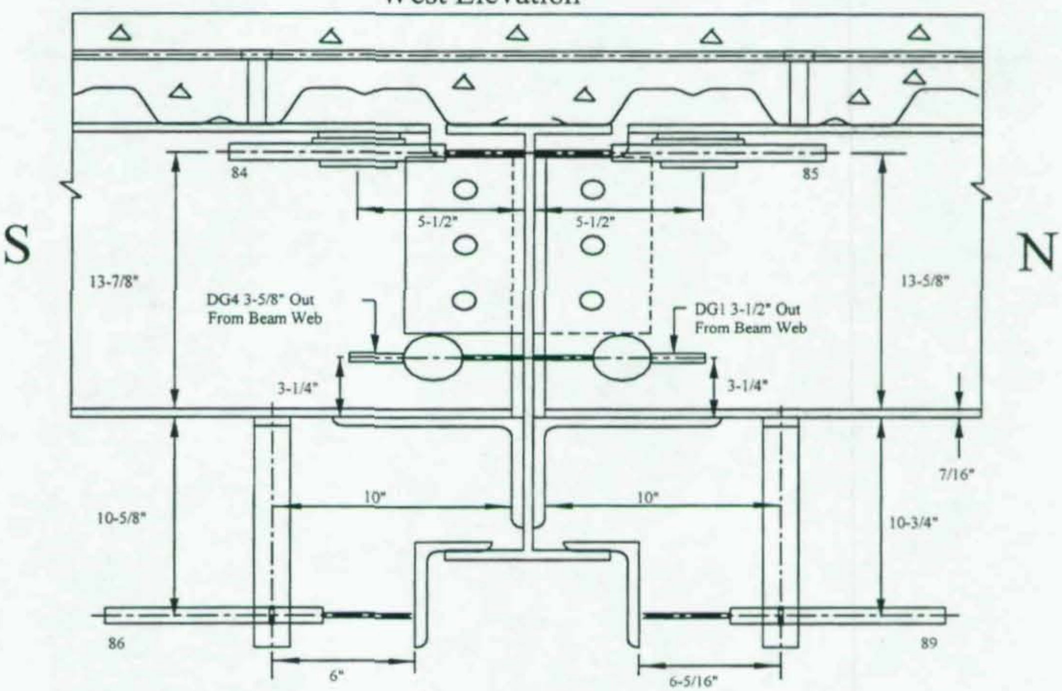

East Elevation

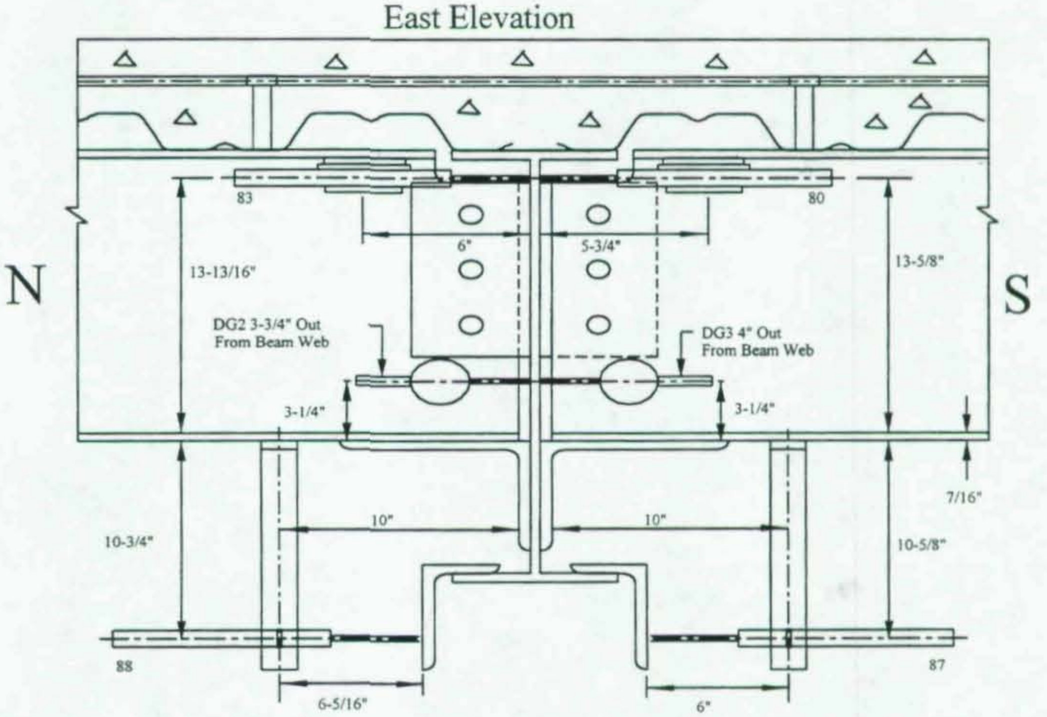

Rotation Instrumentation Live Loading Stage

Raw Data

Load Stage	Channel Data Point	0 (lbs)	1 (lbs)	80 (in.)	83 (in.)	84 (in.)	85 (in.)	86 (in.)	87 (in.)	88 (in.)	89 (in.)
Dead	1	-14	-14	0.003	-0.002	0.001	0.005	-0.008	-0.009	-0.007	-0.007
	2	196	178	0.004	-0.002	0.001	0.005	-0.006	-0.007	-0.009	-0.010
	3	1191	1190	0.007	0.001	0.003	0.008	-0.011	-0.012	-0.012	-0.013
	4	2130	2107	0.009	0.002	0.004	0.011	-0.013	-0.015	-0.019	-0.019
	5	4359	4405	0.019	0.007	0.011	0.021	-0.024	-0.025	-0.028	-0.028
	6	5144	5062	0.023	0.010	0.013	0.024	-0.027	-0.027	-0.033	-0.034
	7	6153	6115	0.030	0.015	0.020	0.031	-0.034	-0.033	-0.039	-0.039
	8	7120	7209	0.039	0.020	0.026	0.039	-0.042	-0.042	-0.048	-0.047
	9	7849	8003	0.048	0.026	0.035	0.046	-0.049	-0.050	-0.054	-0.054
	10	9110	9070	0.062	0.037	0.046	0.059	-0.059	-0.061	-0.067	-0.066
	11	10189	10096	0.078	0.048	0.061	0.072	-0.071	-0.073	-0.077	-0.076
	12	10946	11218	0.102	0.065	0.083	0.093	-0.089	-0.092	-0.093	-0.093
	13	11563	11683	0.108	0.069	0.087	0.098	-0.090	-0.094	-0.099	-0.099
	1	0	0	0.000	0.000	0.000	0.000	0.000	0.000	0.000	0.000
	2	-2775	-2750	0.000	0.000	0.000	0.000	0.002	0.002	0.002	0.002
	3	-4751	-4720	-0.001	0.000	0.000	-0.001	0.003	0.004	0.004	0.004
	4	-7246	-7264	-0.002	-0.001	-0.001	-0.002	0.004	0.006	0.006	0.009
	5	-8900	-8933	-0.004	-0.002	-0.002	-0.005	0.007	0.009	0.010	0.012
	6	-10498	-10575	-0.007	-0.004	-0.003	-0.008	0.009	0.010	0.013	0.015
	7	-11969	-12161	-0.008	-0.005	-0.004	-0.010	0.011	0.013	0.016	0.018
	8	-11997	-12189	-0.009	-0.006	-0.004	-0.010	0.011	0.014	0.016	0.019
Live	1	126	0	0.000	0.000	-0.001	0.000	-0.001	-0.001	-0.001	-0.001
	2	2261	2179	0.001	0.001	0.000	0.001	-0.001	-0.002	-0.006	-0.004
	3	3015	2949	0.001	0.001	0.000	0.001	-0.002	-0.003	-0.006	-0.004
	4	5653	5641	0.002	0.002	0.001	0.001	-0.007	-0.006	-0.007	-0.005
	5	8040	7949	0.005	0.004	0.001	0.004	-0.010	-0.009	-0.012	-0.009
	6	9799	9744	0.006	0.005	0.002	0.006	-0.012	-0.011	-0.015	-0.012
	7	11181	11282	0.008	0.007	0.003	0.007	-0.014	-0.013	-0.017	-0.014
	8	3894	4103	0.002	0.002	0.000	0.001	-0.010	-0.010	-0.002	-0.001
	9	0	128	0.001	0.000	-0.001	-0.001	-0.001	0.000	-0.001	-0.001
	10	6030	6026	0.004	0.002	0.001	0.002	-0.007	-0.006	-0.009	-0.006
	11	11432	11538	0.009	0.007	0.003	0.007	-0.014	-0.013	-0.017	-0.015
	12	12814	12949	0.009	0.008	0.004	0.009	-0.016	-0.014	-0.019	-0.016
	13	14447	14615	0.009	0.009	0.004	0.010	-0.017	-0.016	-0.022	-0.018
	14	16332	16538	0.011	0.009	0.005	0.011	-0.020	-0.018	-0.026	-0.023
	15	17462	17692	0.012	0.010	0.006	0.012	-0.020	-0.018	-0.032	-0.029
	16	19975	20128	0.013	0.011	0.007	0.015	-0.022	-0.019	-0.042	-0.038
	17	22111	22308	0.020	0.013	0.013	0.017	-0.027	-0.024	-0.061	-0.058
	18	23618	23846	0.022	0.017	0.015	0.020	-0.035	-0.032	-0.069	-0.065
	19	25126	25385	0.027	0.020	0.020	0.024	-0.043	-0.039	-0.082	-0.079
	20	26005	26282	0.030	0.027	0.023	0.030	-0.048	-0.044	-0.093	-0.089
	21	26884	27179	0.032	0.032	0.024	0.037	-0.052	-0.048	-0.104	-0.099
	22	28015	28333	0.038	0.037	0.031	0.041	-0.066	-0.059	-0.129	-0.124
	23	28266	28718	0.042	0.043	0.035	0.046	-0.074	-0.067	-0.159	-0.154
	24	26005	26282	0.043	0.051	0.043	0.053	-0.144	-0.132	-0.183	-0.180
	25	28643	28974	0.051	0.057	0.049	0.060	-0.158	-0.144	-0.192	-0.188
	26	30025	30256	0.060	0.068	0.057	0.072	-0.185	-0.171	-0.202	-0.198
	27	30905	31154	0.067	0.085	0.063	0.090	-0.206	-0.191	-0.226	-0.224
	28	31030	31282	0.071	0.090	0.067	0.096	-0.214	-0.199	-0.242	-0.240
	29	31658	31923	0.077	0.103	0.073	0.109	-0.228	-0.212	-0.274	-0.271
	30	32412	32692	0.084	0.120	0.079	0.129	-0.248	-0.234	-0.302	-0.300
	31	33040	33333	0.089	0.140	0.083	0.154	-0.265	-0.252	-0.333	-0.330
	32	33166	33590	0.092	0.160	0.085	0.178	-0.278	-0.264	-0.355	-0.350
	33	33920	34359	0.097	0.184	0.088	0.206	-0.295	-0.280	-0.383	-0.378
	34	33920	34359	0.100	0.198	0.090	0.222	-0.305	-0.290	-0.396	-0.390
	35	33794	34359	0.104	0.230	0.092	0.259	-0.322	-0.305	-0.436	-0.429
	36	33417	33974	0.108	0.259	0.095	0.294	-0.334	-0.316	-0.462	-0.453
	37	33417	33974	0.114	0.321	0.099	0.371	-0.360	-0.341	-0.509	-0.496
	38	34171	34872	0.121	0.357	0.103	0.416	-0.380	-0.361	-0.542	-0.526
	39	34171	34872	0.127	0.412	0.107	0.484	-0.402	-0.382	-0.586	-0.568
	40	34673	35513	0.136	0.484	0.113	0.569	-0.431	-0.409	-0.643	-0.622
	41	15829	16538	0.117	0.462	0.104	0.538	-0.403	-0.386	-0.604	-0.584
	42	-126	-128	0.092	0.429	0.089	0.496	-0.315	-0.304	-0.596	-0.579
	43	15578	16282	0.110	0.453	0.098	0.528	-0.360	-0.344	-0.626	-0.606
	44	29900	30513	0.132	0.476	0.112	0.561	-0.407	-0.388	-0.648	-0.625

<u>Raw Data</u>

Load Stage	Channel Data Point	0 (lbs)	1 (lbs)	80 (in.)	83 (in.)	84 (in.)	85 (in.)	86 (in.)	87 (in.)	88 (in.)	89 (in.)
	45	34171	34872	0.147	0.509	0.122	0.603	-0.437	-0.416	-0.674	-0.651
	46	35050	35897	0.159	0.574	0.132	0.677	-0.474	-0.453	-0.712	-0.690
	47	35678	36667	0.169	0.614	0.140	0.724	-0.502	-0.479	-0.736	-0.715
	48	35930	37051	0.189	0.712	0.160	0.838	-0.571	-0.543	-0.792	-0.768
	49	34045	35128	0.275	0.753	0.266	0.886	-0.665	-0.644	-0.818	-0.793
	50	33668	35128	0.455	0.785	0.492	0.937	-0.850	-0.835	-0.834	-0.808
	51	34296	36154	0.605	0.844	0.690	1.013	-1.025	-1.017	-0.869	-0.842
	52	33920	37436	1.020	0.890	1.272	1.063	-1.428	-1.451	-0.910	-0.881

Raw Data

Load Stage	Channel Data Point	90 (in.)	91 (in.)	92 (in.)	93 (in.)	94 (in.)	95 (in.)	96 (in.)	97 (in.)	98 (in.)	99 (in.)
Dead	1	-	-	-	-	-	-	-	-	-	-
	2	-	-	-	-	-	-	-	-	-	-
	3	-	-	-	-	-	-	-	-	-	-
	4	-	-	-	-	-	-	-	-	-	-
	5	-	-	-	-	-	-	-	-	-	-
	6	-	-	-	-	-	-	-	-	-	-
	7	-	-	-	-	-	-	-	-	-	-
	8	-	-	-	-	-	-	-	-	-	-
	9	-	-	-	-	-	-	-	-	-	-
	10	-	-	-	-	-	-	-	-	-	-
	11	-	-	-	-	-	-	-	-	-	-
	12	-	-	-	-	-	-	-	-	-	-
	13	-	-	-	-	-	-	-	-	-	-
	1	-	-	-	-	-	-	-	-	-	-
	2	-	-	-	-	-	-	-	-	-	-
	3	-	-	-	-	-	-	-	-	-	-
	4	-	-	-	-	-	-	-	-	-	-
	5	-	-	-	-	-	-	-	-	-	-
	6	-	-	-	-	-	-	-	-	-	-
	7	-	-	-	-	-	-	-	-	-	-
	8	-	-	-	-	-	-	-	-	-	-
Live	1	0.000	0.000	0.000	0.000	0.000	0.000	-0.001	-0.001	-0.001	-0.001
	2	0.000	0.001	0.000	0.000	0.000	0.000	-0.001	-0.001	-0.001	-0.001
	3	0.000	0.001	0.000	0.000	0.000	0.000	-0.001	0.000	-0.001	-0.001
	4	0.000	0.004	0.000	0.000	0.002	0.000	-0.001	0.000	-0.001	0.000
	5	0.003	0.007	0.000	0.000	0.005	0.000	0.000	0.002	-0.001	0.003
	6	0.004	0.011	0.000	0.004	0.007	0.000	-0.001	0.006	-0.001	0.005
	7	0.006	0.013	0.000	0.006	0.010	0.000	0.000	0.007	-0.001	0.006
	8	0.005	0.004	0.000	0.006	0.005	0.000	-0.001	0.007	-0.001	0.002
	9	0.004	-0.001	0.000	0.006	0.002	0.000	0.000	0.007	-0.001	0.000
	10	0.004	0.005	0.000	0.006	0.002	0.000	-0.001	0.007	-0.001	0.001
	11	0.008	0.014	-0.001	0.010	0.010	0.000	0.003	0.009	-0.001	0.007
	12	0.008	0.017	0.000	0.010	0.011	0.000	0.003	0.010	-0.001	0.007
	13	0.009	0.018	0.000	0.011	0.012	0.000	0.003	0.012	-0.001	0.008
	14	0.010	0.020	0.000	0.013	0.014	0.000	0.006	0.013	-0.001	0.009
	15	0.012	0.021	0.000	0.015	0.016	0.000	0.007	0.015	-0.001	0.010
	16	0.014	0.023	0.000	0.017	0.018	0.000	0.009	0.015	-0.001	0.010
	17	0.016	0.023	0.007	0.019	0.020	0.020	0.012	0.018	0.013	0.012
	18	0.018	0.024	0.007	0.021	0.023	0.020	0.013	0.018	0.013	0.014
	19	0.021	0.027	0.007	0.024	0.024	0.020	0.016	0.021	0.013	0.017
	20	0.023	0.028	0.007	0.026	0.030	0.020	0.018	0.024	0.013	0.020
	21	0.024	0.028	0.007	0.028	0.039	0.020	0.018	0.027	0.013	0.021
	22	0.026	0.029	0.007	0.029	0.044	0.020	0.020	0.031	0.013	0.029
	23	0.029	0.031	0.007	0.032	0.050	0.020	0.024	0.036	0.013	0.034
	24	0.035	0.032	0.037	0.046	0.057	0.029	0.036	0.047	0.030	0.040
	25	0.037	0.032	0.037	0.046	0.063	0.031	0.036	0.047	0.030	0.044
	26	0.043	0.035	0.037	0.050	0.072	0.037	0.037	0.051	0.030	0.051
	27	0.046	0.044	0.037	0.053	0.087	0.041	0.040	0.062	0.030	0.056
	28	0.048	0.046	0.037	0.056	0.093	0.045	0.043	0.066	0.030	0.061
	29	0.053	0.050	0.037	0.061	0.103	0.050	0.046	0.071	0.030	0.067
	30	0.056	0.054	0.037	0.064	0.120	0.054	0.050	0.079	0.030	0.072
	31	0.057	0.057	0.038	0.068	0.141	0.057	0.053	0.086	0.030	0.076
	32	0.059	0.059	0.038	0.069	0.162	0.059	0.054	0.096	0.030	0.078
	33	0.060	0.060	0.037	0.070	0.189	0.059	0.054	0.106	0.030	0.079
	34	0.061	0.061	0.037	0.071	0.205	0.060	0.056	0.111	0.030	0.080
	35	0.061	0.061	0.038	0.072	0.243	0.061	0.056	0.119	0.030	0.081
	36	0.062	0.061	0.037	0.072	0.259	0.061	0.057	0.122	0.030	0.081
	37	0.062	0.061	0.037	0.072	0.295	0.062	0.057	0.126	0.030	0.082
	38	0.062	0.062	0.037	0.073	0.320	0.062	0.058	0.128	0.030	0.082
	39	0.062	0.062	0.037	0.073	0.369	0.062	0.058	0.131	0.030	0.082
	40	0.062	0.064	0.037	0.074	0.418	0.062	0.058	0.136	0.030	0.083
	41	0.061	0.064	0.037	0.074	0.411	0.062	0.058	0.136	0.030	0.076
	42	0.048	0.051	0.046	0.068	0.363	0.058	0.057	0.133	0.036	0.062
	43	0.054	0.056	0.046	0.068	0.382	0.058	0.058	0.134	0.036	0.070
	44	0.060	0.064	0.046	0.074	0.412	0.059	0.058	0.134	0.036	0.079

Raw Data

Load Stage	Channel Data Point	90 (in.)	91 (in.)	92 (in.)	93 (in.)	94 (in.)	95 (in.)	96 (in.)	97 (in.)	98 (in.)	99 (in.)
	45	0.062	0.068	0.046	0.076	0.440	0.061	0.060	0.139	0.036	0.083
	46	0.063	0.070	0.046	0.077	0.487	0.062	0.060	0.145	0.036	0.085
	47	0.065	0.072	0.046	0.079	0.518	0.063	0.062	0.148	0.036	0.087
	48	0.066	0.075	0.046	0.080	0.556	0.065	0.064	0.152	0.036	0.089
	49	0.069	0.076	0.046	0.084	0.575	0.068	0.066	0.154	0.036	0.091
	50	0.069	0.076	0.046	0.084	0.572	0.068	0.067	0.154	0.036	0.105
	51	0.069	0.076	0.046	0.084	0.572	0.069	0.066	0.154	0.036	0.125
	52	0.067	0.077	0.046	0.084	0.573	0.072	0.066	0.154	0.036	0.165

Raw Data

Load Stage	Channel / Data Point	104 (in.)	105 (in.)	106 (in.)	107 (in.)	108 (in.)	DG1 (in.)	DG2 (in.)	DG3 (in.)	DG4 (in.)
Dead	*1*	-	-	-	-	-	-	-	-	-
	2	-	-	-	-	-	-	-	-	-
	3	-	-	-	-	-	-	-	-	-
	4	-	-	-	-	-	-	-	-	-
	5	-	-	-	-	-	-	-	-	-
	6	-	-	-	-	-	-	-	-	-
	7	-	-	-	-	-	-	-	-	-
	8	-	-	-	-	-	-	-	-	-
	9	-	-	-	-	-	-	-	-	-
	10	-	-	-	-	-	-	-	-	-
	11	-	-	-	-	-	-	-	-	-
	12	-	-	-	-	-	-	-	-	-
	13	-	-	-	-	-	-	-	-	-
	1	-	-	-	0.002	0.002	-	-	-	-
	2	-	-	-	0.015	0.009	-	-	-	-
	3	-	-	-	0.022	0.021	-	-	-	-
	4	-	-	-	0.041	0.041	-	-	-	-
	5	-	-	-	0.061	0.060	-	-	-	-
	6	-	-	-	0.074	0.082	-	-	-	-
	7	-	-	-	0.102	0.095	-	-	-	-
	8	-	-	-	0.099	0.095	-	-	-	-
Live	1	0.000	0.001	0.001	0.000	0.002	0.0000	0.0000	0.0000	0.0000
	2	0.000	0.000	-0.001	0.024	-0.058	-	-	-	-
	3	-0.002	-0.001	-0.003	-0.009	-0.045	-0.0010	0.0000	-0.0010	0.0000
	4	-0.004	-0.003	-0.005	-0.063	-0.030	-0.0015	-0.0001	-0.0012	0.0000
	5	-0.006	-0.005	-0.009	-0.074	-0.073	-0.0013	-0.0007	-0.0009	-0.0006
	6	-0.011	-0.009	-0.014	-0.095	-0.092	-0.0011	-0.0013	-0.0007	-0.0011
	7	-0.013	-0.010	-0.017	-0.108	-0.105	-0.0010	-0.0014	-0.0005	-0.0012
	8	-0.011	-0.007	-0.008	-0.154	0.082	-0.0008	-0.0002	-0.0009	0.0002
	9	-0.006	-0.005	-0.004	0.017	-0.013	0.0002	0.0005	-0.0004	0.0004
	10	-0.009	-0.005	-0.008	-0.056	-0.054	-0.0010	-0.0001	-0.0014	0.0001
	11	*-0.015*	*-0.011*	*-0.019*	*-0.112*	*-0.114*	*-0.0007*	*-0.0015*	*-0.0009*	*-0.0011*
	12	-0.017	-0.013	-0.022	-0.123	-0.127	-0.0008	-0.0018	-0.0010	-0.0015
	13	-0.021	-0.015	-0.025	-0.143	-0.142	-0.0009	-0.0020	-0.0011	-0.0018
	14	-0.030	-0.018	-0.032	-0.167	-0.168	-0.0013	-0.0020	-0.0027	-0.0022
	15	-0.034	-0.021	-0.039	-0.190	-0.187	-0.0024	-0.0021	-0.0022	-0.0029
	16	-0.038	-0.025	-0.045	-0.223	-0.221	-0.0038	-0.0027	-0.0033	-0.0048
	17	-0.045	-0.029	-0.051	-0.283	-0.282	-0.0097	-0.0051	-0.0058	-0.0043
	18	-0.049	-0.033	-0.057	-0.324	-0.327	-0.0112	-0.0052	-0.0079	-0.0073
	19	-0.056	-0.037	-0.061	-0.376	-0.370	-0.0148	-0.0065	-0.0100	-0.0085
	20	-0.060	-0.040	-0.068	-0.411	-0.424	-0.0159	-0.0074	-0.0100	-0.0099
	21	-0.064	-0.042	-0.072	-0.456	-0.456	-0.0175	-0.0085	-0.0102	-0.0106
	22	-0.066	-0.044	-0.077	-0.530	-0.535	-0.0281	-0.0100	-0.0153	-0.0114
	23	-0.071	-0.047	-0.079	-0.603	-0.596	-0.0445	-0.0125	-0.0200	-0.0101
	24	-0.071	-0.048	-0.077	-0.709	-0.703	-0.0138	-0.0030	-0.0485	-0.0079
	25	-0.073	-0.049	-0.081	-0.772	-0.763	-0.0121	-0.0050	-0.0471	-0.0110
	26	-0.077	-0.051	-0.084	-0.859	-0.852	-0.0131	-0.0050	-0.0511	-0.0161
	27	-0.077	-0.054	-0.090	-0.958	-0.957	-0.0183	-0.0075	-0.0561	-0.0191
	28	-0.079	-0.054	-0.093	-1.010	-1.004	-0.0234	-0.0091	-0.0571	-0.0200
	29	-0.081	-0.057	-0.095	-1.103	-1.099	-0.0345	-0.0123	-0.0602	-0.0208
	30	-0.083	-0.058	-0.097	-1.211	-1.206	-0.0392	-0.0160	-0.0632	-0.0236
	31	-0.085	-0.059	-0.098	-1.311	-1.318	-0.0429	-0.0202	-0.0649	-0.0269
	32	-0.088	-0.060	-0.100	-1.412	-1.385	-0.0421	-0.0240	-0.0630	-0.0300
	33	-0.090	-0.061	-0.102	-1.503	-1.505	-0.0420	-0.0280	-0.0611	-0.0341
	34	*-0.092*	*-0.061*	*-0.103*	*-1.585*	*-1.546*	*-0.0419*	*-0.0300*	*-0.0600*	*-0.0360*
	35	-0.092	-0.062	-0.103	-1.685	-1.699	-0.0421	-0.0352	-0.0575	-0.0394
	36	-0.094	-0.062	-0.104	-1.778	-1.806	-0.0360	-0.0370	-0.0535	-0.0421
	37	-0.094	-0.062	-0.104	-1.983	-2.006	-0.0208	-0.0370	-0.0479	-0.0451
	38	-0.094	-0.061	-0.104	-2.145	-2.127	-0.0119	-0.0400	-0.0455	-0.0478
	39	-0.094	-0.061	-0.105	-2.325	-2.314	0.0011	-0.0390	-0.0430	-0.0505
	40	-0.096	-0.062	-0.106	-2.578	-2.540	0.0198	-0.0388	-0.0395	-0.0532
	41	-0.079	-0.047	-0.076	-2.364	-2.286	0.0138	-0.0305	-0.0470	-0.0433
	42	*-0.060*	*-0.035*	*-0.047*	*-1.027*	*-3.041*	*0.0440*	*-0.0205*	*-0.0595*	*-0.0305*
	43	-0.075	-0.047	-0.072	-1.602	-2.955	0.0450	-0.0275	-0.0530	-0.0380
	44	-0.092	-0.061	-0.096	-2.169	-2.843	0.0520	-0.0361	-0.0440	-0.0475

Raw Data

Load Stage	Channel Data Point	104 (in.)	105 (in.)	106 (in.)	107 (in.)	108 (in.)	DG1 (in.)	DG2 (in.)	DG3 (in.)	DG4 (in.)
	45	-0.098	-0.065	-0.105	-2.530	-2.802	0.0600	-0.0405	-0.0370	-0.0510
	46	-0.098	-0.065	-0.106	-3.004	-2.780	0.0730	-0.0390	-0.0312	-0.0535
	47	-0.098	-0.065	-0.106	-3.307	-2.774	0.0820	-0.0380	-0.0290	-0.0490
	48	-0.100	-0.061	-0.106	-3.854	-2.752	0.1039	-0.0341	-0.0250	-0.0570
	49	-0.098	-0.056	-0.101	-3.852	-2.761	0.1189	-0.0321	-0.0130	-0.0410
	50	-0.096	-0.049	-0.097	5.190	-2.752	0.1420	-0.0265	0.0080	-0.0050
	51	-0.096	-0.047	-0.096	3.906	-2.737	0.1680	-0.0190	0.0180	0.0130
	52	-0.094	-0.049	-0.096	1.146	-2.739	0.2020	-0.0118	0.0710	0.0440

Test Comments

Data Point (With respect to the live stage of loading.)

2 Marked cracks in slab some small ones mainly transverse and near middle. Some of these may have existed before the test started from the unloading of the pre-load.

15 One of the initial transverse cracks about 4" on the north side of center has propagated from one edge of the slab to the

17 Sounded like additional cracking. Inspection showed a transverse crack from one side of slab to other about 8" south of centerline.

18 Notice a little flaking of white wash on top edge of south seat angle along the west side of angle between beam flange and top of angle.

19 Transverse crack from edge to edge about 36" north of centerline. Small flakes on south shear tab. Small flaking on girder, backside of north shear tab.

20 First yielding around all bolts in both shear tabs noticed. Top bolts appear to be resisting mostly moment based on the direction of the yielding while middle and bottom bolts appear to be resisting mostly shear forces.
Also notice yielding on girder face opposite of the shear tab on the opposite girder face.

22 Heard popping like concrete cracking. Transverse cracks edge to edge about 24" either side of centerline.

24 Loud pop noticed south side rotation increased significantly. Looks like seat angle slipped into bearing on south side. Connections seem to be swinging toward the web side of the connection
Yielding around top bolts in both shear tabs has progressed most noticeably in the north connection. Also see some yielding along the fillet of the seat angle on the bottom side of the angle.

27 Notice some yielding along bottom of seat angle fillet mostly at edges of seat angle.

28 First yielding in north connection web in front of top bolt. Notice some yielding around the top of the bolt in the south connection seat angle and in the bottom flange of the south connection at the free edge of the outstanding angle,

30 Yielding around the top of the bolts in the north connection seat angle.

32 North side of slab generally more cracked than south side.

36 Yielding in north connection shear tab such that yielding patterns between the bolts have connected to each other.

37 Crack running from North load ram to end of slab, parallel with beam. South side has almost all but quit rotating, mainly because cannot increase load. Deck is pulling in tension on the connection side of the first two studs on the Yielding in north connection seat angle bottom side along angle fillet and around bolts closest to the girder face has progresses significantly.

41 Start unloading to add lateral brace to north side of specimen

42 unloaded

43 re-loading

44 Yielding of web in front of top bolt noticed on south connection.

46 Yielding in front of second middle noticed on north web. Criss-cross yielding pattern bottom of bottom flange middle

47 The deck definitely appears to be carrying load out to the pour stop by way of deck shear deformations.

49 Notice yielding in front of middle bolt web side of south connection.

50 Notice yielding in front of bottom bolt in web in both north and south connections. Had to reset the displacement gage for the south connection the wire had reached its limit. Starting local buckling of bottom flange south connection

52 Shear yielding pattern web south side, end test for excessive deformations.

Composite Connection Test Summary **Connection #5**

<u>**Calculated Data**</u> **Data Point**	***Using POTS Only*** **North Rotation** **(rad)**	**North Moment** **(k-in.)**	***Using POTS Only*** **South Rotation** **(rad)**	**South Moment** **(k-in.)**	***POTS & DG*** **North Rotation** **(rad)**	***POTS & DG*** **South Rotation** **(rad)**
1	0.0003	81	0.0004	81		
2	0.0005	96	0.0003	94		
3	0.0007	165	0.0007	165		
4	0.0010	230	0.0008	228		
5	0.0017	385	0.0016	388		
6	0.0020	439	0.0018	434		
7	0.0025	510	0.0023	507		
8	0.0031	577	0.0030	583		
9	0.0036	627	0.0036	638		
10	0.0046	715	0.0046	712		
11	0.0055	790	0.0057	784		
12	0.0069	843	0.0073	862		
13	0.0073	886	0.0076	894		
1	0.0073	886	0.0076	894		
2	0.0073	693	0.0075	703		
3	0.0072	555	0.0074	566		
4	0.0070	382	0.0073	389		
5	0.0067	267	0.0072	273		
6	0.0065	156	0.0070	159		
7	0.0064	54	0.0069	49		
8	0.0063	52	0.0068	47		
1	0.0064	91	0.0068	82	0.0063	0.0068
2	0.0065	239	0.0069	233		
3	0.0065	292	0.0070	287	0.0064	0.0069
4	0.0067	475	0.0072	474	0.0066	0.0070
5	0.0069	641	0.0073	634	0.0068	0.0072
6	0.0071	763	0.0075	759	0.0069	0.0073
7	0.0072	859	0.0076	866	0.0071	0.0074
8	0.0064	353	0.0073	367	0.0065	0.0070
9	0.0063	82	0.0068	91	0.0062	0.0068
10	0.0067	501	0.0072	501	0.0066	0.0071
11	0.0072	877	0.0076	884	0.0071	0.0075
12	0.0074	973	0.0077	982	0.0072	0.0075
13	0.0075	1086	0.0078	1098	0.0073	0.0076
14	0.0077	1217	0.0079	1231	0.0074	0.0078
15	0.0080	1296	0.0080	1312	0.0075	0.0079
16	0.0084	1470	0.0081	1481	0.0078	0.0082
17	0.0093	1619	0.0085	1632	0.0084	0.0088
18	0.0097	1723	0.0089	1739	0.0088	0.0092
19	0.0104	1828	0.0094	1846	0.0093	0.0098
20	0.0111	1889	0.0097	1909	0.0100	0.0101
21	0.0118	1950	0.0100	1971	0.0107	0.0103
22	0.0130	2029	0.0107	2051	0.0117	0.0112
23	0.0144	2047	0.0112	2078	0.0130	0.0117
24	0.0157	1889	0.0141	1909	0.0119	0.0133
25	0.0163	2073	0.0149	2096	0.0125	0.0141
26	0.0172	2169	0.0164	2185	0.0136	0.0153
27	0.0189	2230	0.0175	2247	0.0155	0.0162
28	0.0197	2239	0.0179	2256	0.0163	0.0166
29	0.0215	2282	0.0187	2301	0.0182	0.0174
30	0.0234	2335	0.0198	2354	0.0203	0.0182
31	0.0255	2378	0.0207	2399	0.0227	0.0189
32	0.0273	2387	0.0213	2416	0.0248	0.0192
33	0.0294	2439	0.0221	2470	0.0274	0.0196
34	0.0305	2439	0.0226	2470	0.0289	0.0199
35	0.0335	2431	0.0234	2470	0.0323	0.0202
36	0.0358	2404	0.0240	2443	0.0350	0.0204

37	0.0404	2404	0.0252	2443	0.0407	0.0208
38	0.0433	2457	0.0263	2506	0.0442	0.0213
39	0.0475	2457	0.0273	2506	0.0491	0.0218
40	0.0529	2492	0.0288	2550	0.0555	0.0225
41	0.0502	1182	0.0272	1231	0.0529	0.0211
42	0.0485	73	0.0230	73	0.0477	0.0192
43	0.0507	1165	0.0252	1214	0.0505	0.0205
44	0.0527	2160	0.0278	2203	0.0531	0.0222
45	0.0552	2457	0.0294	2506	0.0564	0.0231
46	0.0596	2518	0.0314	2577	0.0621	0.0240
47	0.0623	2562	0.0328	2630	0.0657	0.0245
48	0.0688	2579	0.0363	2657	0.0742	0.0265
49	0.0716	2448	0.0441	2523	0.0775	0.0340
50	0.0739	2422	0.0599	2523	0.0800	0.0500
51	0.0779	2466	0.0741	2595	0.0846	0.0646
52	0.0815	2439	0.1110	2684	0.0871	0.1063

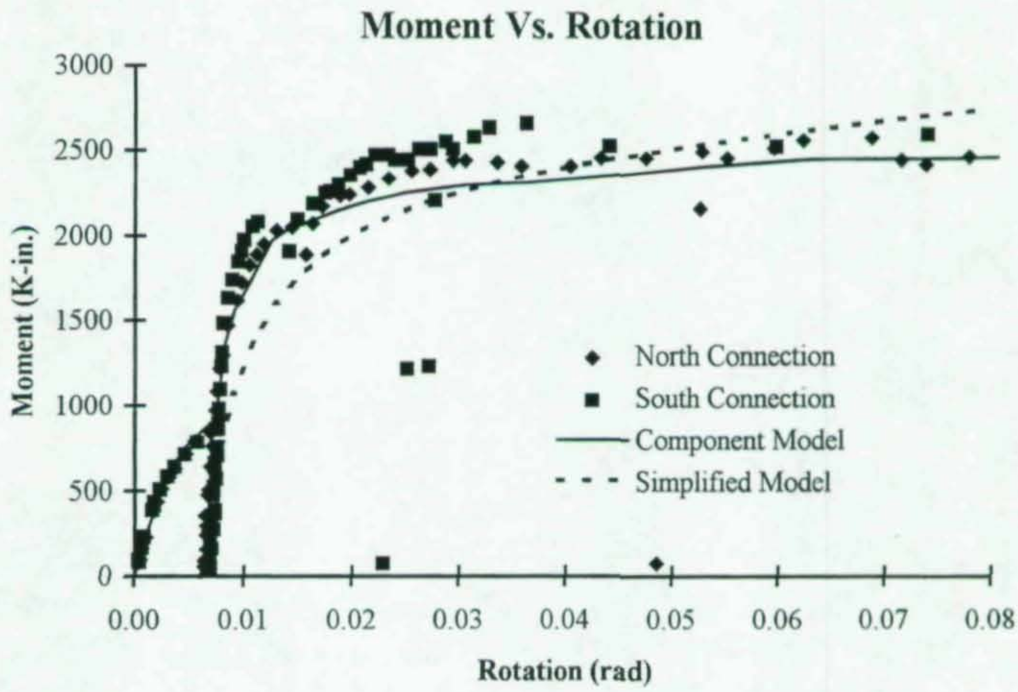
Moment Vs. Rotation
Moment (K-in.)
Rotation (rad)
North Connection
South Connection
Component Model
Simplified Model
3000
2500
2000
1500
1000
500
0
0.00
0.01
0.02
0.03
0.04
0.05
0.06
0.07
0.08

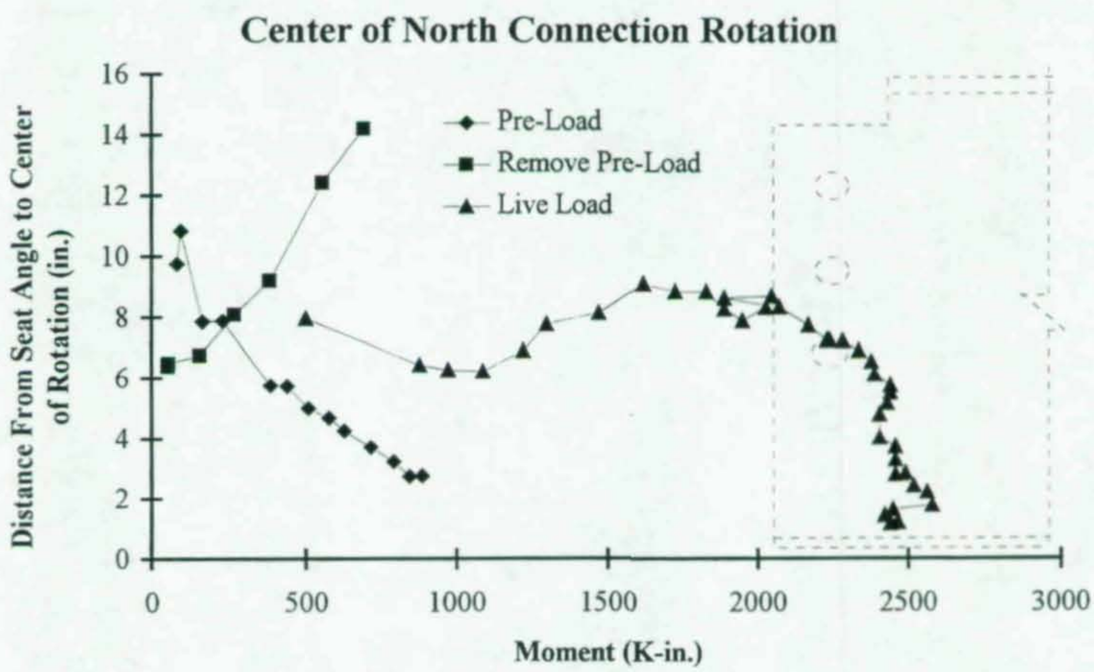
Center of North Connection Rotation
Distance From Seat Angle to Center of Rotation (in.)
Moment (K-in.)
Pre-Load
Remove Pre-Load
Live Load
16
14
12
10
8
6
4
2
0
0
500
1000
1500
2000
2500
3000

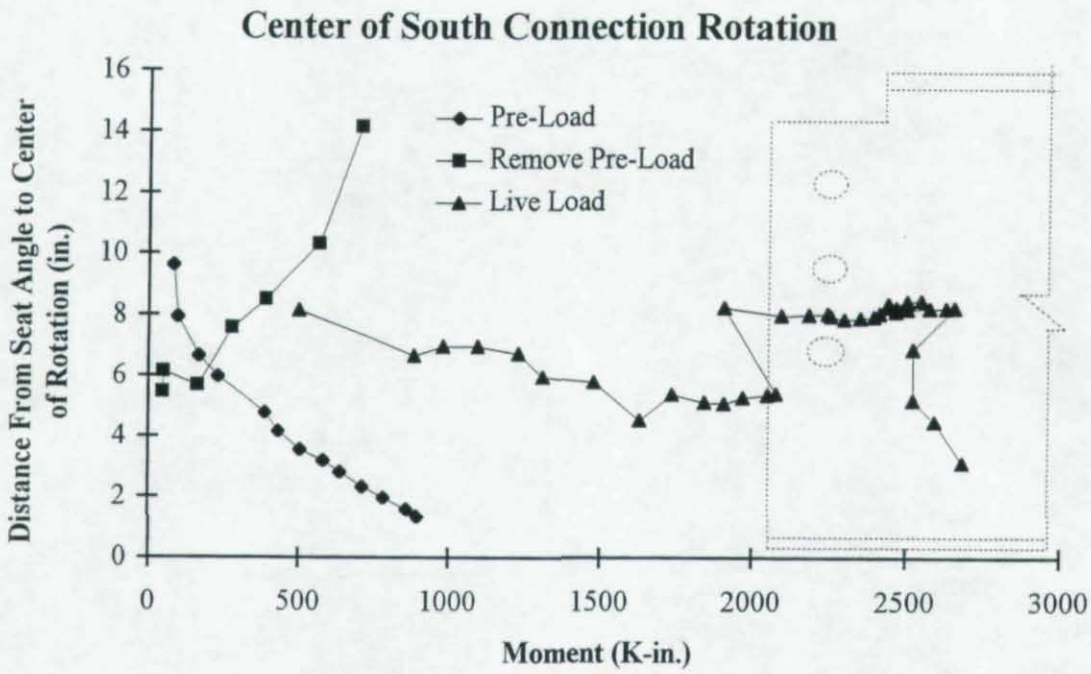
Center of South Connection Rotation
Distance From Seat Angle to Center of Rotation (in.)
Moment (K-in.)
Pre-Load
Remove Pre-Load
Live Load
0
2
4
6
8
10
12
14
16
0
500
1000
1500
2000
2500
3000

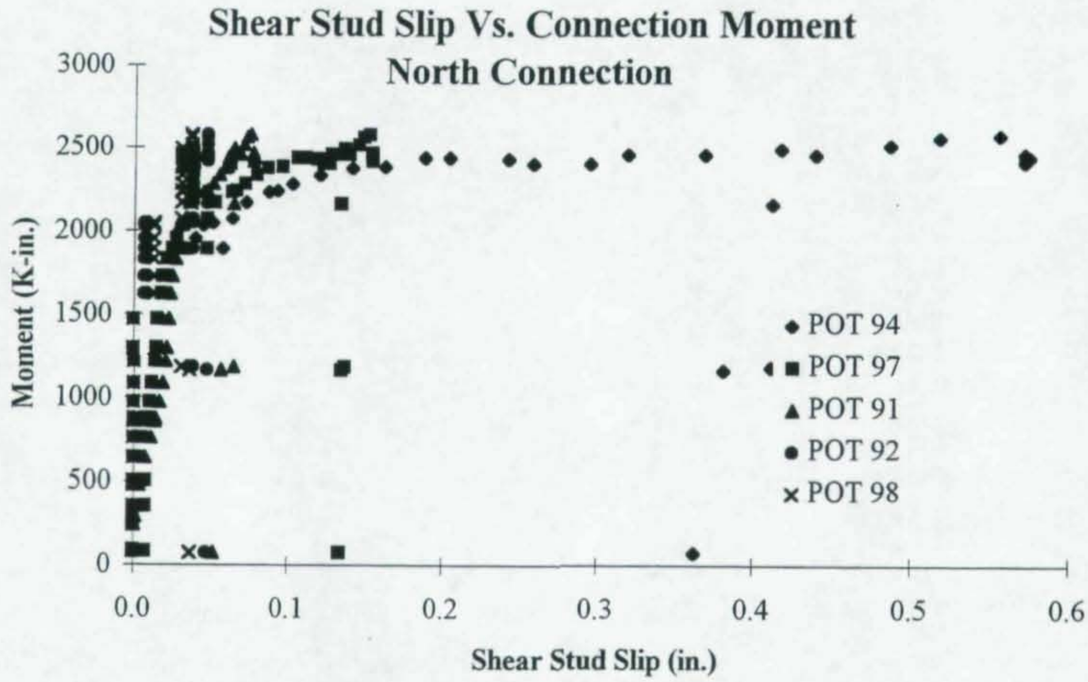
Shear Stud Slip Vs. Connection Moment
North Connection
Moment (K-in.)
Shear Stud Slip (in.)
POT 94
POT 97
POT 91
POT 92
POT 98
0
500
1000
1500
2000
2500
3000
0.0
0.1
0.2
0.3
0.4
0.5
0.6

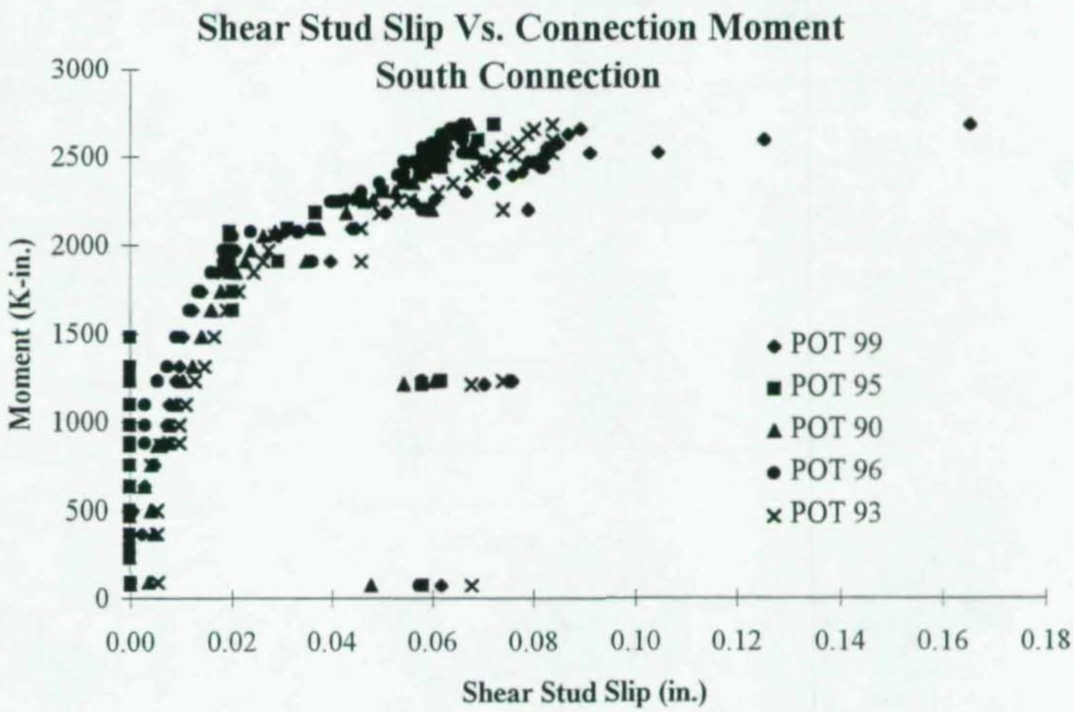
Shear Stud Slip Vs. Connection Moment
South Connection
Moment (K-in.)
3000
2500
2000
1500
1000
500
0
0.00
0.02
0.04
0.06
0.08
0.10
0.12
0.14
0.16
0.18
Shear Stud Slip (in.)
POT 99
POT 95
POT 90
POT 96
POT 93

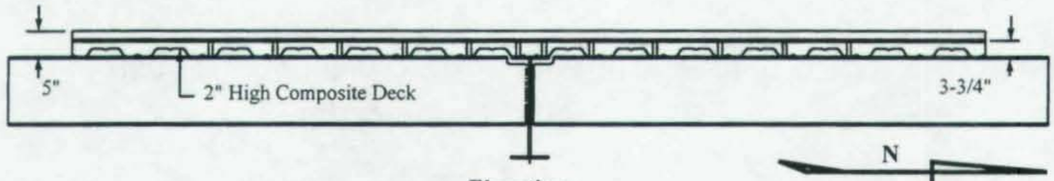

Elevation

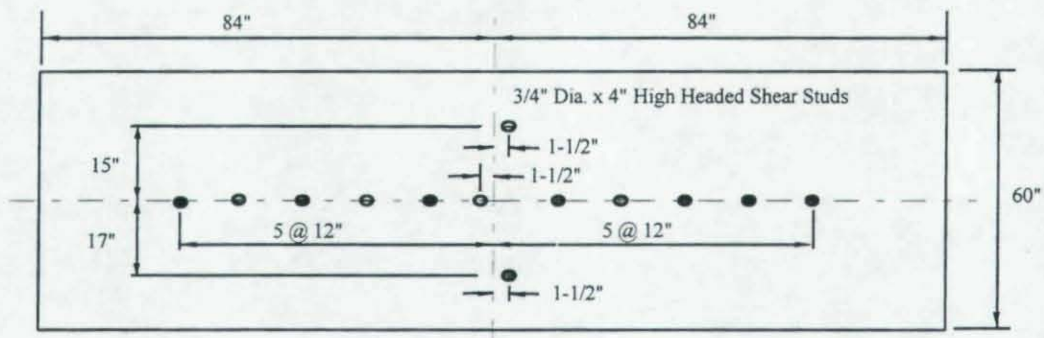

Shear Stud Layout

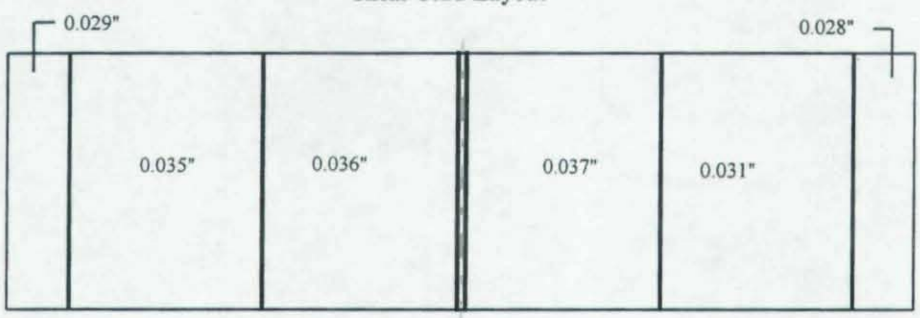

Deck Layout & Thickness

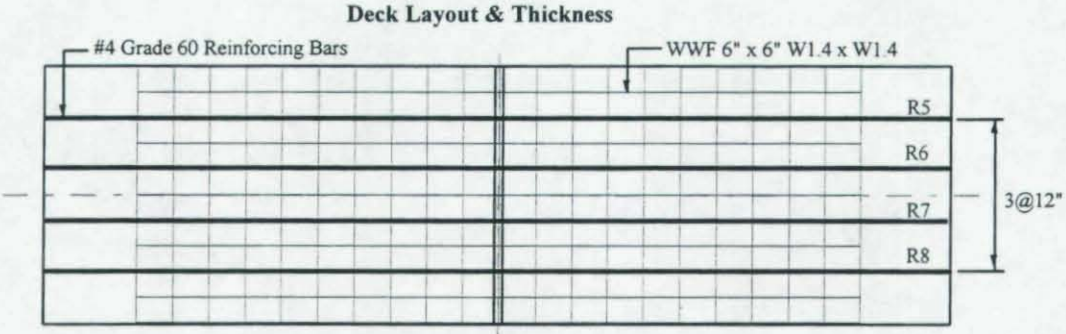

Reinforcing Identification & Layout

Reinforced Composite Deck Information

Description of Instrumentation

Channel	Sense of Extension	Description of Measurement	Load Stage	Gage Type	Sensitivity	Full Scale
0	Compression (-)	North Load Ram	Live	Load Cell	1.99	500 kips
1	Compression (-)	South Load Ram	Live	Load Cell	1.95	500 kips
80	-**	Connection Rotation	Live	POT		6"
83	-**	Connection Rotation	Live	POT		6"
84	-**	Connection Rotation	Live	POT		6"
85	-**	Connection Rotation	Live	POT		6"
86	-**	Connection Rotation	Live	POT		6"
87	-**	Connection Rotation	Live	POT		6"
88	-**	Connection Rotation	Live	POT		6"
89	-**	Connection Rotation	Live	POT		6"
90	-**	Stud Slip	Live	POT		6"
91	-**	Stud Slip	Live	POT		6"
92	-**	Stud Slip	Live	POT		6"
93	-**	Stud Slip	Live	POT		6"
94	-**	Stud Slip	Live	POT		6"
95	-**	Stud Slip	Live	POT		6"
96	-**	Stud Slip	Live	POT		6"
97	-**	Stud Slip	Live	POT		6"
98	-**	Stud Slip	Live	POT		6"
99	-**	Stud Slip	Live	POT		6"
104	-**	Girder Deflection	Live	DCDT 7	0.95	20"
105	+	Girder Deflection	Live	DCDT 8	0.949	10"
106	+	Girder Deflection	Live	DCDT 11	0.943	10"
107	+	Filler Beam Deflection	Live	DCDT 9	0.942	20"
108	+	Filler Beam Deflection	Live	DCDT 4	0.948	20"
DG1	-**	Connection Rotation	Live	Dial Gage		1"
DG2	-**	Connection Rotation	Live	Dial Gage		1"
DG3	-**	Connection Rotation	Live	Dial Gage		1"
DG4	-**	Connection Rotation	Live	Dial Gage		1"

** All data has been modified so that (+) readings indicate extension.

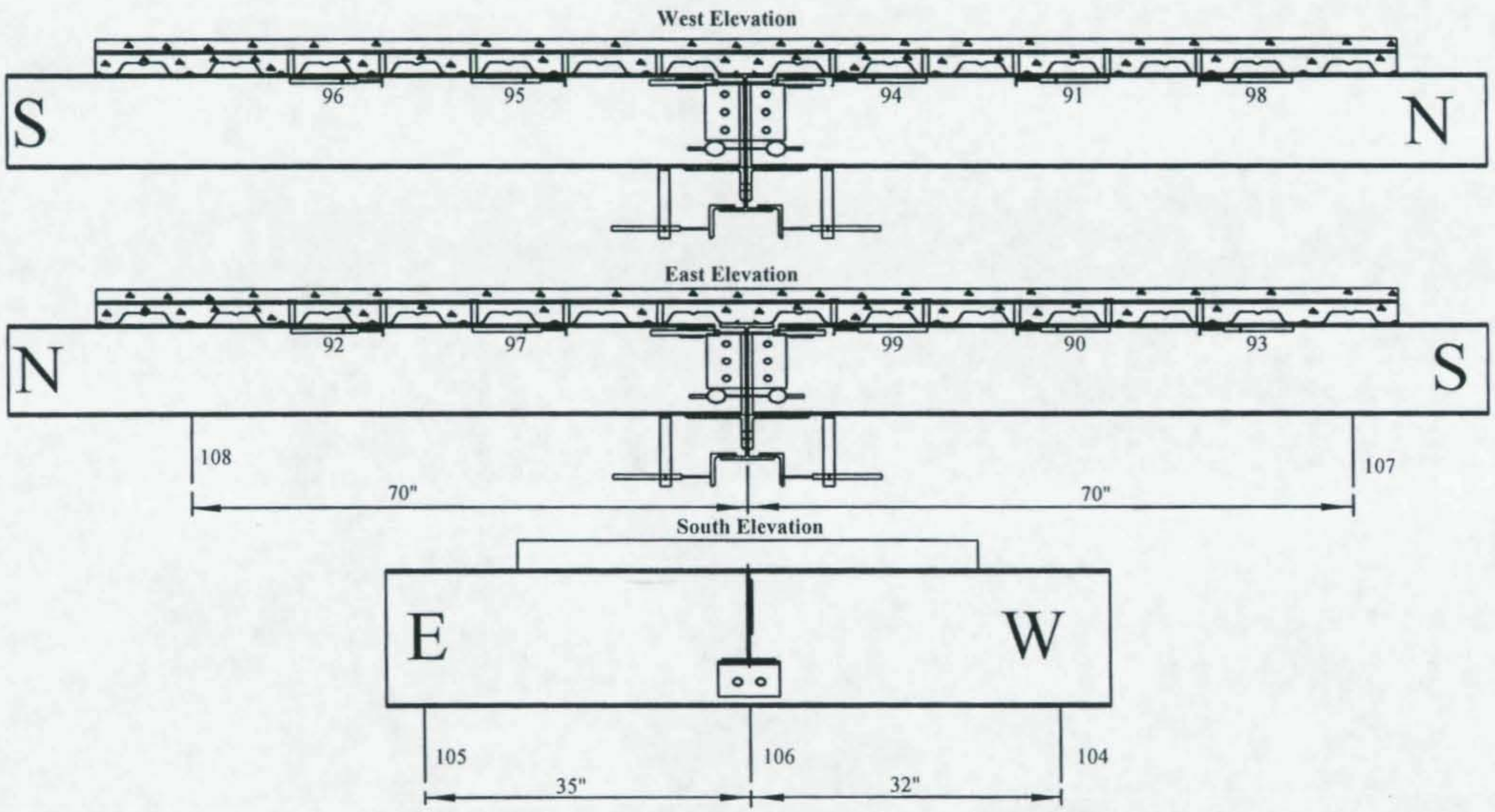

Stud Slip & Beam Deflection Instrumentation Live Loading Stage

West Elevation

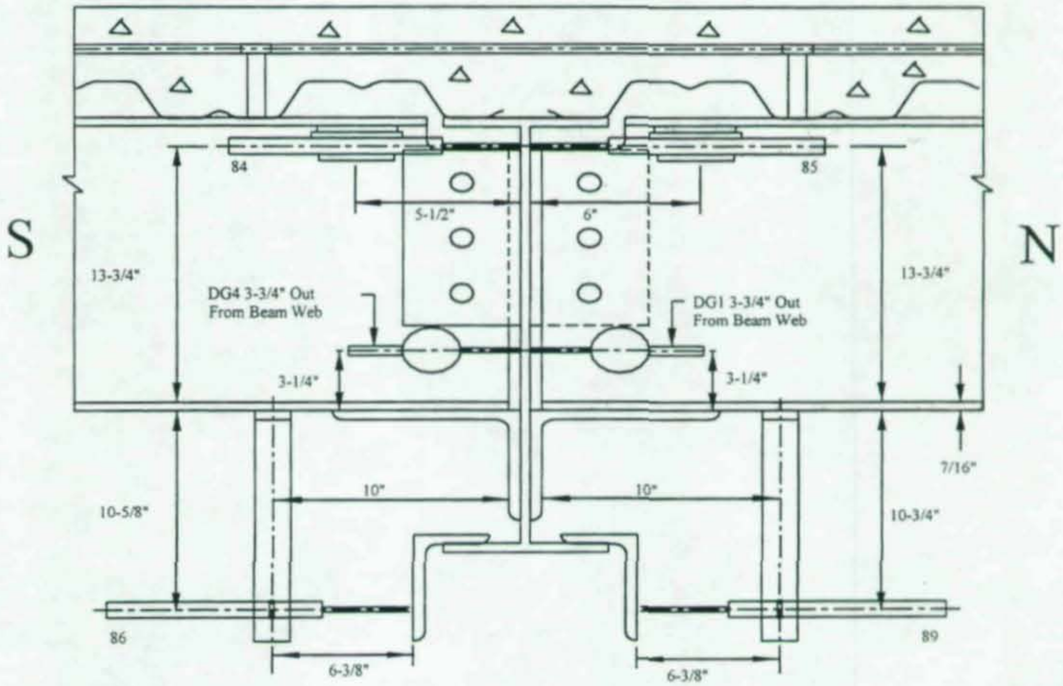

East Elevation

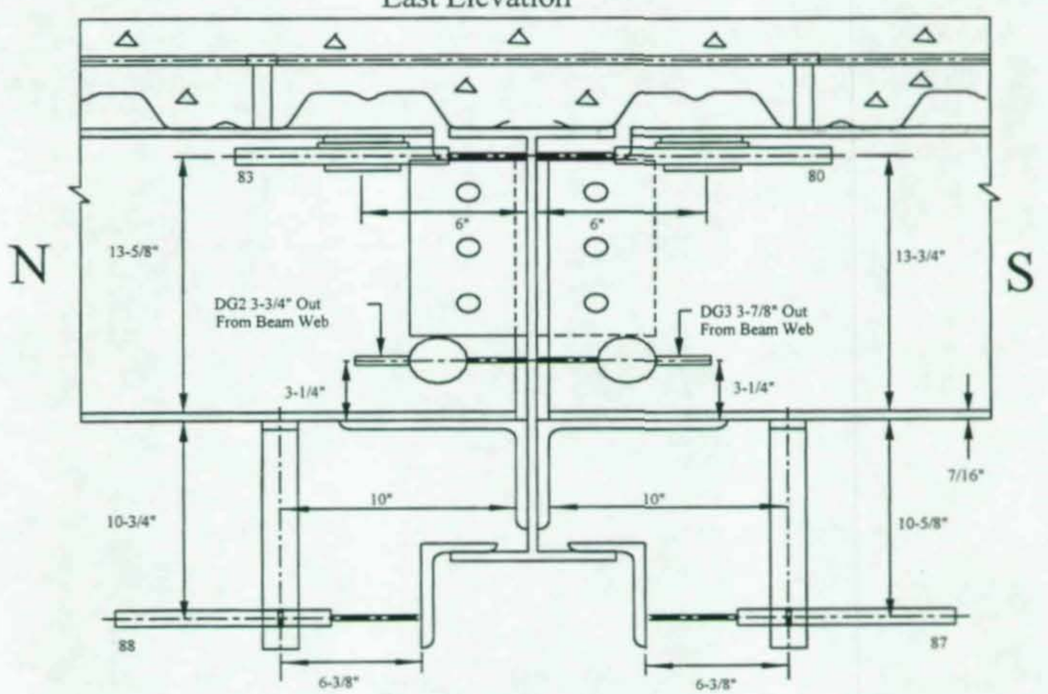

Rotation Instrumentation Live Loading Stage

Raw Data

Load Stage	Channel / Data Point	0 (lbs)	1 (lbs)	80 (in.)	83 (in.)	84 (in.)	85 (in.)	86 (in.)	87 (in.)	88 (in.)	89 (in.)
Live	1	0	0	0.000	0.000	0.000	0.000	0.000	0.000	0.000	0.000
	2	-126	0	0.001	0.000	0.000	-0.001	-0.001	0.000	0.000	0.000
	3	4523	4744	0.000	0.000	0.000	-0.001	-0.007	-0.007	-0.004	-0.004
	4	8291	8718	0.002	0.000	0.002	0.001	-0.015	-0.014	-0.008	-0.009
	5	10050	10385	0.003	0.001	0.002	0.002	-0.017	-0.017	-0.012	-0.012
	6	5779	6026	0.002	0.001	0.002	0.002	-0.010	-0.010	-0.012	-0.012
	7	0	0	0.001	0.000	0.001	0.001	-0.003	-0.002	-0.003	-0.004
	8	5779	6026	0.002	0.001	0.001	0.002	-0.009	-0.009	-0.013	-0.013
	9	*10050*	*10256*	*0.003*	*0.001*	*0.002*	*0.003*	*-0.017*	*-0.017*	*-0.013*	*-0.013*
	10	11307	11667	0.003	0.002	0.002	0.004	-0.020	-0.020	-0.013	-0.013
	11	13191	13590	0.004	0.002	0.003	0.005	-0.023	-0.023	-0.017	-0.016
	12	14950	15385	0.005	0.004	0.004	0.007	-0.026	-0.025	-0.018	-0.019
	13	15829	16282	0.007	0.004	0.005	0.008	-0.029	-0.028	-0.021	-0.020
	14	16332	16795	0.015	0.007	0.010	0.013	-0.035	-0.035	-0.025	-0.025
	15	19347	20000	0.018	0.009	0.013	0.015	-0.041	-0.040	-0.031	-0.030
	16	22613	23333	0.027	0.015	0.021	0.024	-0.054	-0.053	-0.042	-0.041
	17	24497	25256	0.036	0.024	0.028	0.040	-0.069	-0.069	-0.059	-0.059
	18	24497	25256	0.043	0.040	0.035	0.059	-0.087	-0.087	-0.076	-0.074
	19	25251	25897	0.049	0.049	0.040	0.075	-0.104	-0.104	-0.092	-0.090
	20	24749	25513	0.052	0.078	0.040	0.120	-0.116	-0.114	-0.119	-0.116
	21	24749	25513	0.054	0.098	0.042	0.148	-0.162	-0.160	-0.142	-0.138
	22	25503	26154	0.059	0.115	0.043	0.174	-0.180	-0.177	-0.158	-0.154
	23	25879	26667	0.060	0.124	0.045	0.187	-0.190	-0.186	-0.167	-0.163
	24	26508	27308	0.062	0.131	0.046	0.197	-0.200	-0.196	-0.175	-0.170
	25	26256	27179	0.068	0.137	0.051	0.208	-0.217	-0.214	-0.189	-0.185
	26	26759	27564	0.077	0.145	0.060	0.220	-0.253	-0.253	-0.196	-0.191
	27	26884	27821	0.082	0.153	0.065	0.231	-0.283	-0.283	-0.201	-0.197
	28	26759	27692	0.106	0.166	0.093	0.250	-0.333	-0.332	-0.212	-0.207
	29	26759	27692	0.136	0.169	0.131	0.256	-0.366	-0.365	-0.219	-0.213
	30	22236	23077	0.133	0.167	0.129	0.252	-0.357	-0.354	-0.216	-0.210
	31	15829	16538	0.126	0.165	0.125	0.245	-0.341	-0.338	-0.212	-0.207
	32	*8794*	*9231*	*0.117*	*0.160*	*0.120*	*0.233*	*-0.318*	*-0.319*	*-0.207*	*-0.204*
	33	0	-128	0.101	0.151	0.112	0.215	-0.279	-0.280	-0.203	-0.201
	34	7789	8077	0.111	0.154	0.115	0.226	-0.306	-0.307	-0.206	-0.201
	35	15327	15769	0.120	0.161	0.121	0.238	-0.322	-0.322	-0.216	-0.213
	36	23995	25128	0.133	0.170	0.128	0.255	-0.339	-0.339	-0.237	-0.232
	37	26759	27949	0.145	0.182	0.141	0.271	-0.351	-0.349	-0.264	-0.259
	38	27261	28590	0.160	0.189	0.159	0.280	-0.369	-0.367	-0.273	-0.268
	39	27638	29103	0.204	0.221	0.209	0.311	-0.416	-0.417	-0.322	-0.318
	40	27764	29487	0.228	0.266	0.228	0.344	-0.447	-0.448	-0.347	-0.346
	41	28266	29487	0.285	0.306	0.275	0.384	-0.475	-0.474	-0.409	-0.408
	42	29271	30513	0.332	0.336	0.312	0.419	-0.512	-0.510	-0.460	-0.458
	43	29774	31026	0.373	0.371	0.348	0.456	-0.547	-0.543	-0.501	-0.498
	44	30276	31282	0.432	0.418	0.400	0.506	-0.594	-0.587	-0.556	-0.553
	45	30905	31795	0.480	0.459	0.444	0.550	-0.632	-0.623	-0.603	-0.600
	46	31281	32179	0.505	0.516	0.466	0.608	-0.656	-0.647	-0.656	-0.653
	47	31658	32308	0.541	0.577	0.497	0.672	-0.696	-0.686	-0.703	-0.699
	48	32035	32821	0.603	0.606	0.569	0.705	-0.764	-0.750	-0.725	-0.721
	49	32538	33205	0.672	0.683	0.636	0.784	-0.820	-0.807	-0.802	-0.798
	50	32915	33462	0.760	0.741	0.718	0.844	-0.912	-0.897	-0.837	-0.834
	51	33291	33077	0.883	0.867	0.838	0.971	-1.011	-0.991	-0.954	-0.948
	52	29271	28846	0.934	0.988	0.888	1.116	-1.061	-1.043	-1.050	-1.045
	53	126	0	0.875	0.941	0.846	1.046	-0.952	-0.938	-1.004	-0.998

Raw Data

Load Stage	Channel Data Point	90 (in.)	91 (in.)	92 (in.)	93 (in.)	94 (in.)	95 (in.)	96 (in.)	97 (in.)	98 (in.)	99 (in.)
Live	1	0.000	0.000	0.000	0.000	0.000	0.000	0.000	0.000	0.000	0.000
	2	0.000	0.000	0.000	0.000	0.000	0.000	0.000	0.000	0.000	0.000
	3	0.000	0.001	0.001	0.002	0.000	0.000	0.001	0.000	0.002	0.001
	4	0.000	0.003	0.004	0.005	0.004	0.001	0.003	0.003	0.006	0.002
	5	0.001	0.004	0.005	0.007	0.004	0.001	0.005	0.004	0.007	0.002
	6	0.001	0.004	0.004	0.006	0.004	0.001	0.005	0.003	0.007	0.002
	7	0.001	0.002	0.002	0.004	0.004	0.001	0.004	0.002	0.003	0.002
	8	0.001	0.003	0.003	0.006	0.005	0.001	0.004	0.002	0.006	0.002
	9	0.002	0.004	0.005	0.007	0.006	0.001	0.005	0.004	0.007	0.002
	10	0.002	0.005	0.006	0.008	0.007	0.002	0.006	0.004	0.008	0.004
	11	0.004	0.007	0.008	0.011	0.008	0.003	0.007	0.006	0.010	0.004
	12	0.004	0.009	0.009	0.012	0.009	0.004	0.007	0.007	0.012	0.004
	13	0.007	0.010	0.010	0.013	0.010	0.006	0.009	0.009	0.014	0.007
	14	0.008	0.012	0.012	0.015	0.011	0.006	0.010	0.010	0.017	0.009
	15	0.008	0.013	0.012	0.016	0.012	0.006	0.010	0.010	0.018	0.009
	16	0.009	0.017	0.017	0.020	0.014	0.008	0.012	0.013	0.023	0.015
	17	0.011	0.019	0.019	0.022	0.016	0.010	0.015	0.016	0.026	0.017
	18	0.013	0.021	0.020	0.024	0.029	0.012	0.016	0.017	0.028	0.018
	19	0.013	0.021	0.021	0.025	0.032	0.012	0.017	0.018	0.028	0.020
	20	0.013	0.021	0.021	0.025	0.034	0.012	0.017	0.018	0.028	0.019
	21	0.013	0.021	0.021	0.024	0.034	0.012	0.017	0.018	0.028	0.019
	22	0.013	0.021	0.021	0.025	0.034	0.012	0.017	0.018	0.028	0.019
	23	0.013	0.021	0.021	0.025	0.034	0.012	0.017	0.018	0.028	0.019
	24	0.013	0.021	0.021	0.025	0.034	0.012	0.017	0.017	0.028	0.019
	25	0.013	0.021	0.021	0.025	0.034	0.012	0.017	0.017	0.028	0.019
	26	0.013	0.021	0.021	0.025	0.034	0.012	0.017	0.017	0.028	0.019
	27	0.013	0.021	0.021	0.026	0.034	0.013	0.017	0.017	0.029	0.019
	28	0.014	0.021	0.021	0.026	0.034	0.013	0.018	0.017	0.029	0.020
	29	0.014	0.021	0.021	0.026	0.035	0.013	0.018	0.018	0.029	0.020
	30	0.014	0.020	0.021	0.026	0.035	0.013	0.018	0.017	0.029	0.019
	31	0.013	0.019	0.020	0.025	0.035	0.013	0.017	0.017	0.028	0.018
	32	0.013	0.017	0.018	0.022	0.035	0.011	0.015	0.015	0.024	0.016
	33	0.005	0.007	0.006	0.012	0.048	0.006	0.007	0.009	0.013	0.009
	34	0.007	0.012	0.012	0.019	0.052	0.007	0.009	0.011	0.021	0.012
	35	0.009	0.015	0.015	0.023	0.055	0.009	0.012	0.013	0.025	0.014
	36	0.013	0.018	0.021	0.027	0.059	0.012	0.015	0.017	0.031	0.017
	37	0.013	0.020	0.022	0.028	0.060	0.012	0.016	0.017	0.032	0.018
	38	0.013	0.021	0.023	0.029	0.060	0.013	0.017	0.018	0.032	0.019
	39	0.013	0.021	0.023	0.029	0.061	0.013	0.017	0.018	0.033	0.020
	40	0.014	0.021	0.023	0.030	0.061	0.013	0.017	0.018	0.033	0.020
	41	0.014	0.021	0.023	0.030	0.061	0.013	0.017	0.018	0.033	0.021
	42	0.013	0.021	0.023	0.030	0.061	0.013	0.017	0.018	0.033	0.022
	43	0.013	0.021	0.023	0.031	0.061	0.013	0.017	0.018	0.033	0.023
	44	0.013	0.022	0.023	0.031	0.061	0.013	0.017	0.018	0.034	0.024
	45	0.014	0.022	0.024	0.031	0.062	0.013	0.017	0.019	0.034	0.024
	46	0.014	0.021	0.024	0.031	0.062	0.013	0.017	0.020	0.034	0.024
	47	0.014	0.022	0.024	0.031	0.062	0.013	0.017	0.020	0.034	0.024
	48	0.014	0.021	0.024	0.031	0.062	0.013	0.017	0.020	0.034	0.024
	49	0.013	0.021	0.024	0.031	0.062	0.013	0.017	0.020	0.034	0.024
	50	0.014	0.022	0.024	0.031	0.063	0.014	0.017	0.020	0.034	0.025
	51	0.014	0.022	0.024	0.031	0.063	0.014	0.017	0.021	0.034	0.026
	52	0.015	0.021	0.023	0.032	0.063	0.015	0.017	0.020	0.034	0.024
	53	*0.004*	*0.006*	*0.006*	*0.012*	*0.063*	*0.005*	*0.004*	*0.010*	*0.010*	*0.010*

<u>Raw Data</u>

Load Stage	Channel Data Point	104 *(in.)*	105 *(in.)*	106 *(in.)*	107 *(in.)*	108 *(in.)*	DG1 *(in.)*	DG2 *(in.)*	DG3 *(in.)*	DG4 *(in.)*
Live	1	0.000	0.000	0.000	0.000	0.000	0.0000	0.0000	0.0000	0.0000
	2	-0.002	0.001	0.000	0.000	0.000	0.0000	0.0000	0.0000	0.0000
	3	-0.004	-0.004	-0.008	-0.054	-0.030	-0.0018	-0.0015	-0.0061	-0.0005
	4	-0.011	-0.010	-0.016	-0.108	-0.047	-0.0035	0.0019	-0.0089	-0.0011
	5	-0.015	-0.013	-0.021	-0.086	-0.108	-0.0040	0.0018	-0.0095	-0.0019
	6	-0.017	-0.013	-0.016	-0.015	-0.127	-0.0027	0.0018	-0.0083	-0.0019
	7	-0.004	-0.005	-0.003	-0.017	-0.022	0.0000	0.0000	-0.0011	-0.0019
	8	-0.011	-0.009	-0.013	0.026	-0.166	-0.0021	0.0018	-0.0082	-0.0018
	9	-0.017	-0.013	-0.022	-0.076	-0.133	-0.0037	0.0018	-0.0100	-0.0019
	10	-0.030	-0.017	-0.032	-0.128	-0.120	-0.0041	0.0016	-0.0100	-0.0020
	11	-0.043	-0.022	-0.041	-0.147	-0.146	-0.0045	0.0012	-0.0107	-0.0021
	12	-0.051	-0.026	-0.049	-0.169	-0.168	-0.0049	0.0010	-0.0109	-0.0028
	13	-0.058	-0.028	-0.053	-0.190	-0.187	-0.0048	0.0005	-0.0105	-0.0033
	14	-0.064	-0.030	-0.061	-0.223	-0.228	-0.0028	0.0001	-0.0082	-0.0049
	15	-0.073	-0.036	-0.069	-0.268	-0.275	-0.0030	-0.0006	-0.0085	-0.0060
	16	-0.088	-0.050	-0.087	-0.361	-0.355	-0.0020	-0.0030	-0.0061	-0.0100
	17	-0.098	-0.056	-0.093	-0.445	-0.441	-0.0030	-0.0052	-0.0043	-0.0151
	18	-0.107	-0.059	-0.100	-0.532	-0.529	0.0000	-0.0085	-0.0022	-0.0204
	19	-0.111	-0.061	-0.103	-0.605	-0.602	-0.0008	-0.0111	-0.0029	-0.0241
	20	-0.111	-0.062	-0.104	-0.711	-0.701	0.0095	-0.0155	0.0050	-0.0295
	21	-0.111	-0.061	-0.103	-0.830	-0.841	0.0059	-0.0158	-0.0115	-0.0398
	22	-0.113	-0.062	-0.103	-0.923	-0.920	0.0088	-0.0187	-0.0112	-0.0445
	23	-0.115	-0.062	-0.104	-0.984	-0.942	0.0092	-0.0200	-0.0112	-0.0465
	24	-0.115	-0.063	-0.105	-1.070	-0.942	0.0085	-0.0211	-0.0119	-0.0481
	25	-0.122	-0.064	-0.107	-1.191	-0.935	0.0025	-0.0240	-0.0135	-0.0485
	26	-0.120	-0.064	-0.107	-1.364	-0.935	-0.0001	-0.0249	-0.0211	-0.0542
	27	-0.122	-0.065	-0.108	-1.503	-0.933	-0.0024	-0.0250	-0.0281	-0.0600
	28	-0.124	-0.066	-0.109	-1.799	-0.933	-0.0005	-0.0291	-0.0285	-0.0667
	29	-0.124	-0.066	-0.110	-2.004	-0.933	0.0053	-0.0325	-0.0240	-0.0675
	30	-0.122	-0.065	-0.104	-1.905	-0.955	0.0058	-0.0321	-0.0245	-0.0661
	31	-0.111	-0.056	-0.088	-1.725	-0.987	0.0059	-0.0310	-0.0251	-0.0640
	32	-0.092	-0.044	-0.070	-1.477	-1.028	0.0060	-0.0292	-0.0269	-0.0612
	33	-0.073	-0.030	-0.048	-1.025	-1.187	0.0055	-0.0262	-0.0295	-0.0554
	34	-0.081	-0.035	-0.061	-1.343	-1.079	0.0041	-0.0273	-0.0289	-0.0599
	35	-0.096	-0.047	-0.079	-1.470	-1.152	0.0041	-0.0288	-0.0278	-0.0622
	36	-0.118	-0.061	-0.101	-1.602	-1.294	0.0055	-0.0300	-0.0253	-0.0668
	37	-0.124	-0.065	-0.105	-1.704	-1.387	0.0058	-0.0300	-0.0239	-0.0709
	38	-0.126	-0.065	-0.107	-1.857	-1.387	0.0072	-0.0299	-0.0215	-0.0715
	39	-0.132	-0.066	-0.108	-2.104	-1.619	0.0083	-0.0290	-0.0195	-0.0708
	40	-0.135	-0.065	-0.111	-2.430	-1.621	0.0107	-0.0218	-0.0129	-0.0721
	41	-0.135	-0.068	-0.117	-2.439	-2.122	0.0190	-0.0150	-0.0025	-0.0722
	42	-0.139	-0.073	-0.121	-2.595	-2.436	0.0226	-0.0120	0.0046	-0.0758
	43	-0.141	-0.074	-0.124	-2.781	-2.655	0.0280	-0.0080	0.0111	-0.0758
	44	-0.145	-0.077	-0.127	-3.034	-2.963	0.0371	-0.0015	0.0220	-0.0724
	45	-0.147	-0.078	-0.130	-3.252	-3.232	0.0350	0.0033	0.0322	-0.0688
	46	-0.147	-0.079	-0.131	-3.399	-3.505	0.0558	0.0111	0.0385	-0.0680
	47	-0.150	-0.080	-0.133	-3.723	-3.692	0.0679	0.0205	0.0469	-0.0671
	48	-0.150	-0.082	-0.135	-4.231	-3.698	0.0750	0.0231	0.0584	-0.0559
	49	-0.154	-0.082	-0.136	-4.567	-4.120	0.0890	0.0345	0.0722	-0.0485
	50	-0.154	-0.082	-0.138	-5.302	-4.128	0.1000	0.0429	0.0922	-0.0384
	51	-0.156	-0.083	-0.141	-5.849	-4.840	0.1230	0.0635	0.1205	-0.0206
	52	-0.158	-0.083	-0.135	-6.240	-5.296	0.1500	0.0811	0.1408	-0.0081
	53	-0.094	-0.038	-0.063	-4.908	-5.592	0.1382	-0.0043	0.0209	0.0089

Test Comments

Data Point (With respect to the live stage of loading.)

1 zero gages
2 re-zero after adjusting rams
5 Small crack about 4" to north of centerline, direction transverse about 10" long.
6 Start unloading to re-align north ram
7 Zero load , re-align north ram
9 Second crack about 6" to north of centerline, about 24" long
14 Crack from edge to edge about 24" south of centerline. Two north cracks have joined and are extend from edge to edge. Crack about 10" south of centerline transverse from edge to edge.
16 New crack transverse from edge to edge about 18" south of centerline.
17 New transverse crack about 12" north of centerline extending to edge on one end and extending to and joining first crack on north side of slab. Small yielding noticed at bottom of shear plate south side directly adjacent to the girder
18 New crack at about 20" north of centerline, about 30" long transverse. New crack from edge to edge transverse about 24" north of centerline.
19 Small yield lines just above top and bottom bolt south plate. Small yield line in front of north seat angle north east
20 First crack on north side has opened to just over 1/4". Small yield lines above top and bottom bolt in north shear tab. Yielding at base of south shear tab continues to increase.
21 Small yielding noticed on north shear tab around all bolt mostly at top bolt though.
23 North ram keeps wanting to push west which is causing one side of the north slab to open up and one side to close.
24 Part of the reason for the increased crack size on the east side of the north part of the slab would be the connection eccentricity. Trying to balance connection rotations back out by displace only the south side.
26 New crack from edge to edge transverse about 4" south of centerline. West side of girder seems to be dropping with respect to middle.
28 Yielding around all bolts in shear tabs continuing as tab seems to be bending under the eccentricity of the connection.
29 Notice yielding around bolt in south seat angle south west bolt. Also notice yielding along bottom fillet of south
30 Start unloading to add lateral braces to top flange of beam. Or to straighten out rams
33 zero load, added lateral braces to top flange, they are arranged such that they should both push the beams to the east thus trying to even out the cracking in the slab
34 Start reloading
36 Noticed small yielding in front of top bolt in web of north connection. Added small jack between flanges on north beam to keep flanges from rotating with respect to each other.
38 Noticed some yielding at fillet on bottom side of north seat angle, also some yielding around bolts in north seat angle
39 Noticed some yielding in front of top bolt in web of south connection. Yielding patterns in both shear tabs suggest that the top bolts are starting to go more into bearing to resist moment rather than resisting shear.
42 Slab cracking appears to be evening out. Notice that flanges have taken an angle that is above that associated with the flange at the seat angle. This would tend to increase the measured angle based on the bottom potentiometers.
42 Yielding of bottom flange along outstanding edge of seat angle.
44 Appears to be some shear yielding patterns in the web of the north connection. *Some yielding in front of middle bolt*
45 Notice some yielding in front of middle bolt web of south connection.
49 Yielding in front of bottom bolt in webs both connections. Yielding pattern in bottom flange of south connection just in front of free edge of angle showing possible soon local buckling.
52 Reinforcing bar #7 ruptured
53 unload and end test

Calculated Data Data Point	*Using POTS Only* North Rotation (rad)	North Moment (k-in.)	*Using POTS Only* South Rotation (rad)	South Moment (k-in.)	*POTS & DG* North Rotation (rad)	*POTS & DG* South Rotation (rad)
1	0.0000	82	0.0000	82	0.0000	0.0000
2	0.0000	73	0.0000	82	0.0000	0.0000
3	0.0002	396	0.0003	412	0.0001	0.0003
4	0.0003	658	0.0007	688	0.0001	0.0006
5	0.0006	780	0.0008	804	0.0003	0.0007
6	0.0006	484	0.0005	501	0.0002	0.0007
7	0.0002	82	0.0001	82	0.0001	0.0002
8	0.0006	484	0.0004	501	0.0001	0.0006
9	0.0006	780	0.0008	795	0.0003	0.0008
10	0.0007	868	0.0009	893	0.0004	0.0008
11	0.0008	999	0.0011	1026	0.0005	0.0009
12	0.0010	1121	0.0012	1151	0.0007	0.0010
13	0.0011	1182	0.0014	1214	0.0008	0.0012
14	0.0014	1217	0.0019	1249	0.0011	0.0018
15	0.0017	1427	0.0023	1472	0.0013	0.0021
16	0.0025	1654	0.0031	1704	0.0020	0.0029
17	0.0037	1785	0.0041	1837	0.0033	0.0038
18	0.0050	1785	0.0051	1837	0.0049	0.0046
19	0.0062	1837	0.0060	1882	0.0063	0.0053
20	0.0087	1802	0.0065	1855	0.0094	0.0053
21	0.0106	1802	0.0084	1855	0.0118	0.0068
22	0.0121	1854	0.0092	1900	0.0137	0.0072
23	0.0129	1881	0.0097	1935	0.0148	0.0074
24	0.0135	1924	0.0102	1980	0.0157	0.0077
25	0.0144	1907	0.0111	1971	0.0168	0.0083
26	0.0151	1942	0.0129	1998	0.0179	0.0097
27	0.0157	1950	0.0144	2016	0.0189	0.0107
28	0.0168	1942	0.0174	2007	0.0205	0.0135
29	0.0172	1942	0.0201	2007	0.0208	0.0164
30	0.0170	1627	0.0196	1686	0.0205	0.0161
31	0.0167	1182	0.0187	1231	0.0200	0.0155
32	0.0162	693	0.0176	724	0.0192	0.0149
33	0.0155	82	0.0156	73	0.0178	0.0136
34	0.0158	623	0.0169	643	0.0185	0.0144
35	0.0166	1147	0.0178	1178	0.0195	0.0151
36	0.0180	1750	0.0189	1828	0.0207	0.0161
37	0.0196	1942	0.0199	2024	0.0220	0.0174
38	0.0203	1977	0.0213	2069	0.0226	0.0188
39	0.0236	2003	0.0251	2105	0.0254	0.0230
40	0.0262	2012	0.0272	2131	0.0286	0.0247
41	0.0303	2047	0.0304	2131	0.0316	0.0290
42	0.0336	2116	0.0336	2203	0.0343	0.0327
43	0.0367	2151	0.0365	2238	0.0371	0.0359
44	0.0408	2186	0.0405	2256	0.0408	0.0403
45	0.0445	2230	0.0439	2292	0.0447	0.0439
46	0.0489	2256	0.0458	2318	0.0486	0.0458
47	0.0533	2282	0.0488	2327	0.0534	0.0483
48	0.0554	2308	0.0541	2363	0.0558	0.0535
49	0.0616	2343	0.0591	2390	0.0618	0.0587
50	0.0654	2370	0.0662	2408	0.0663	0.0651
51	0.0752	2396	0.0751	2381	0.0760	0.0741
52	0.0844	2116	0.0791	2087	0.0861	0.0772
53	0.0802	91	0.0728	82	0.0852	0.0773

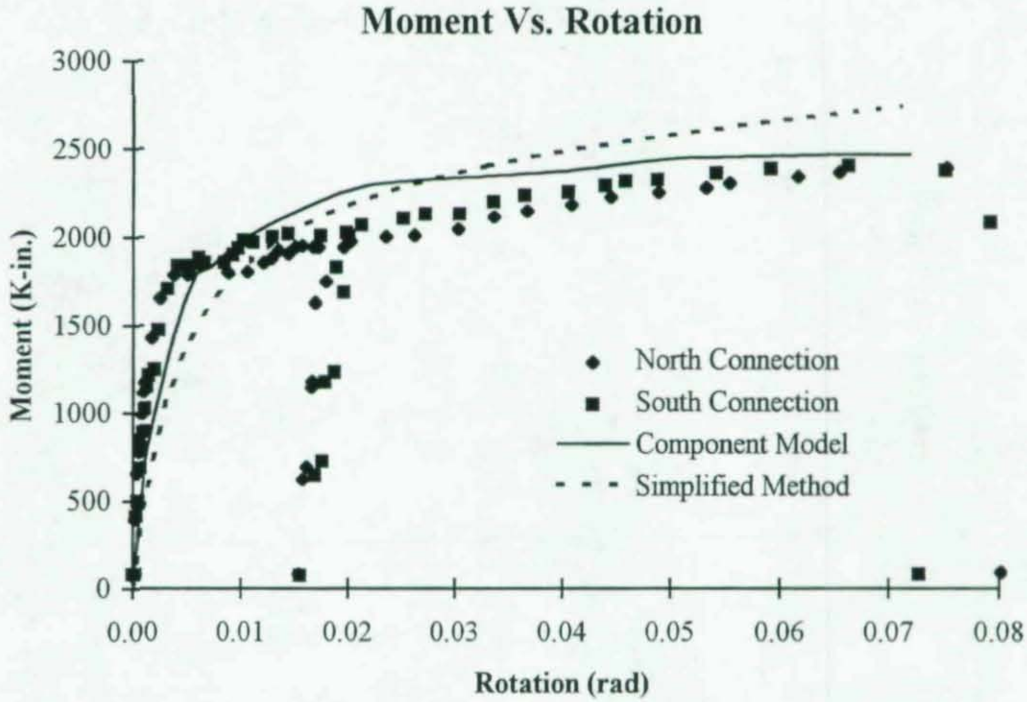
Moment Vs. Rotation
3000
2500
2000
1500
1000
500
0
Moment (K-in.)
0.00
0.01
0.02
0.03
0.04
0.05
0.06
0.07
0.08
Rotation (rad)
North Connection
South Connection
Component Model
Simplified Method

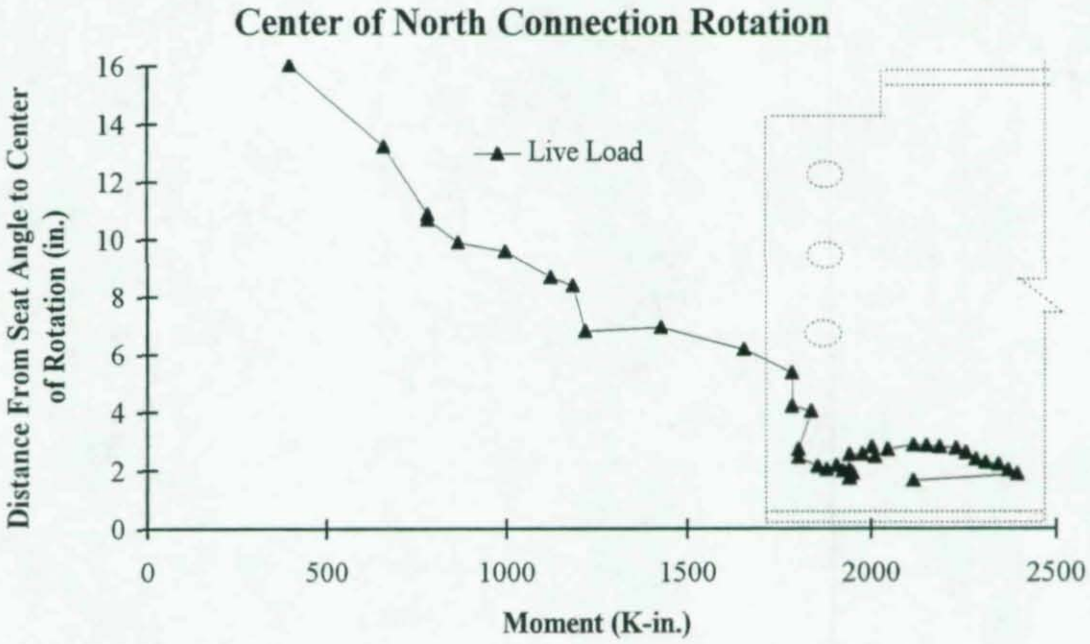
Center of North Connection Rotation
16
14
12
10
8
6
4
2
0
Distance From Seat Angle to Center of Rotation (in.)
0
500
1000
1500
2000
2500
Moment (K-in.)
Live Load

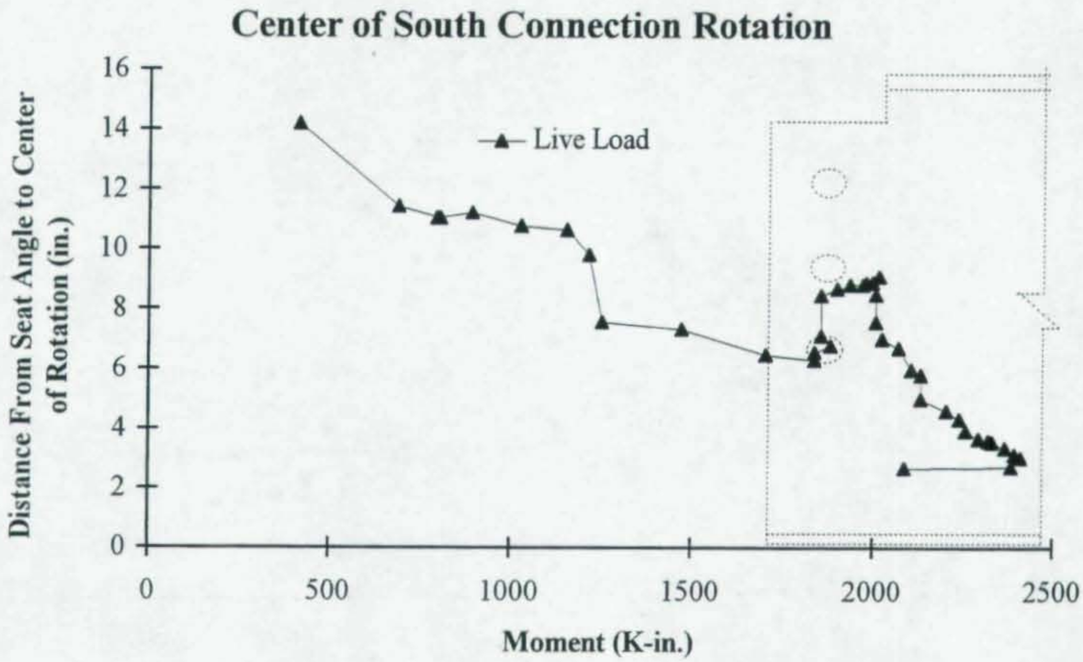
Center of South Connection Rotation
Distance From Seat Angle to Center of Rotation (in.)
Live Load
Moment (K-in.)
0
2
4
6
8
10
12
14
16
0
500
1000
1500
2000
2500

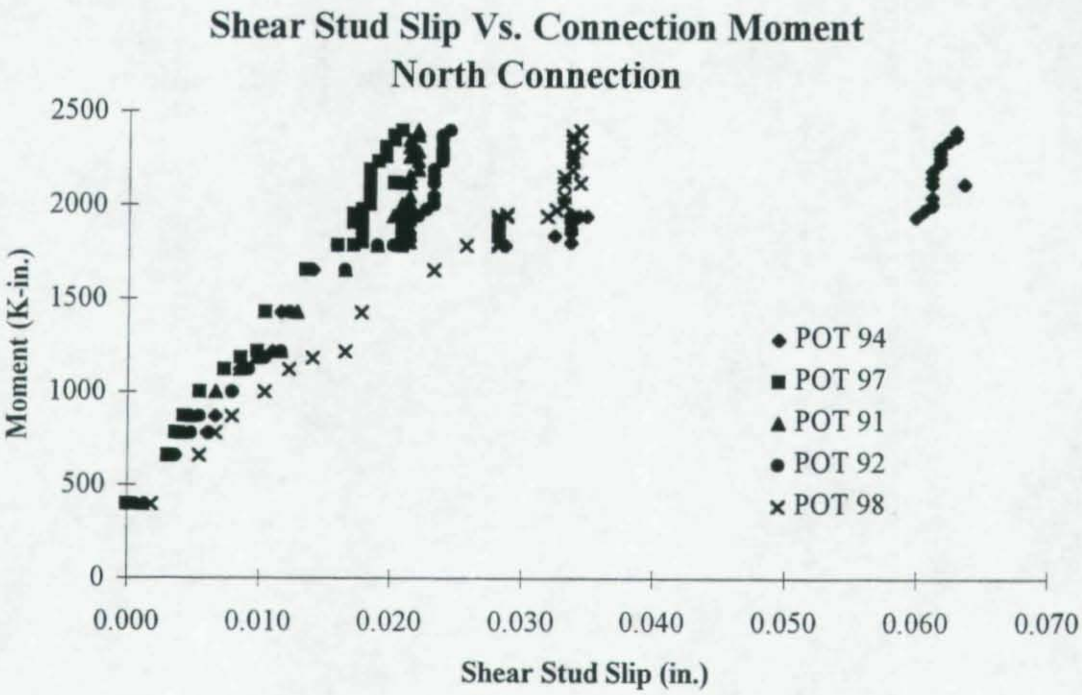
Shear Stud Slip Vs. Connection Moment
North Connection
Moment (K-in.)
Shear Stud Slip (in.)
POT 94
POT 97
POT 91
POT 92
POT 98
0
500
1000
1500
2000
2500
0.000
0.010
0.020
0.030
0.040
0.050
0.060
0.070

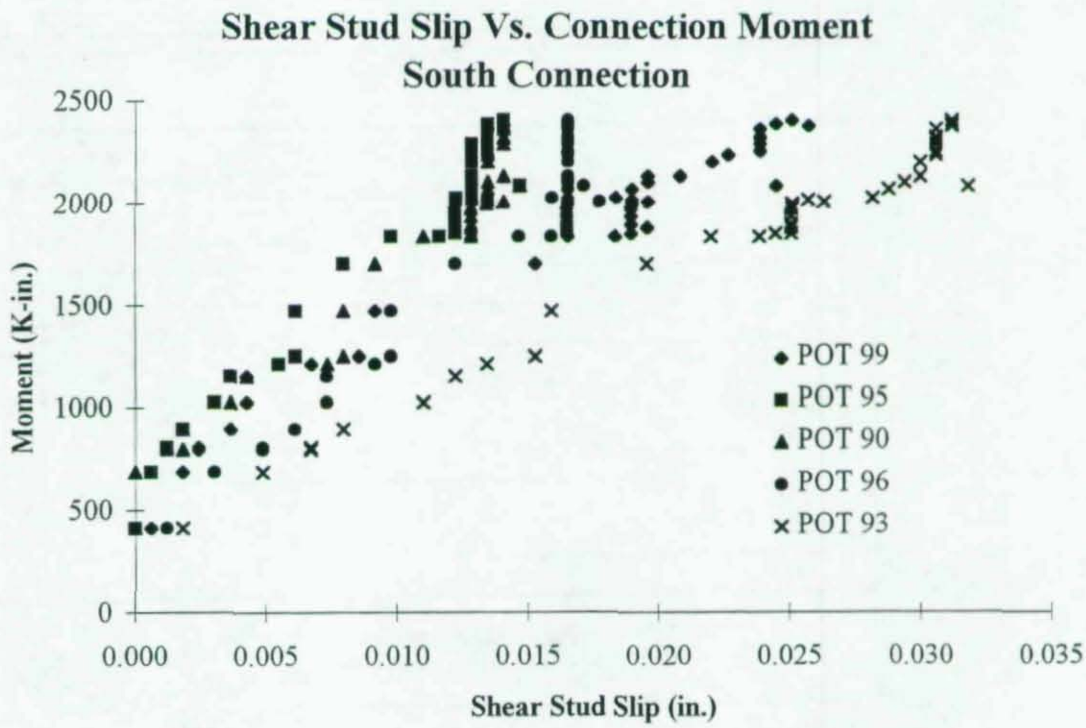
Shear Stud Slip Vs. Connection Moment
South Connection
Moment (K-in.)
2500
2000
1500
1000
500
0
0.000
0.005
0.010
0.015
0.020
0.025
0.030
0.035
Shear Stud Slip (in.)
POT 99
POT 95
POT 90
POT 96
POT 93

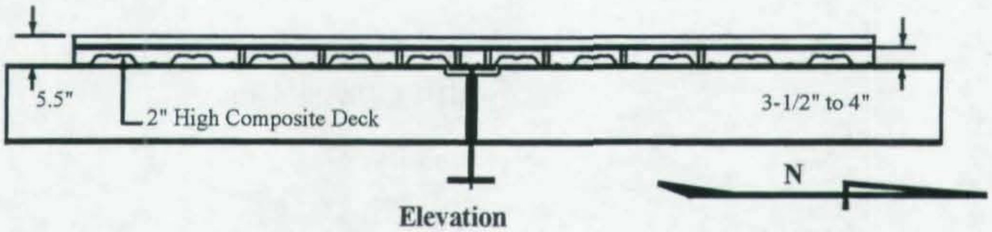

Elevation

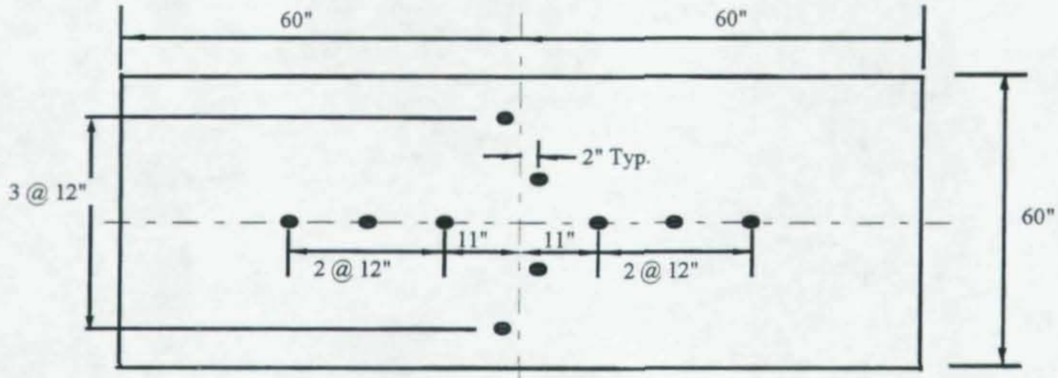

Shear Stud Layout
(3/4" Dia. x 4" High Headed Shear Studs)

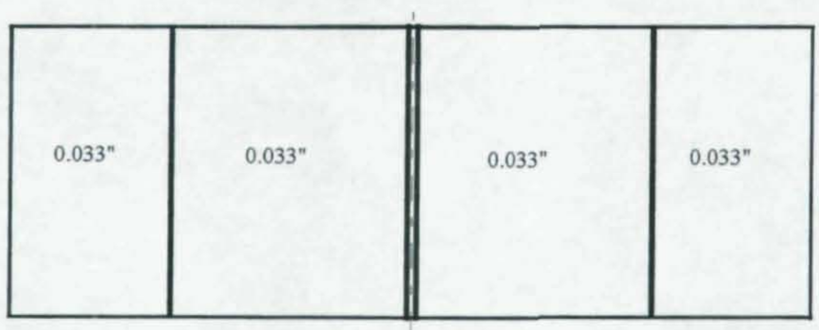

Deck Layout & Thickness

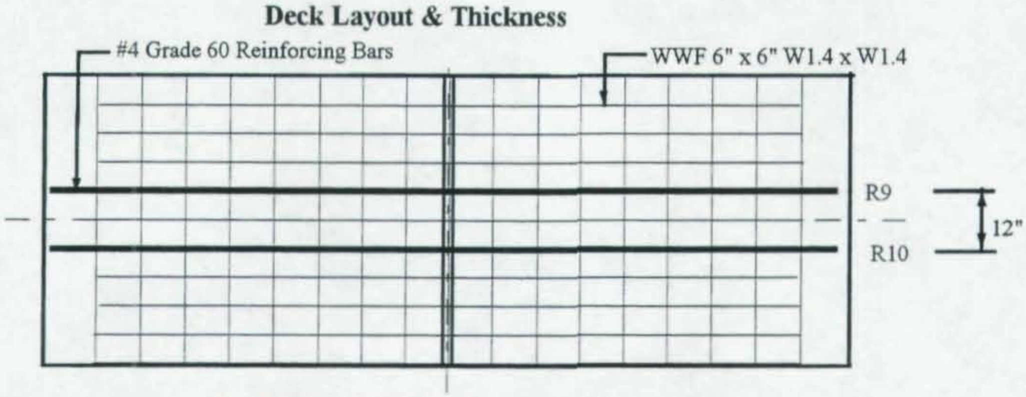

Reinforcing Identification & Layout

Reinforced Composite Deck Information

Description of Instrumentation

Channel	Sense of Extension	Description of Measurement	Load Stage	Gage Type	Sensitivity	Full Scale
2	Compression (-)	North Load Ram	Dead	Load Cell	0.7135	20,000 lbs
1	Compression (-)	South Load Ram	Dead	Load Cell	0.731	20,000 lbs
2	Compression (-)	North Load Ram	Live	Load Cell	0.92	150 kips
1	Compression (-)	South Load Ram	Live	Load Cell	1.95	500 kips
80	-**	Connection Rotation	Dead/Live	POT		6"
83	-**	Connection Rotation	Dead/Live	POT		6"
84	-**	Connection Rotation	Dead/Live	POT		6"
85	-**	Connection Rotation	Dead/Live	POT		6"
86	-**	Connection Rotation	Dead/Live	POT		6"
87	-**	Connection Rotation	Dead/Live	POT		6"
88	-**	Connection Rotation	Dead/Live	POT		6"
89	-**	Connection Rotation	Dead/Live	POT		6"
92	-**	Stud Slip	Live	POT		6"
93	-**	Stud Slip	Live	POT		6"
94	-**	Stud Slip	Live	POT		6"
95	-**	Stud Slip	Live	POT		6"
96	-**	Stud Slip	Live	POT		6"
97	-**	Stud Slip	Live	POT		6"
104	+	Girder Deflection	Dead/Live	DCDT 5	0.939	20"
105	-**	Girder Deflection	Dead/Live	DCDT 8	0.949	10"
106	+	Girder Deflection	Dead/Live	DCDT 11	0.943	10"
107	-**	Filler Beam Deflection	Dead/Live	DCDT 9	0.942	20"
108	+	Filler Beam Deflection	Dead/Live	DCDT 4	0.948	20"
DG1	-**	Connection Rotation	Live	Dial Gage		1"
DG2	-**	Connection Rotation	Live	Dial Gage		1"
DG3	-**	Connection Rotation	Live	Dial Gage		1"
DG4	-**	Connection Rotation	Live	Dial Gage		1"

** All data has been modified so that (+) readings indicate extension.

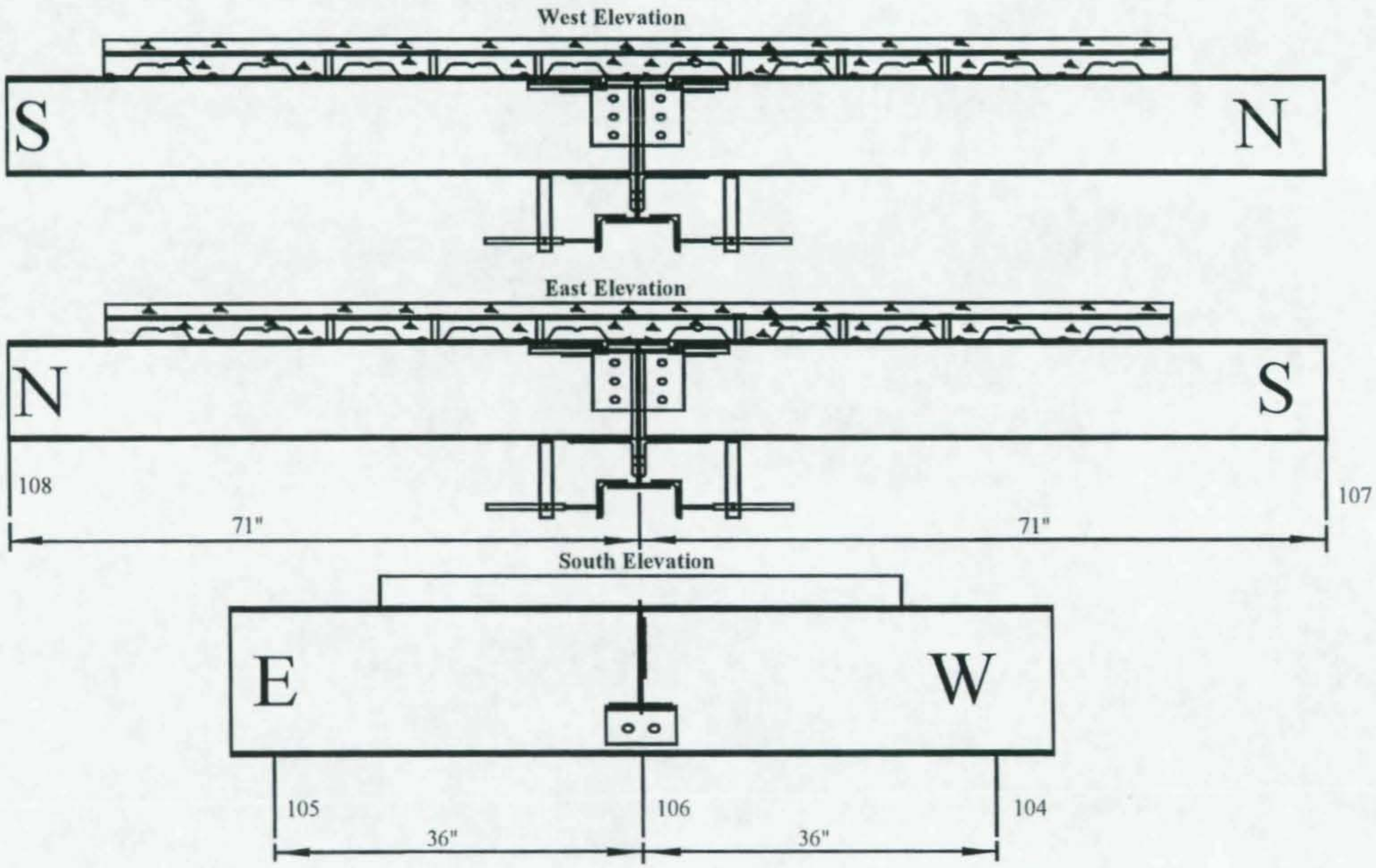

Stud Slip & Beam Deflection Instrumentation Dead Loading Stage

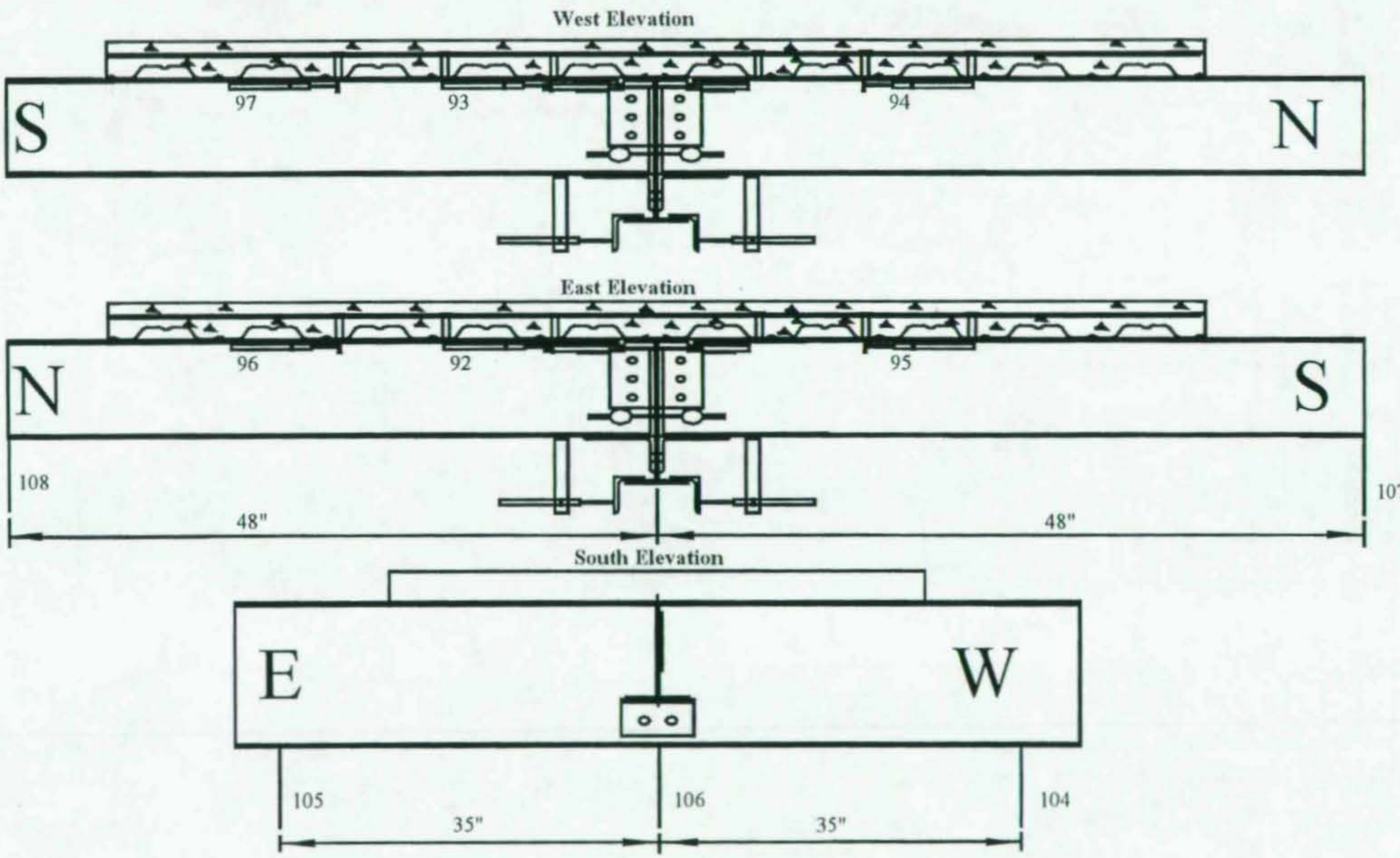

Stud Slip & Beam Deflection Instrumentation Live Loading Stage

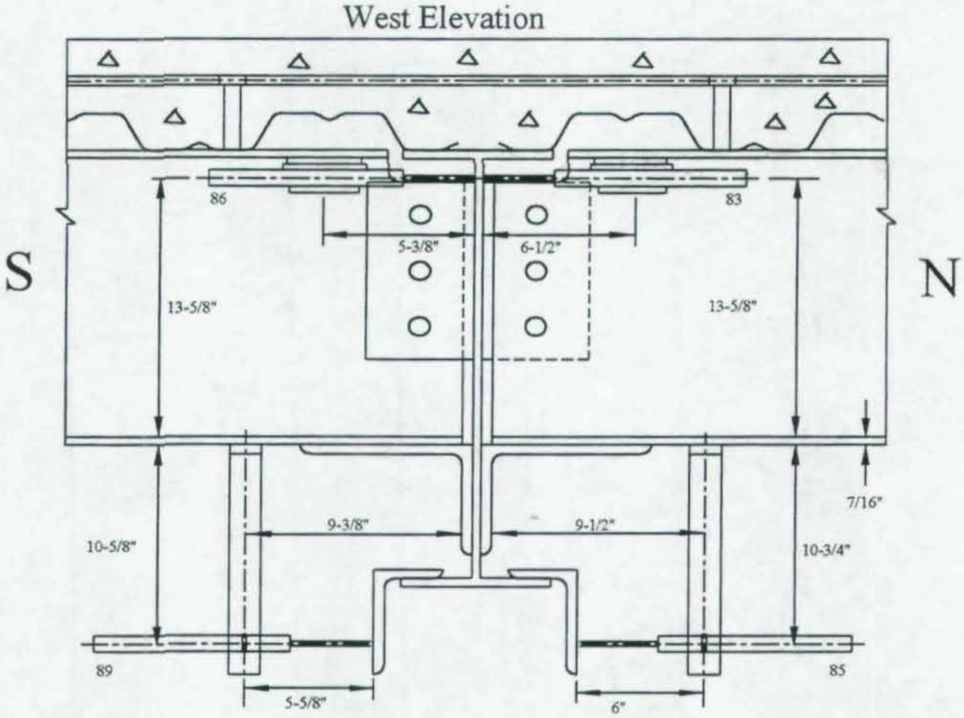

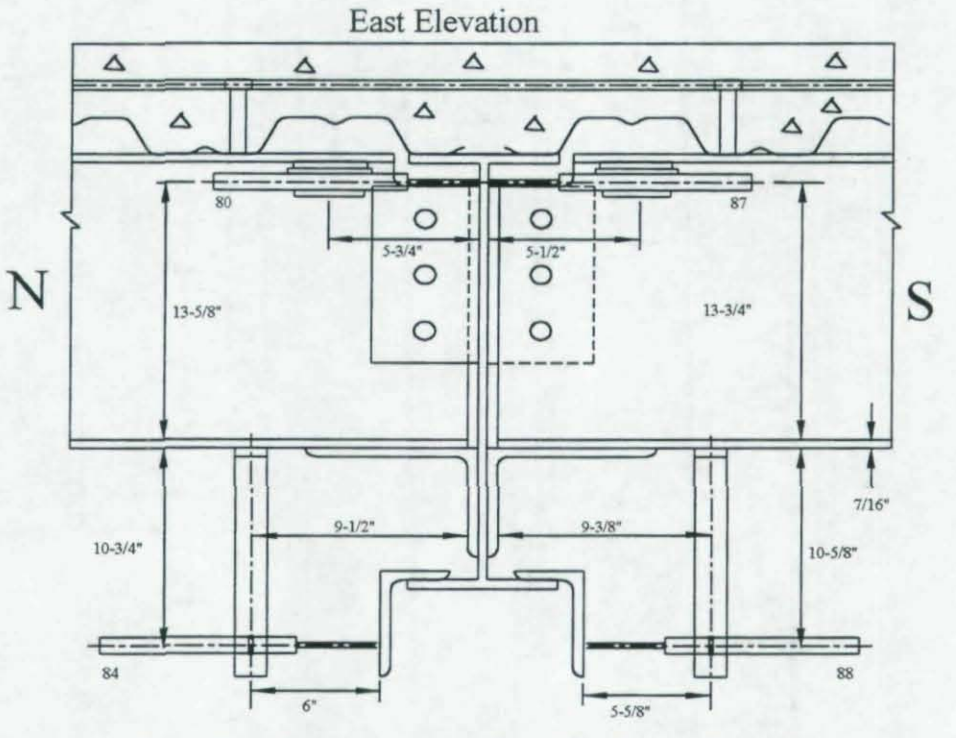

Rotation Instrumentation Dead Loading Stage

West Elevation

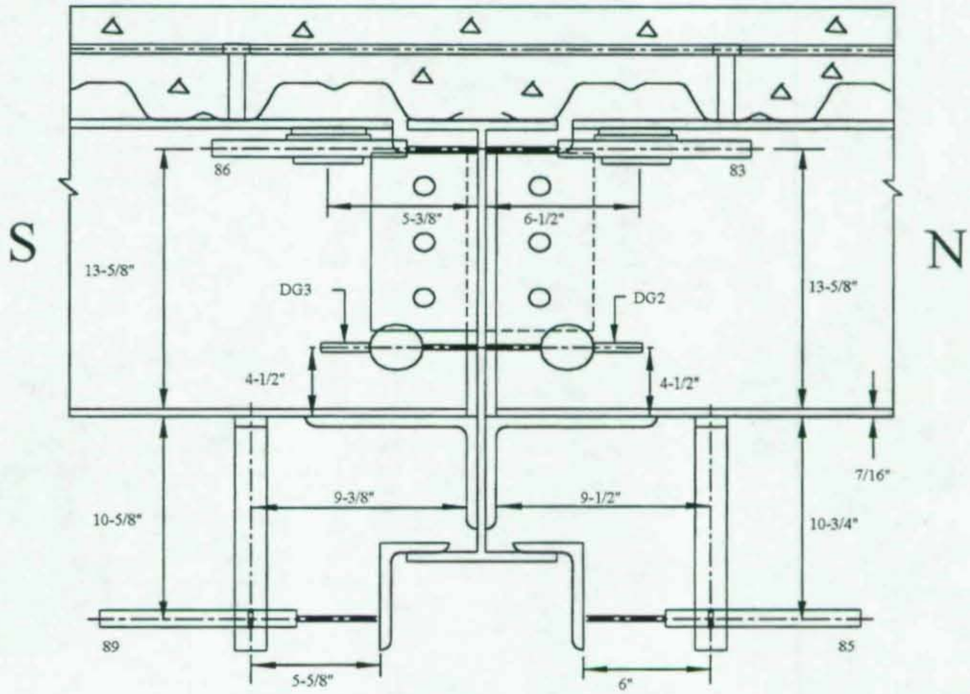

East Elevation

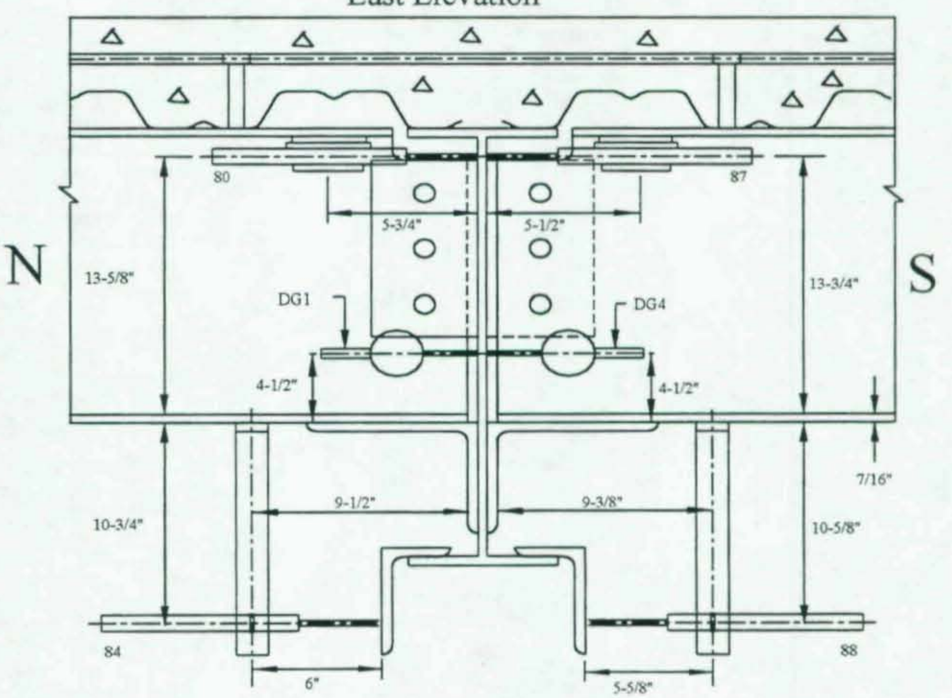

Rotation Instrumentation Live Loading Stage

Raw Data

Load Stage	Channel Data Point	2 (lbs)	1 (lbs)	80 (in.)	83 (in.)	84 (in.)	85 (in.)	86 (in.)	87 (in.)	88 (in.)	89 (in.)	92 (in.)	93 (in.)
Dead Load	1	0	0	0.001	0.000	0.001	0.001	0.000	0.000	0.001	0.000	-	-
	2	0	0	0.002	0.001	0.002	0.001	0.001	0.001	0.001	0.001	-	-
	3	0	0	0.002	0.001	0.001	-0.001	0.002	0.002	-0.006	-0.005	-	-
	4	0	0	0.002	0.001	0.001	-0.001	0.002	0.002	-0.006	-0.005	-	-
	5	631	616	0.002	0.002	-0.002	-0.004	0.002	0.003	-0.007	-0.007	-	-
	6	1009	1012	0.003	0.003	-0.002	-0.004	0.002	0.005	-0.009	-0.009	-	-
	7	2018	1970	0.005	0.006	-0.007	-0.010	0.003	0.006	-0.010	-0.009	-	-
	8	2985	3037	0.007	0.007	-0.009	-0.011	0.004	0.009	-0.015	-0.014	-	-
	9	3980	3926	0.008	0.010	-0.013	-0.015	0.006	0.011	-0.015	-0.015	-	-
	10	5046	5048	0.010	0.013	-0.015	-0.017	0.009	0.013	-0.021	-0.020	-	-
	11	5816	5937	0.012	0.015	-0.021	-0.021	0.010	0.016	-0.023	-0.021	-	-
	12	6685	6949	0.015	0.020	-0.023	-0.024	0.012	0.019	-0.027	-0.027	-	-
	13	7989	7962	0.019	0.024	-0.030	-0.032	0.015	0.023	-0.028	-0.027	-	-
	14	8802	8837	0.025	0.031	-0.037	-0.038	0.017	0.025	-0.032	-0.032	-	-
	15	9671	9836	0.032	0.039	-0.044	-0.045	0.023	0.033	-0.038	-0.037	-	-
	16	10792	10848	0.038	0.047	-0.052	-0.052	0.032	0.042	-0.045	-0.045	-	-
	17	11731	11778	0.051	0.059	-0.063	-0.065	0.038	0.050	-0.054	-0.054	-	-
	18	12908	13119	0.067	0.078	-0.081	-0.081	0.055	0.070	-0.068	-0.068	-	-
	19	14198	14077	0.085	0.097	-0.096	-0.097	0.070	0.086	-0.082	-0.081	-	-
	20	14968	14788	0.100	0.114	-0.118	-0.118	0.090	0.108	-0.097	-0.096	-	-
Dead Un-Loa	21	14688	14555	0.102	0.114	-0.108	-0.113	0.090	0.107	-0.082	-0.080	-	-
	22	14702	14569	0.102	0.114	-0.108	-0.113	0.090	0.108	-0.082	-0.080	-	-
	23	14702	14583	0.102	0.114	-0.108	-0.113	0.090	0.108	-0.082	-0.080	-	-
	24	12880	12859	0.102	0.114	-0.105	-0.111	0.090	0.107	-0.082	-0.080	-	-
	25	10764	10752	0.101	0.113	-0.104	-0.109	0.089	0.107	-0.081	-0.079	-	-
	26	9264	9330	0.101	0.113	-0.102	-0.107	0.089	0.106	-0.081	-0.079	-	-
	27	7204	7264	0.101	0.111	-0.099	-0.105	0.088	0.105	-0.079	-0.077	-	-
	28	5354	5431	0.099	0.110	-0.097	-0.103	0.088	0.104	-0.077	-0.076	-	-
	29	3280	3228	0.097	0.107	-0.093	-0.099	0.087	0.102	-0.075	-0.074	-	-
	30	589	602	0.095	0.103	-0.086	-0.092	0.085	0.098	-0.073	-0.073	-	-
	31	0	0	0.095	0.103	-0.085	-0.090	0.085	0.097	-0.072	-0.071	-	-
Live	1	0	0	0.095	0.103	-0.085	-0.090	0.085	0.097	-0.072	-0.071	0.000	0.000
	2	815	897	0.095	0.103	-0.086	-0.090	0.085	0.097	-0.073	-0.072	0.000	0.000
	3	2609	2564	0.095	0.105	-0.090	-0.095	0.085	0.097	-0.072	-0.071	0.001	0.001
	4	3016	3077	0.095	0.105	-0.090	-0.095	0.085	0.097	-0.073	-0.073	0.001	0.001
	5	4321	4487	0.095	0.105	-0.091	-0.096	0.085	0.098	-0.074	-0.074	0.001	0.002
	6	5543	5769	0.095	0.106	-0.091	-0.096	0.086	0.098	-0.078	-0.077	0.002	0.002
	7	7337	7692	0.096	0.108	-0.094	-0.099	0.087	0.100	-0.078	-0.079	0.004	0.005
	8	9946	10513	0.098	0.110	-0.098	-0.104	0.088	0.103	-0.080	-0.079	0.008	0.008
	9	9946	10769	0.099	0.111	-0.096	-0.101	0.088	0.103	-0.084	-0.083	0.009	0.009
	10	13696	14615	0.101	0.113	-0.103	-0.109	0.088	0.105	-0.084	-0.084	0.010	0.010
	11	16630	17692	0.102	0.114	-0.110	-0.115	0.090	0.106	-0.088	-0.087	0.013	0.013
	12	18179	19103	0.103	0.115	-0.115	-0.120	0.091	0.108	-0.090	-0.089	0.013	0.014
	13	19728	20513	0.104	0.117	-0.122	-0.127	0.095	0.111	-0.111	-0.109	0.015	0.015
	14	21277	22051	0.107	0.121	-0.131	-0.135	0.098	0.116	-0.126	-0.126	0.015	0.015
	15	22500	23205	0.111	0.126	-0.148	-0.153	0.101	0.120	-0.132	-0.130	0.015	0.015
	16	23234	23974	0.114	0.129	-0.161	-0.167	0.106	0.124	-0.161	-0.155	0.017	0.016
	17	25109	25769	0.118	0.133	-0.169	-0.174	0.109	0.128	-0.169	-0.165	0.017	0.017
	18	26250	26923	0.122	0.137	-0.178	-0.184	0.114	0.133	-0.180	-0.175	0.017	0.018
	19	27310	27949	0.129	0.145	-0.195	-0.200	0.120	0.139	-0.199	-0.193	0.018	0.018
	20	28500	29000	0.145	0.162	-0.215	-0.220	0.130	0.150	-0.238	-0.230	0.018	0.020
	21	25190	26154	0.211	0.216	-0.261	-0.269	0.133	0.155	-0.267	-0.259	0.019	0.020
	22	26576	27564	0.268	0.266	-0.292	-0.299	0.135	0.157	-0.283	-0.275	0.019	0.020
	23	27473	28718	0.318	0.308	-0.324	-0.332	0.137	0.161	-0.302	-0.294	0.019	0.020
	24	28451	29872	0.362	0.347	-0.343	-0.353	0.141	0.166	-0.329	-0.319	0.019	0.020
	25	29103	30769	0.426	0.403	-0.371	-0.381	0.146	0.171	-0.365	-0.355	0.019	0.019
	26	29755	31538	0.503	0.470	-0.403	-0.414	0.153	0.179	-0.413	-0.401	0.020	0.018
	27	29837	31923	0.590	0.547	-0.446	-0.459	0.187	0.223	-0.476	-0.465	0.020	0.017
	28	27962	30000	0.599	0.557	-0.444	-0.457	0.273	0.330	-0.559	-0.549	0.020	0.018
	29	29592	31667	0.607	0.566	-0.446	-0.460	0.399	0.476	-0.680	-0.671	0.020	0.019
	30	30489	32821	0.628	0.587	-0.459	-0.472	0.505	0.596	-0.789	-0.782	0.020	0.020
	31	29348	31410	0.692	0.657	-0.527	-0.542	0.604	0.697	-0.865	-0.859	0.020	0.020
	32	30245	31667	0.876	0.845	-0.691	-0.708	0.729	0.786	-0.910	-0.901	0.020	0.020
	33	13043	14615	1.287	1.233	-0.909	-0.928	0.713	0.761	-0.923	-0.911	0.020	0.021

Raw Data

Load Stage	94 (in.)	95 (in.)	96 (in.)	97 (in.)	104 (in.)	105 (in.)	106 (in.)	107 (in.)	108 (in.)	DG1 (in.)	DG2 (in.)	DG3 (in.)	DG4 (in.)
Dead Load	-	-	-	-	0.000	0.003	-0.003	0.004	0.000	-	-	-	-
	-	-	-	-	-0.002	0.004	-0.005	0.006	-0.006	-	-	-	-
	-	-	-	-	-0.002	0.004	-0.005	0.004	-0.006	-	-	-	-
	-	-	-	-	-0.002	0.005	-0.004	0.004	-0.004	-	-	-	-
	-	-	-	-	-0.002	0.004	-0.004	0.004	-0.026	-	-	-	-
	-	-	-	-	-0.002	0.005	-0.004	-0.028	-0.011	-	-	-	-
	-	-	-	-	-0.002	0.005	-0.005	-0.015	-0.039	-	-	-	-
	-	-	-	-	-0.002	0.005	-0.006	-0.069	-0.045	-	-	-	-
	-	-	-	-	-0.002	0.005	-0.009	-0.063	-0.058	-	-	-	-
	-	-	-	-	-0.004	0.005	-0.011	-0.117	-0.058	-	-	-	-
	-	-	-	-	-0.009	0.005	-0.012	-0.108	-0.092	-	-	-	-
	-	-	-	-	-0.009	0.004	-0.014	-0.156	-0.092	-	-	-	-
	-	-	-	-	-0.009	0.002	-0.017	-0.149	-0.146	-	-	-	-
	-	-	-	-	-0.022	-0.064	-0.053	-0.210	-0.204	-	-	-	-
	-	-	-	-	-0.028	-0.064	-0.053	-0.236	-0.252	-	-	-	-
	-	-	-	-	-0.028	-0.064	-0.053	-0.292	-0.292	-	-	-	-
	-	-	-	-	-0.076	-0.070	-0.081	-0.363	-0.378	-	-	-	-
	-	-	-	-	-0.082	-0.070	-0.081	-0.463	-0.473	-	-	-	-
	-	-	-	-	-0.082	-0.074	-0.084	-0.551	-0.561	-	-	-	-
	-	-	-	-	-0.082	-0.077	-0.087	-0.648	-0.666	-	-	-	-
Dead Un-Loa	-	-	-	-	-0.082	-0.077	-0.087	-0.648	-0.666	-	-	-	-
	-	-	-	-	-0.080	-0.078	-0.089	-0.651	-0.666	-	-	-	-
	-	-	-	-	-0.078	-0.078	-0.089	-0.653	-0.666	-	-	-	-
	-	-	-	-	-0.078	-0.078	-0.090	-0.666	-0.660	-	-	-	-
	-	-	-	-	-0.078	-0.078	-0.090	-0.653	-0.662	-	-	-	-
	-	-	-	-	-0.078	-0.078	-0.090	-0.646	-0.641	-	-	-	-
	-	-	-	-	-0.078	-0.078	-0.090	-0.640	-0.615	-	-	-	-
	-	-	-	-	-0.078	-0.078	-0.088	-0.599	-0.621	-	-	-	-
	-	-	-	-	-0.078	-0.079	-0.083	-0.588	-0.589	-	-	-	-
	-	-	-	-	-0.076	-0.078	-0.079	-0.573	-0.535	-	-	-	-
	-	-	-	-	-0.073	-0.078	-0.078	-0.540	-0.555	-	-	-	-
Live	0.000	0.000	0.000	0.000	0.000	0.000	0.000	0.000	0.000	0.0000	0.0000	0.0000	0.0000
	0.000	0.000	0.001	0.000	0.000	0.000	0.000	-0.024	0.013	0.0000	0.0000	0.0000	0.0000
	0.002	0.000	0.003	0.000	0.000	-0.003	0.000	0.011	-0.034	0.0000	0.0000	0.0000	0.0000
	0.002	0.000	0.004	0.000	0.000	-0.002	0.001	-0.017	-0.022	0.0000	-0.0010	0.0000	-0.0010
	0.002	0.001	0.006	0.002	-0.006	-0.002	-0.002	-0.030	-0.015	0.0000	-0.0010	0.0000	-0.0010
	0.004	0.002	0.008	0.003	-0.006	-0.005	-0.005	-0.078	0.013	0.0000	-0.0010	-0.0050	-0.0010
	0.005	0.004	0.011	0.005	-0.006	-0.006	-0.008	-0.102	0.013	0.0000	-0.0010	-0.0010	-0.0010
	0.009	0.007	0.015	0.010	-0.013	-0.010	-0.017	-0.104	-0.015	0.0000	-0.0010	-0.0010	0.0000
	0.009	0.009	0.017	0.011	-0.013	-0.013	-0.019	-0.164	0.045	0.0000	0.0000	-0.0010	0.0000
	0.012	0.010	0.018	0.013	-0.015	-0.013	-0.022	-0.158	-0.009	0.0000	0.0000	-0.0010	0.0000
	0.015	0.012	0.021	0.015	-0.019	-0.019	-0.031	-0.158	-0.047	-0.0010	0.0000	0.0000	-0.0040
	0.016	0.014	0.023	0.017	-0.026	-0.022	-0.038	-0.158	-0.082	-0.0010	0.0000	0.0010	-0.0060
	0.018	0.018	0.024	0.020	-0.032	-0.028	-0.045	-0.164	-0.142	-0.0010	-0.0040	0.0010	-0.0170
	0.019	0.019	0.026	0.020	-0.035	-0.031	-0.049	-0.186	-0.189	-0.0020	-0.0050	0.0000	-0.0230
	0.021	0.020	0.026	0.021	-0.067	-0.037	-0.067	-0.236	-0.228	-0.0050	-0.0080	-0.0010	-0.0250
	0.022	0.023	0.028	0.024	-0.067	-0.042	-0.076	-0.272	-0.275	-0.0060	-0.0100	-0.0030	-0.0350
	0.024	0.023	0.029	0.024	-0.073	-0.044	-0.080	-0.305	-0.301	-0.0070	-0.0110	-0.0040	-0.0360
	0.025	0.024	0.031	0.026	-0.080	-0.048	-0.085	-0.335	-0.342	-0.0080	-0.0120	-0.0050	-0.0380
	0.027	0.026	0.032	0.028	-0.086	-0.052	-0.092	-0.385	-0.396	-0.0100	-0.0130	-0.0070	-0.0420
	0.030	0.030	0.034	0.031	-0.102	-0.058	-0.101	-0.458	-0.503	-0.0130	-0.0150	-0.0110	-0.0490
	0.030	0.031	0.035	0.032	-0.108	-0.061	-0.109	-0.612	-0.602	-0.0110	-0.0040	-0.0140	-0.0390
	0.031	0.031	0.035	0.032	-0.106	-0.061	-0.109	-0.705	-0.701	0.0020	0.0070	-0.0140	-0.0340
	0.032	0.031	0.035	0.032	-0.106	-0.062	-0.109	-0.804	-0.802	0.0110	0.0150	-0.0150	-0.0320
	0.032	0.031	0.035	0.032	-0.115	-0.064	-0.111	-0.992	-0.802	0.0190	0.0220	-0.0140	-0.0280
	0.032	0.031	0.036	0.032	-0.115	-0.067	-0.114	-1.245	-0.802	0.0330	0.0340	-0.0130	-0.0250
	0.032	0.031	0.036	0.032	-0.121	-0.070	-0.117	-1.561	-0.789	0.0500	0.0480	-0.0120	-0.0210
	0.033	0.032	0.037	0.034	-0.128	-0.074	-0.119	-1.993	-0.768	0.0690	0.0630	-0.0020	-0.0040
	0.032	0.032	0.037	0.034	-0.128	-0.074	-0.120	-2.302	-0.768	0.0750	0.0730	0.0160	0.0250
	0.032	0.032	0.037	0.034	-0.128	-0.076	-0.120	-2.812	-0.770	0.0820	0.0820	0.0410	0.0670
	0.033	0.033	0.037	0.033	-0.128	-0.078	-0.123	-3.294	-0.770	0.0920	0.0930	0.0580	0.0960
	0.032	0.033	0.037	0.033	-0.130	-0.082	-0.128	-3.560	-1.064	0.1120	0.1130	0.0800	0.1240
	0.032	0.033	0.037	0.034	-0.130	-0.082	-0.129	-3.567	-2.038	0.1700	0.1820	0.1100	0.1500
	0.031	0.031	0.035	0.032	-0.115	-0.083	-0.098	-3.675	-2.959	-	-	-	-

__Test Comments__

Data Point (With respect to the pre-load stage of loading.)

20 Cracks present in slab after applying preload, two cracks near girder centerline and parrallel with girder that go from edge to edge of the composite slab.

21 Before unloading dead load noticed bearing yield patterns around all three bolts in the shear plate. See
North: Shear Plate: Bearing yielding around all three bolt holes, primary yielding at top bolt hole with small yield patterns around bottom two bolt holes, also notice some slight yielding at the bottom support
North: Beam Web: Small bearing yield pattern at bolt hole #2
South: Shear plate: Bearing yielding around all three bolt holes, primary yielding at top bolt hole with small yield patterns around bottom two bolt holes
South: Beam Web: Bearing yielding around top two bolts, main yielding at top bolt hole (primarily above
Girder Web: Notice yield patterns on the face of the girder web near the location of the top of the shear plate, one or two inches away from the connection, perhaps local bending in the girder web induced by the tension in the shear tab

23 Removed screws from pour stop to see if any difference in the moment before and after screws removed.

24 Start unloading dead load.

31 Rods completely unloaded.

Data Point (With respect to the live-load stage of loading.)

1 zero all channels and take data point

2 applying about 1 kip on each ram

3 Power outage caused shutdown

4 Power outage caused shutdown

9 As loading up to this point heard a loud bang and load dropped, north deflection decreased, possibly load frame bolts slipping into bearing.

12 North: Shear Plate: tension yield at top support corner of plate

14 First real new crack in concrete since preload. About 1' south of girder centerline and parallel to girder from edge of slab to edge of slab.

16 On way to this point loud bang and load drop. Beam deflections remained about equal. South rotation increased but can't see anything of major slipping or cracking.

17 South: Shear Plate: yielding at bottom support corner of plate

18 Slab: Main crack right over girder centerline is expanding and now reaches from edge to edge of slab. This crack was initiated under the preloading stage.

19 South: Top side bottom flange: Web side: bolt farthest away from girder has small yield flakes around the bolt washer. Note this is the side that is taking the most deformation toward the girder.

20 South: Beam web: bearing yielding at Bolt #2 toward girder
South: Top side bottom flange: plate side: bolt fathest away from girder bearing yielding on side away
South: Bottom side of seat angle: Plate side: bolt farthest away from girder bearing yielding on side
****Note: forgot to take data point on sys 4000 here, make sure to add this point back into the data later

21 Loud sound like concrete cracking, can see that north side loosened up, visual inspection of north side slab shows crack over centerline of girder had widened significantly, almost 3/8" in some locations
North: Plate side: bolts #2 and #3 bearing yielding increasing around these bolts from the original yielding seen under the preload.
North: beam web: bolts #2 and #3 bearing yielding around these bolts increasing beyond what original yielding after preload was

22 North: top side bottom angle: web side: bolt farthest away from girder some bearing yielding on side away from girder
South side: web side: bearing yielding increasing around bolts #2 and #3

23 North: web side: bolt #1 bearing yielding toward support and inclined

24 North: Shear plate: bearing yielding around top two bolts progressing rapidly as the crack at the centerline of the girder in the concrete continues to widen,most of the crack is on the north side of the beam
Note: puposely trying to rotate the south side by only loading this side that is why the north deflection is not increasing while the south is. I hope to be able to increase the flexibility of the south side before the north side contiues to failure

25 Slab on north side of specimen is opening on the west side but not the east thus causing the beam to move to the east at the top but the bottom is held in place by the lateral braces. This results in the end of the beam becoming warped like LTB

26 Both sides: Bottom side of seat angle: yielding along outstanding toe of angle basically from edge to edge

28 Slab: new crack just south of girder centerline, this crack will start to soften the slab stiffness on the south side and increase these rotations, hopefully the rotations can then be balanced
South: Shear plate: bearing yielding around all bolts increased significantly as the slab softens, also on web side of connection

29 South slab: opening at crack but primarily on west side causing beam to lean to the east side

30 South: top side bottom flange: bearing yielding around most seat angle bolts
Rotations evened out now start to load both sides again

32 Top bolts on both sides are rotating to account for the plate bending of the web and shear plate (caused by the eccentric load being transferred)

33 Rebar fracture, end test, fracture was in the crack at the centline of girder on just the north side, the rebar was rebar #9 (west side of slab)
When the rebar fractured all the load was dumped onto the plate and it fractured in tension from the top of the plate through the top bolt hole all the way down to bolt hole #2

Calculated Data Data Point	*Using POTS Only* North Rotation (rad)	North Moment (k-in.)	*Using POTS Only* South Rotation (rad)	South Moment (k-in.)	*POTS & DG* North Rotation (rad)	*POTS & DG* South Rotation (rad)
1	0.0000	0	0.0000	0	-	-
2	0.0000	0	0.0000	0	-	-
3	0.0001	46	0.0003	46	-	-
4	0.0001	46	0.0003	46	-	-
5	0.0002	75	0.0004	74	-	-
6	0.0002	92	0.0005	92	-	-
7	0.0006	138	0.0006	136	-	-
8	0.0007	182	0.0008	184	-	-
9	0.0009	227	0.0010	225	-	-
10	0.0011	275	0.0013	276	-	-
11	0.0014	311	0.0014	316	-	-
12	0.0017	350	0.0017	362	-	-
13	0.0021	409	0.0019	408	-	-
14	0.0026	446	0.0021	448	-	-
15	0.0032	486	0.0026	493	-	-
16	0.0038	537	0.0033	539	-	-
17	0.0048	580	0.0039	582	-	-
18	0.0062	633	0.0053	643	-	-
19	0.0076	692	0.0064	686	-	-
20	0.0091	727	0.0079	719	-	-
21	0.0088	714	0.0072	708	-	-
22	0.0088	715	0.0073	709	-	-
23	0.0088	715	0.0073	709	-	-
24	0.0087	632	0.0072	631	-	-
25	0.0086	536	0.0072	535	-	-
26	0.0085	467	0.0072	470	-	-
27	0.0084	374	0.0070	376	-	-
28	0.0082	290	0.0070	293	-	-
29	0.0080	195	0.0068	193	-	-
30	0.0076	73	0.0066	73	-	-
31	0.0075	46	0.0066	46	-	-
1	0.0075	46	0.0066	46	0.0075	0.0066
2	0.0075	83	0.0066	87	0.0075	0.0066
3	0.0078	165	0.0065	163	0.0076	0.0066
4	0.0077	183	0.0066	186	0.0077	0.0066
5	0.0078	242	0.0067	250	0.0077	0.0067
6	0.0078	298	0.0068	308	0.0077	0.0070
7	0.0080	380	0.0069	396	0.0079	0.0069
8	0.0083	498	0.0071	524	0.0081	0.0071
9	0.0082	498	0.0072	536	0.0081	0.0071
10	0.0086	669	0.0073	711	0.0084	0.0072
11	0.0089	803	0.0075	851	0.0085	0.0075
12	0.0091	873	0.0076	915	0.0086	0.0077
13	0.0095	944	0.0086	979	0.0090	0.0086
14	0.0100	1014	0.0094	1049	0.0095	0.0094
15	0.0108	1070	0.0097	1102	0.0102	0.0099
16	0.0115	1103	0.0110	1137	0.0107	0.0110
17	0.0120	1188	0.0115	1218	0.0112	0.0115
18	0.0125	1240	0.0121	1271	0.0117	0.0121
19	0.0135	1288	0.0131	1318	0.0127	0.0131
20	0.0149	1343	0.0151	1365	0.0147	0.0148
21	0.0193	1192	0.0164	1236	0.0203	0.0148
22	0.0227	1255	0.0171	1300	0.0246	0.0148
23	0.0258	1296	0.0180	1353	0.0285	0.0150
24	0.0283	1340	0.0192	1405	0.0321	0.0152
25	0.0319	1370	0.0209	1446	0.0370	0.0155
26	0.0361	1400	0.0231	1481	0.0429	0.0161
27	0.0412	1403	0.0272	1498	0.0497	0.0187
28	0.0415	1318	0.0345	1411	0.0499	0.0263
29	0.0419	1392	0.0449	1487	0.0499	0.0370
30	0.0432	1433	0.0539	1539	0.0510	0.0463
31	0.0487	1381	0.0610	1475	0.0559	0.0541
32	0.0629	1422	0.0670	1487	0.0688	0.0623
33	0.0878	639	0.0666	711		

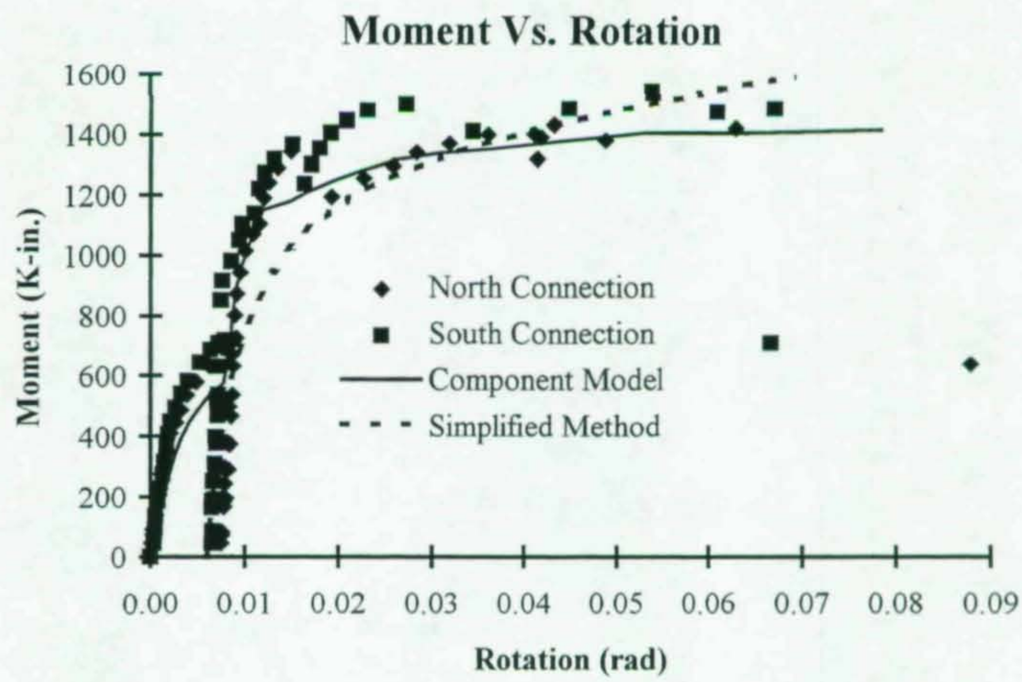

Moment Vs. Rotation
1600
1400
1200
1000
800
600
400
200
0
Moment (K-in.)
North Connection
South Connection
Component Model
Simplified Method
0.00
0.01
0.02
0.03
0.04
0.05
0.06
0.07
0.08
0.09
Rotation (rad)

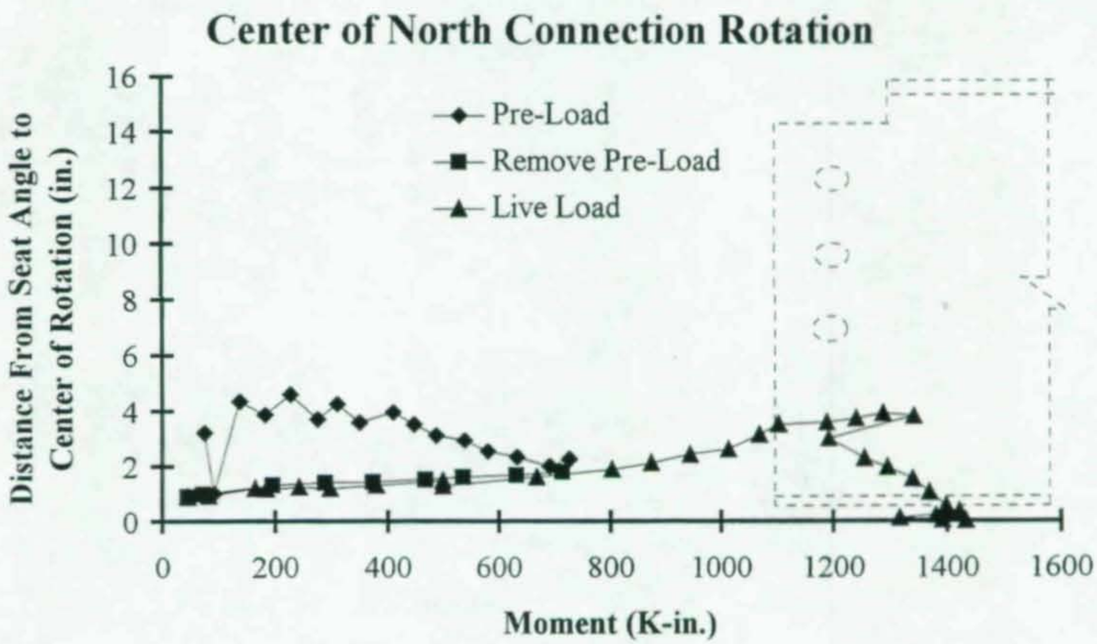

Center of North Connection Rotation
16
14
12
10
8
6
4
2
0
Distance From Seat Angle to Center of Rotation (in.)
Pre-Load
Remove Pre-Load
Live Load
0
200
400
600
800
1000
1200
1400
1600
Moment (K-in.)

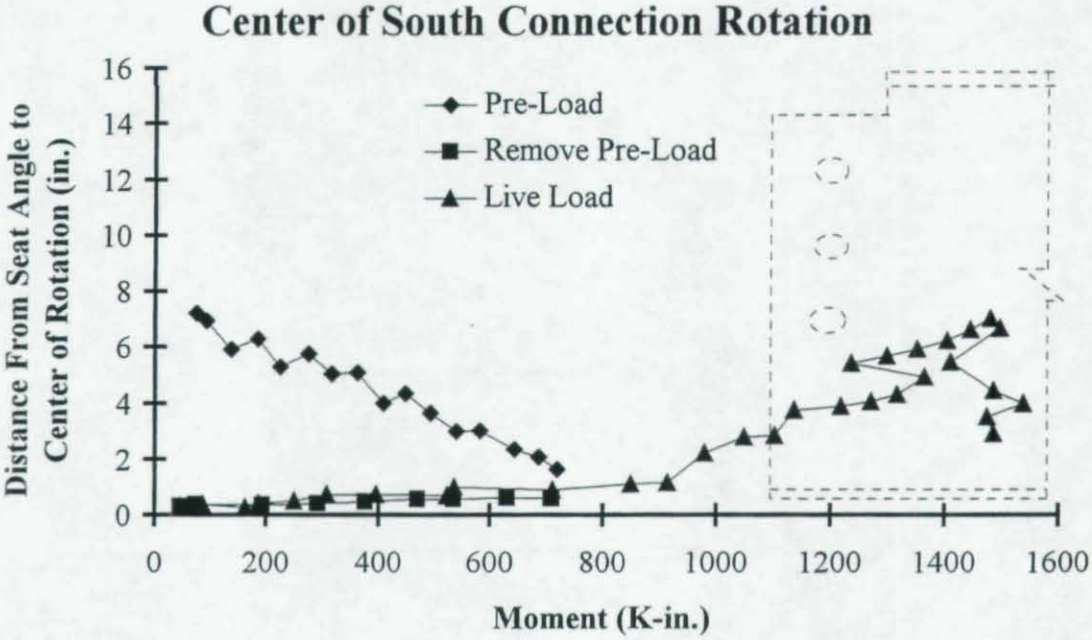
Center of South Connection Rotation
Distance From Seat Angle to Center of Rotation (in.)
Pre-Load
Remove Pre-Load
Live Load
Moment (K-in.)
0
2
4
6
8
10
12
14
16
0
200
400
600
800
1000
1200
1400
1600

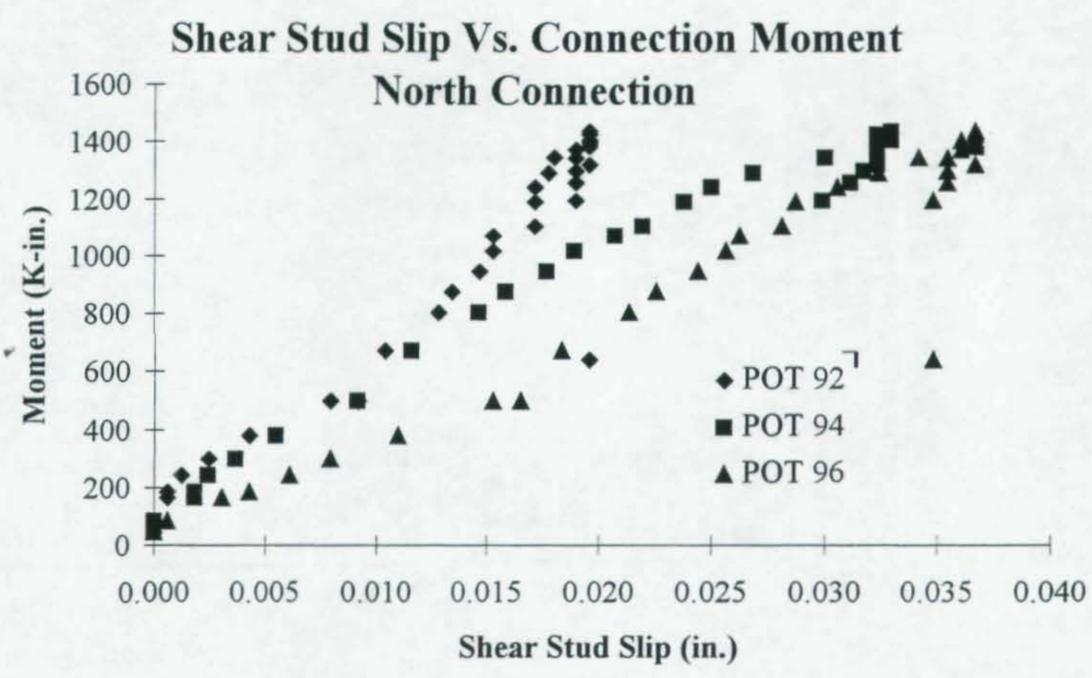
Shear Stud Slip Vs. Connection Moment
North Connection
Moment (K-in.)
POT 92
POT 94
POT 96
Shear Stud Slip (in.)
0
200
400
600
800
1000
1200
1400
1600
0.000
0.005
0.010
0.015
0.020
0.025
0.030
0.035
0.040

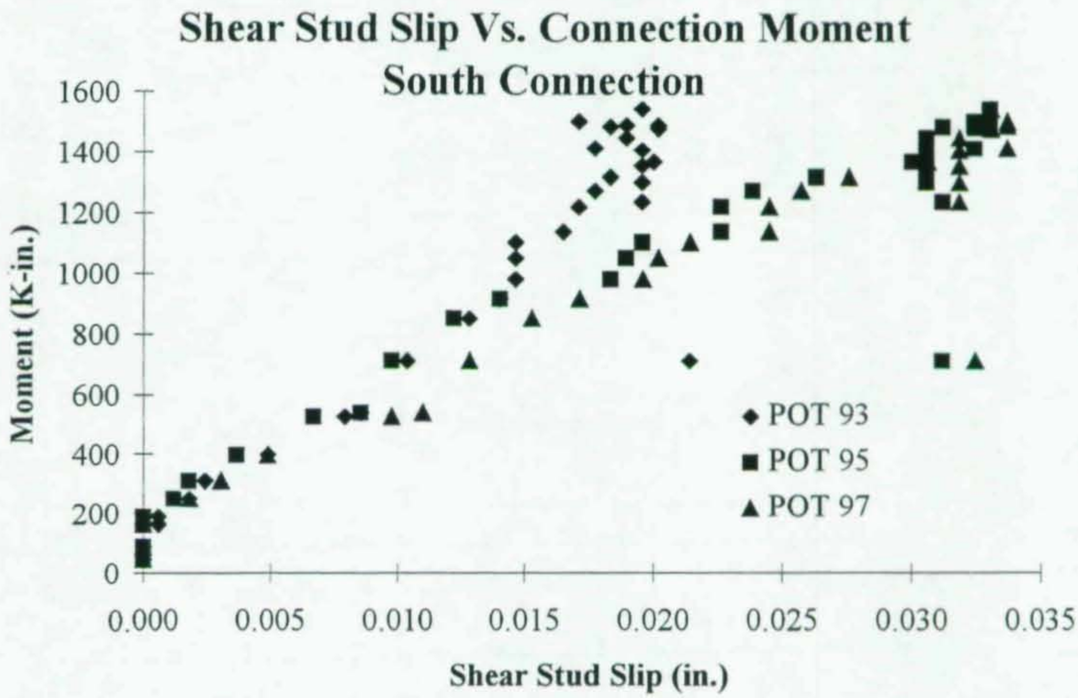
Shear Stud Slip Vs. Connection Moment
South Connection
Moment (K-in.)
1600
1400
1200
1000
800
600
400
200
0
0.000
0.005
0.010
0.015
0.020
0.025
0.030
0.035
Shear Stud Slip (in.)
POT 93
POT 95
POT 97

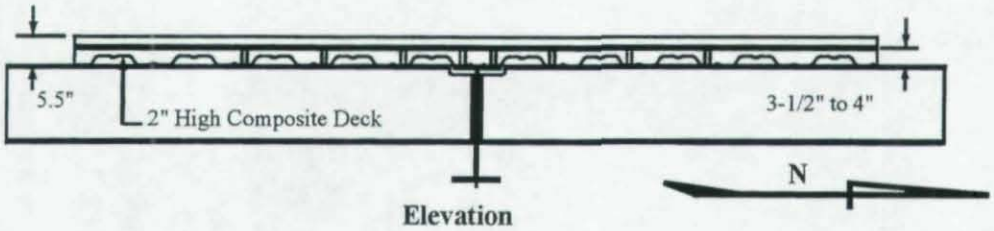

Elevation

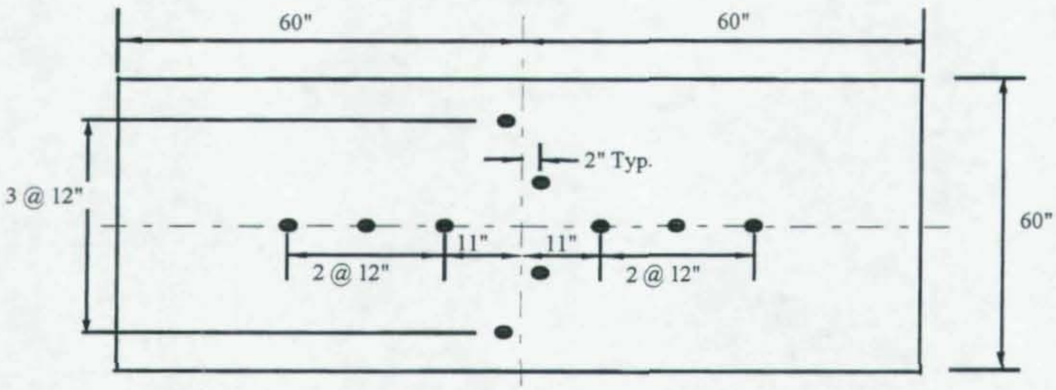

Shear Stud Layout
(3/4" Dia. x 4" High Headed Shear Studs)

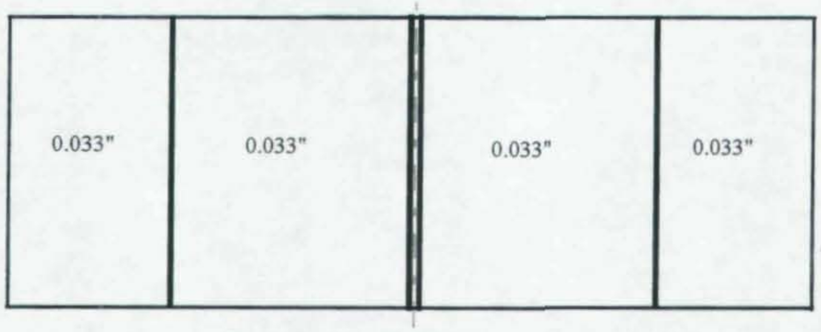

Deck Layout & Thickness

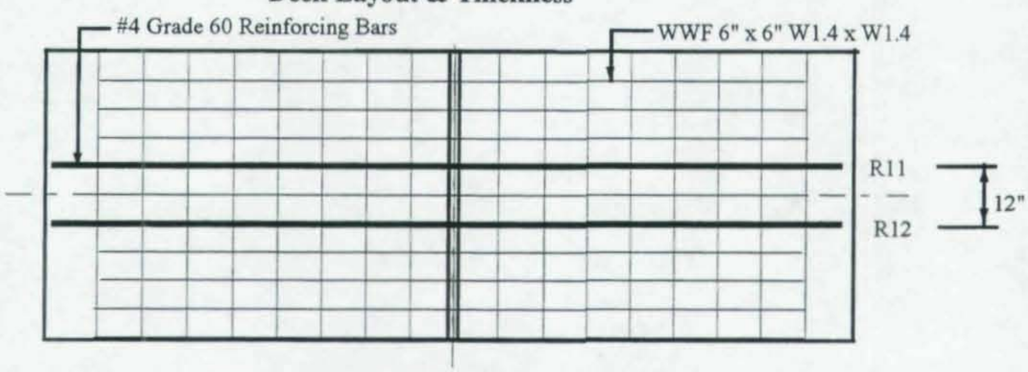

Reinforcing Identification & Layout

Reinforced Composite Deck Information

Description of Instrumentation

Channel	Sense of Extension	Description of Measurement	Load Stage	Gage Type	Sensitivity	Full Scale
2	Compression (-)	North Load Ram	Live	Load Cell	0.92	150 kips
1	Compression (-)	South Load Ram	Live	Load Cell	1.95	500 kips
80	-**	Connection Rotation	Live	POT		6"
83	-**	Connection Rotation	Live	POT		6"
84	-**	Connection Rotation	Live	POT		6"
85	-**	Connection Rotation	Live	POT		6"
86	-**	Connection Rotation	Live	POT		6"
87	-**	Connection Rotation	Live	POT		6"
88	-**	Connection Rotation	Live	POT		6"
89	-**	Connection Rotation	Live	POT		6"
92	-**	Stud Slip	Live	POT		6"
93	-**	Stud Slip	Live	POT		6"
94	-**	Stud Slip	Live	POT		6"
95	-**	Stud Slip	Live	POT		6"
96	-**	Stud Slip	Live	POT		6"
97	-**	Stud Slip	Live	POT		6"
104	+	Girder Deflection	Live	DCDT 5	0.939	20"
105	-**	Girder Deflection	Live	DCDT 8	0.949	10"
106	+	Girder Deflection	Live	DCDT 11	0.943	10"
107	-**	Filler Beam Deflection	Live	DCDT 9	0.942	20"
108	+	Filler Beam Deflection	Live	DCDT 4	0.948	20"
DG1	-**	Connection Rotation	Live	Dial Gage		1"
DG2	-**	Connection Rotation	Live	Dial Gage		1"
DG3	-**	Connection Rotation	Live	Dial Gage		1"
DG4	-**	Connection Rotation	Live	Dial Gage		1"

** All data has been modified so that (+) readings indicate extension.

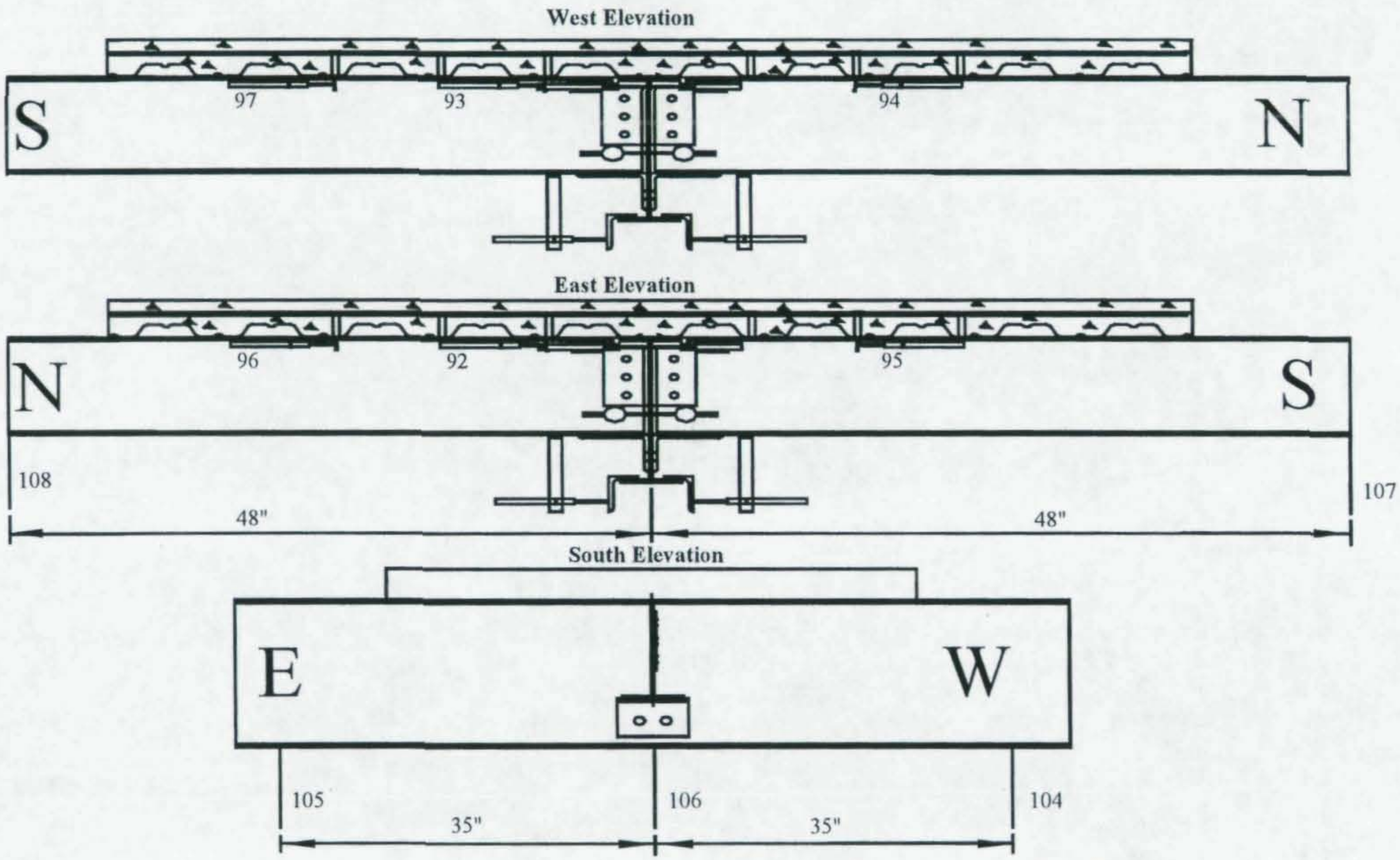

Stud Slip & Beam Deflection Instrumentation Live Loading Stage

West Elevation

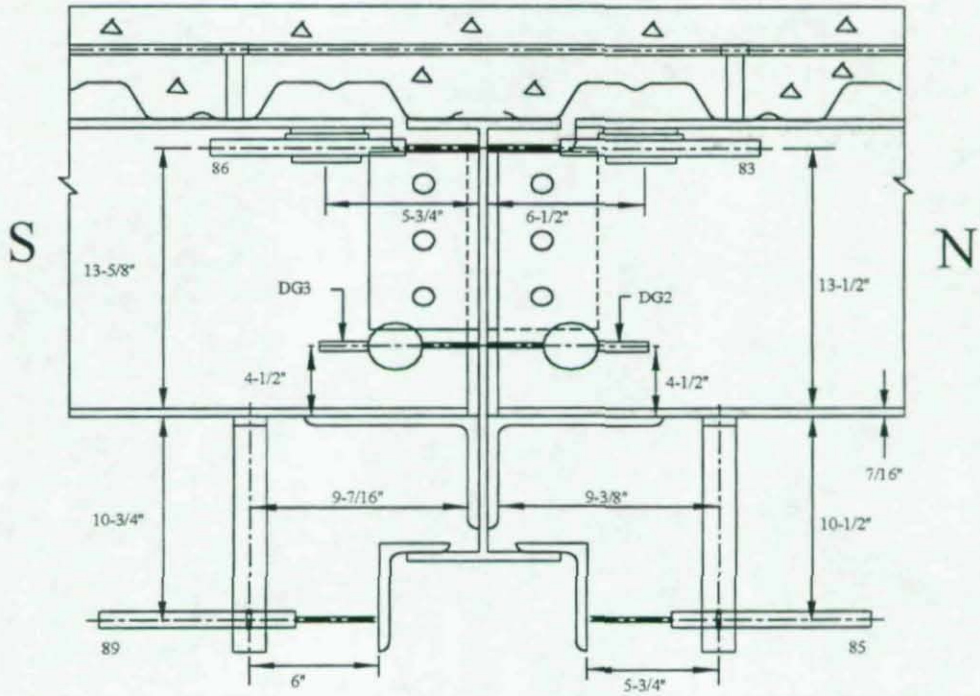

East Elevation

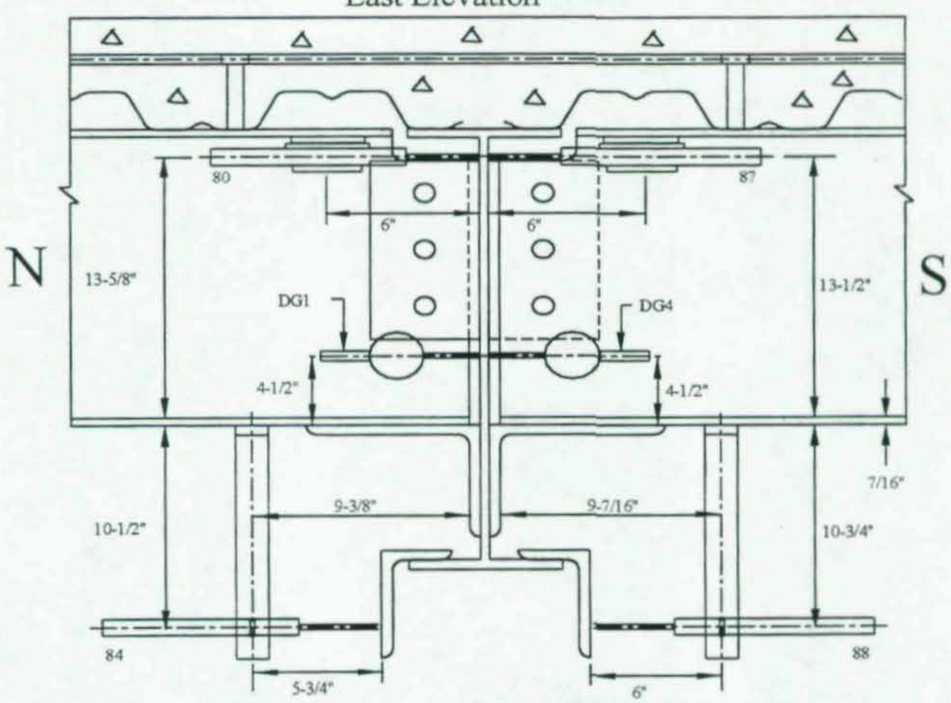

Rotation Instrumentation Live Loading Stage

Raw Data

Load Stage	Channel Data Point	2 (lbs)	1 (lbs)	80 (in.)	83 (in.)	84 (in.)	85 (in.)	86 (in.)	87 (in.)	88 (in.)	89 (in.)	92 (in.)	93 (in.)	94 (in.)
Live	1	0	0	0.000	0.000	0.000	0.000	0.000	0.000	0.000	0.000	0.000	0.000	0.000
	2	1154	1223	0.000	-0.001	-0.002	-0.001	0.000	0.000	-0.002	-0.002	0.000	0.000	0.001
	3	2821	2772	0.000	-0.001	-0.003	-0.002	0.000	-0.001	-0.004	-0.004	0.000	0.000	0.001
	4	6026	5951	0.000	-0.001	-0.007	-0.005	0.000	0.000	-0.007	-0.007	0.000	0.001	0.002
	5	8462	8397	0.001	0.000	-0.007	-0.006	0.000	0.000	-0.010	-0.010	0.001	0.001	0.003
	6	11026	10924	0.001	0.001	-0.011	-0.010	0.001	0.001	-0.011	-0.012	0.002	0.002	0.005
	7	12179	12147	0.004	0.006	-0.016	-0.015	0.002	0.006	-0.017	-0.017	0.004	0.003	0.006
	8	12564	12391	0.005	0.007	-0.021	-0.021	0.003	0.006	-0.023	-0.021	0.007	0.004	0.007
	9	15769	15652	0.005	0.010	-0.025	-0.024	0.005	0.007	-0.027	-0.026	0.007	0.005	0.008
	10	18846	18668	0.008	0.014	-0.031	-0.030	0.007	0.012	-0.034	-0.033	0.011	0.007	0.012
	11	20513	20299	0.011	0.018	-0.041	-0.041	0.014	0.023	-0.048	-0.048	0.012	0.008	0.013
	12	21795	21685	0.015	0.023	-0.052	-0.051	0.018	0.028	-0.054	-0.055	0.012	0.009	0.013
	13	24359	24049	0.026	0.034	-0.071	-0.072	0.024	0.035	-0.072	-0.073	0.013	0.010	0.015
	14	21923	21603	0.060	0.056	-0.095	-0.095	0.029	0.043	-0.091	-0.090	0.013	0.010	0.015
	15	23333	22826	0.087	0.077	-0.115	-0.117	0.031	0.046	-0.108	-0.107	0.013	0.010	0.015
	16	24359	23641	0.113	0.097	-0.149	-0.153	0.033	0.049	-0.130	-0.129	0.013	0.010	0.015
	17	25000	24212	0.136	0.116	-0.167	-0.171	0.036	0.052	-0.152	-0.151	0.013	0.010	0.015
	18	26154	25109	0.172	0.143	-0.186	-0.192	0.040	0.057	-0.189	-0.188	0.013	0.010	0.015
	19	27436	26087	0.207	0.167	-0.203	-0.209	0.045	0.064	-0.228	-0.225	0.014	0.010	0.015
	20	28846	27228	0.274	0.220	-0.242	-0.250	0.057	0.078	-0.292	-0.287	0.014	0.012	0.015
	21	26795	25190	0.297	0.245	-0.262	-0.272	0.119	0.167	-0.368	-0.362	0.014	0.012	0.015
	22	29359	27799	0.317	0.266	-0.289	-0.297	0.209	0.285	-0.453	-0.449	0.014	0.012	0.015
	23	30000	28696	0.348	0.297	-0.346	-0.355	0.299	0.384	-0.508	-0.506	0.015	0.012	0.016
	24	28718	28370	0.396	0.339	-0.403	-0.414	0.391	0.427	-0.543	-0.535	0.015	0.012	0.016
	25	30000	29837	0.458	0.389	-0.481	-0.494	0.480	0.495	-0.577	-0.570	0.016	0.012	0.016
	26	30513	30571	0.520	0.443	-0.550	-0.561	0.524	0.536	-0.597	-0.589	0.017	0.012	0.016
	27	30897	31060	0.619	0.537	-0.646	-0.658	0.590	0.598	-0.630	-0.620	0.017	0.012	0.016
	28	31154	30489	0.673	0.656	-0.700	-0.711	0.620	0.634	-0.683	-0.673	0.018	0.012	0.016
	29	31410	30652	0.726	0.715	-0.740	-0.749	0.668	0.681	-0.727	-0.716	0.018	0.012	0.017
	30	31538	30571	0.754	0.741	-0.750	-0.759	0.765	0.774	-0.810	-0.798	0.018	0.012	0.017
	31	23205	23071	0.757	0.747	-0.781	-0.786	0.887	0.823	-0.858	-0.838	0.016	0.007	0.014
	32	10769	10761	0.736	0.722	-0.742	-0.747	0.848	0.809	-0.833	-0.815	0.013	0.007	0.012
	33	-128	82	0.717	0.699	-0.705	-0.709	0.805	0.792	-0.795	-0.779	0.009	0.005	0.007

Raw Data

Load Stage	Channel Data Point	95 (in.)	96 (in.)	97 (in.)	104 (in.)	105 (in.)	106 (in.)	107 (in.)	108 (in.)	DG1 (in.)	DG2 (in.)	DG3 (in.)	DG4 (in.)
Live	1	-0.001	0.000	0.000	0.000	0.001	0.000	0.000	0.000	0.0000	0.0000	0.0000	0.0000
	2	-0.001	0.001	0.001	0.000	0.000	-0.001	-0.009	-0.013	0.0000	-0.0010	0.0010	-0.0020
	3	-0.001	0.002	0.001	0.000	0.000	-0.001	-0.006	-0.026	0.0000	-0.0020	0.0010	-0.0040
	4	-0.001	0.004	0.002	0.000	0.000	-0.006	-0.035	-0.039	0.0010	-0.0030	0.0020	-0.0060
	5	0.001	0.006	0.005	0.000	0.000	-0.010	-0.026	-0.047	0.0010	-0.0040	0.0020	-0.0070
	6	0.002	0.008	0.007	-0.013	0.000	-0.028	-0.030	-0.092	0.0010	-0.0050	0.0030	-0.0080
	7	0.003	0.009	0.008	-0.013	0.000	-0.029	-0.041	-0.114	0.0000	-0.0040	0.0030	-0.0070
	8	0.004	0.010	0.009	-0.028	-0.033	-0.053	-0.067	-0.140	0.0000	-0.0040	0.0030	-0.0060
	9	0.004	0.012	0.011	-0.035	-0.037	-0.064	-0.095	-0.168	-0.0010	-0.0040	0.0030	-0.0050
	10	0.005	0.015	0.015	-0.048	-0.064	-0.084	-0.134	-0.213	-0.0010	-0.0040	0.0020	-0.0040
	11	0.006	0.017	0.015	-0.054	-0.087	-0.099	-0.179	-0.267	-0.0030	-0.0050	0.0010	-0.0030
	12	0.006	0.018	0.016	-0.061	-0.112	-0.120	-0.195	-0.340	-0.0040	-0.0050	0.0000	-0.0030
	13	0.007	0.019	0.017	-0.073	-0.131	-0.132	-0.275	-0.394	-0.0060	-0.0080	-0.0020	-0.0030
	14	0.007	0.020	0.017	-0.073	-0.132	-0.137	-0.361	-0.434	-0.0080	-0.0040	-0.0030	0.0070
	15	0.007	0.020	0.018	-0.073	-0.132	-0.137	-0.497	-0.434	-0.0080	-0.0050	-0.0040	0.0130
	16	0.007	0.020	0.017	-0.073	-0.132	-0.136	-0.661	-0.434	-0.0070	-0.0160	-0.0030	0.0130
	17	0.007	0.020	0.018	-0.080	-0.132	-0.137	-0.780	-0.434	-0.0070	-0.0190	-0.0030	0.0140
	18	0.007	0.020	0.018	-0.080	-0.132	-0.138	-0.975	-0.434	-0.0060	-0.0210	-0.0030	0.0160
	19	0.007	0.020	0.018	-0.086	-0.136	-0.141	-1.154	-0.428	-0.0070	-0.0210	-0.0030	0.0160
	20	0.007	0.020	0.018	-0.086	-0.137	-0.147	-1.522	-0.421	-0.0070	-0.0200	-0.0030	0.0230
	21	0.007	0.020	0.018	-0.093	-0.141	-0.148	-1.883	-0.413	-0.0030	-0.0080	0.0060	0.0470
	22	0.007	0.020	0.018	-0.093	-0.146	-0.151	-2.116	-0.628	0.0080	0.0070	0.0160	0.0740
	23	0.007	0.020	0.018	-0.102	-0.153	-0.162	-2.114	-1.082	0.0170	0.0210	0.0300	0.1000
	24	0.007	0.021	0.018	-0.102	-0.155	-0.164	-2.116	-1.471	0.0320	0.0360	0.0520	0.1160
	25	0.007	0.021	0.018	-0.102	-0.159	-0.168	-2.116	-1.957	0.0440	0.0540	0.0780	0.1360
	26	0.007	0.021	0.018	-0.108	-0.163	-0.172	-2.116	-2.331	0.0570	0.0690	0.0890	0.1500
	27	0.007	0.021	0.018	-0.108	-0.168	-0.175	-2.114	-2.884	0.0820	0.0980	0.1080	0.1720
	28	0.007	0.021	0.018	-0.108	-0.172	-0.178	-2.430	-2.995	0.0930	0.1300	0.1190	0.1860
	29	0.007	0.021	0.018	-0.106	-0.172	-0.179	-2.605	-3.157	0.1050	0.1490	0.1350	0.2010
	30	0.007	0.021	0.018	-0.108	-0.172	-0.178	-3.005	-3.157	0.1120	0.1580	0.1650	0.2320
	31	0.004	0.019	0.018	-0.106	-0.171	-0.178	-3.042	-3.361	0.1180	0.1660	0.2000	0.2540
	32	0.004	0.014	0.013	-0.108	-0.171	-0.156	-3.072	-3.071	0.1240	0.1520	0.2010	0.2420
	33	0.002	0.007	0.008	-0.099	-0.161	-0.142	-3.035	-2.832	0.1270	0.1430	0.2020	0.2370

<u>Test Comments</u>

Data Point (With respect to the live stage of loading.)

pre-load about 200 lbs on each ram, then unload re-zero and start test

1 zero point, start tests

4 Both sides of connection bending away from the shear plate causing dial gage readings to be positive on one side and negative on plate side

7 Slab: First crack in slab parrallel with girder from edge to edge of slab about 4 to 6 inches north of girder

8 Banging sound, possibly north seat angle bolt slipping into bearing, no new cracking, however, girder appears to have dropped some - may be girder slipping down on connections

11 Slab: new crack parrallel with girder from west edge of slab to within 4" of east edge, about 6 to 8 in. south of girder centerline: also small crack near the south west corner of slab about 2' north of corner and

12 Slab: crack near south west corner now extends from edge to edge of slab running parrallel with girder and about 3' south of girder centerline

South: Shear Tab: small bearing yielding at bottom bolt on weld side of plate and slightly declined

13 Girder: yield patterns in web near top corner of where shear plate is welded to the girder

14 Slab: original north crack expanding and some secondary cracks around this crack showing up

North: Shear Tab: bearing yielding around top bolt hole on side away from support and slightly declined

16 Slab: original crack on north side continues to open, trying to load south side heavier to try to increase cracking and balance rotations

North: Bottom side seat angle: bolt to north west corner: bearing yielding on support side of bolt

17 North: Shear tab: yielding around top bolt increasing significantly as slab continues to soften

North: web: bearing yielding around top bolt on the support side

North: top side bottom flange: bearing yielding near two bolts farthest from support

18 North: Shear tab: bearing yielding around middle bolt away from support, also some vertical yield lines going from top bolt to middle bolt and from middle bolt to bottom bolt

North: beam web: bearing yielding around top and middle bolts on support side of bolt holes

South: Shear tab: appears to be some tension yielding at top middle of shear tab

19 South: Shear tab: scattered bearing yielding around all bolts, no real definite direction however the majority of lines are below the bolts

20 South: Top side bottom flange: south east bolt bearing yielding on side away from support

North: web: bearing yielding at bottom bolt support side and slightly inclined

North: shear tab: bearing yielding around top bolt increasing, now yielding on both sides of bolt hole and extends almost all the way to top support side corner of plate

21 Slab: original crack on south side finally starting open up more and the slab stiffness on south side

South: Shear tab: scattered yielding around all bolts increased significantly, particuarily around top bolt

South: web: some bearing yielding around all bolt holes

South: bottom side seat angle: bearing yielding on support side of two bolts farthest from support

22 Slab: new cracks spurring off the original crack on the north side

Bolts are rotating to accomidate the eccentricity between the web and plate

23 South: top side bottom flange: plate side: bearing yielding around both bolts this side

South: bottom of seat angle: bending yielding along outstanding toe of seat angle

24 South crack continues to open and is very even from edge to edge of slab (even crack width)

Girder web behind each shear plate is yielding, guess that the axial load in the shear plate is causing the yielding in the girder web on the opposite side that the plate is welded to

26 North: bottom side of seat angle: bending yielding along outstanding toe of angle

28 Slab: original north crack just evened out so that crack width is about the same from edge to edge of slab

31 Loud bang, sounds and looks like (based on pot readings) that rebar on south side ruptured , visual inspection shows that rebar #12 on the south side ruptured, can just see rupture inside crack onsouth side

Unload

32 Unload

33 End Test

00919

Composite Connection Test Summary

Connection #8

Calculated Data Data Point	*Using POTS Only* North Rotation (rad)	North Moment (k-in.)	*Using POTS Only* South Rotation (rad)	South Moment (k-in.)	*POTS & DG* North Rotation (rad)	*POTS & DG* South Rotation (rad)
1	0.0000	0	0.0000	0	0.0000	0.0000
2	0.0000	52	0.0001	56	0.0000	0.0001
3	0.0001	128	0.0001	126	0.0001	0.0001
4	0.0002	274	0.0003	271	0.0001	0.0002
5	0.0003	385	0.0004	382	0.0002	0.0003
6	0.0005	502	0.0005	497	0.0003	0.0004
7	0.0008	554	0.0008	553	0.0007	0.0006
8	0.0011	572	0.0011	564	0.0009	0.0006
9	0.0013	717	0.0013	712	0.0010	0.0007
10	0.0017	857	0.0017	849	0.0014	0.0011
11	0.0023	933	0.0027	924	0.0020	0.0021
12	0.0029	992	0.0031	987	0.0025	0.0025
13	0.0042	1108	0.0041	1094	0.0039	0.0034
14	0.0062	998	0.0051	983	0.0067	0.0036
15	0.0081	1062	0.0059	1039	0.0093	0.0036
16	0.0104	1108	0.0069	1076	0.0123	0.0038
17	0.0120	1138	0.0079	1102	0.0146	0.0041
18	0.0141	1190	0.0096	1142	0.0180	0.0045
19	0.0160	1248	0.0113	1187	0.0212	0.0050
20	0.0201	1312	0.0144	1239	0.0274	0.0060
21	0.0220	1219	0.0205	1146	0.0291	0.0123
22	0.0239	1336	0.0282	1265	0.0299	0.0213
23	*0.0275*	*1365*	*0.0343*	*1306*	*0.0320*	*0.0291*
24	0.0317	1307	0.0383	1291	0.0351	0.0342
25	0.0372	1365	0.0429	1358	0.0394	0.0401
26	0.0423	1388	0.0454	1391	0.0441	0.0432
27	0.0502	1406	0.0492	1413	0.0514	0.0478
28	0.0559	1418	0.0527	1387	0.0582	0.0500
29	0.0598	1429	0.0564	1395	0.0625	0.0534
30	0.0613	1435	0.0636	1391	0.0645	0.0601
31	0.0627	1056	0.0688	1050	0.0642	0.0661
32	0.0602	490	0.0668	490	0.0622	0.0639
33	0.0578	-6	0.0640	4	0.0603	0.0609

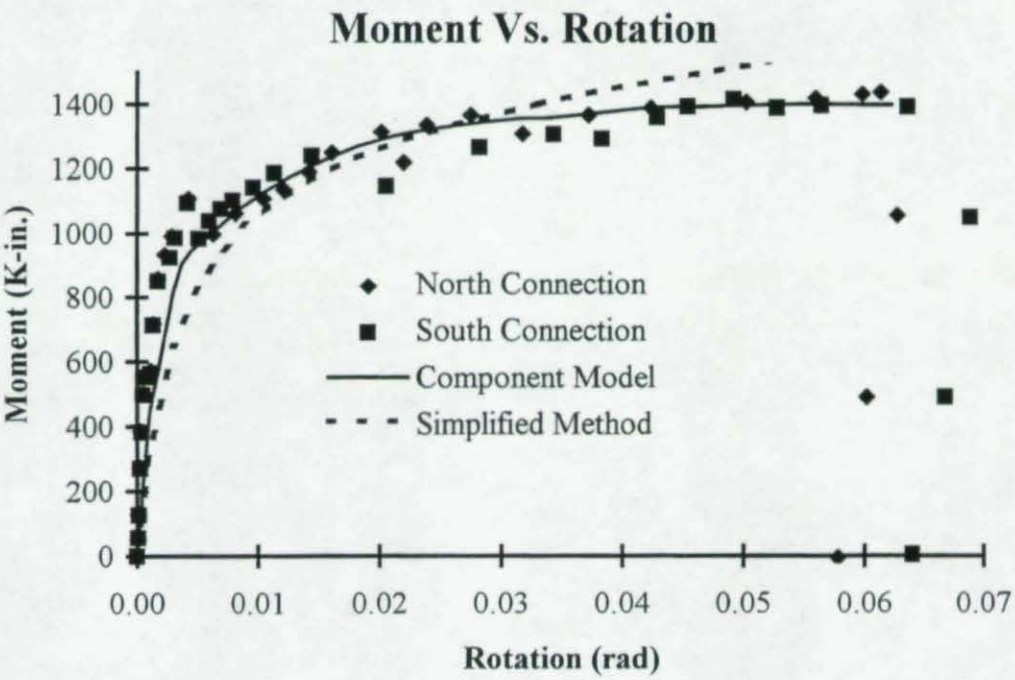

Moment Vs. Rotation
Moment (K-in.)
Rotation (rad)
North Connection
South Connection
Component Model
Simplified Method
0
200
400
600
800
1000
1200
1400
0.00
0.01
0.02
0.03
0.04
0.05
0.06
0.07

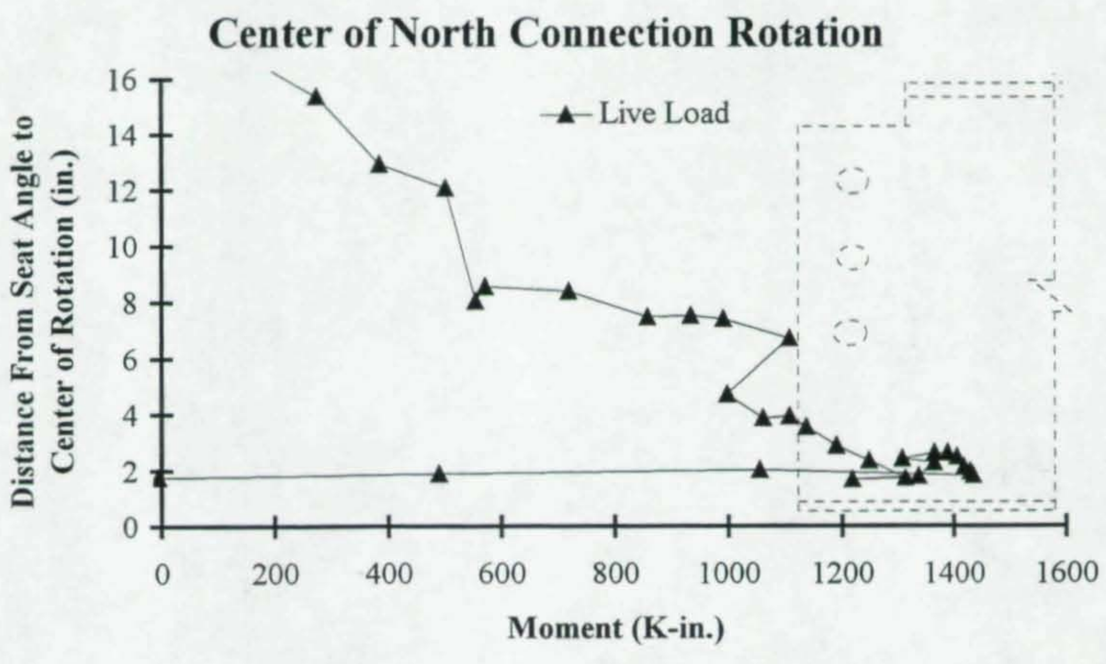

Center of North Connection Rotation
Distance From Seat Angle to Center of Rotation (in.)
Moment (K-in.)
Live Load
0
2
4
6
8
10
12
14
16
0
200
400
600
800
1000
1200
1400
1600

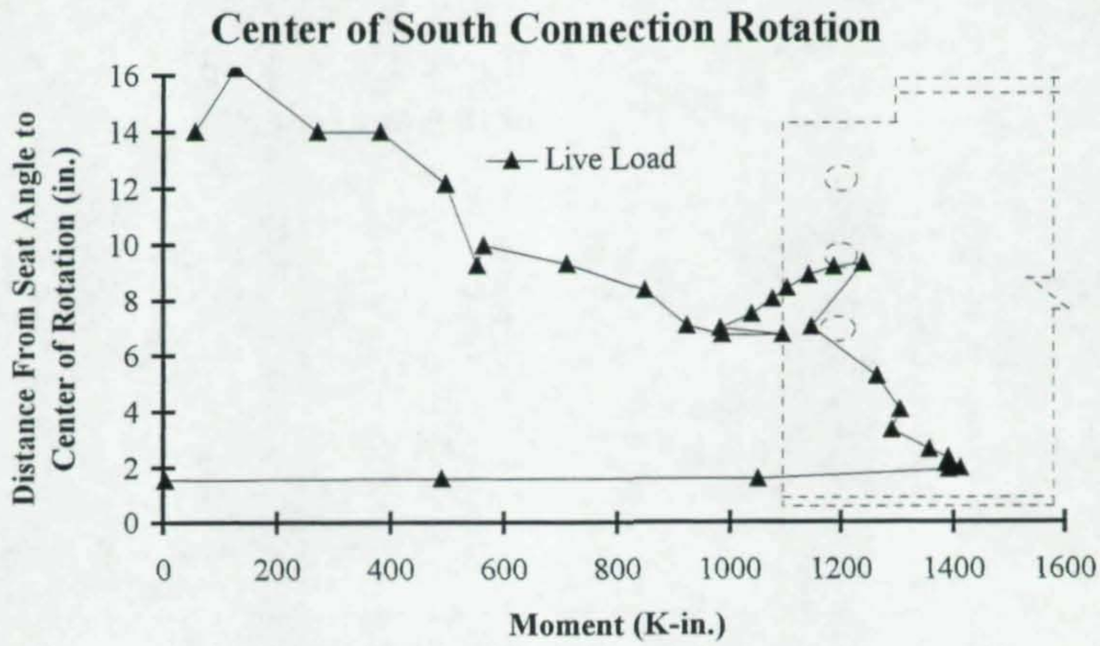
Center of South Connection Rotation
Distance From Seat Angle to Center of Rotation (in.)
Live Load
Moment (K-in.)
0
2
4
6
8
10
12
14
16
0
200
400
600
800
1000
1200
1400
1600

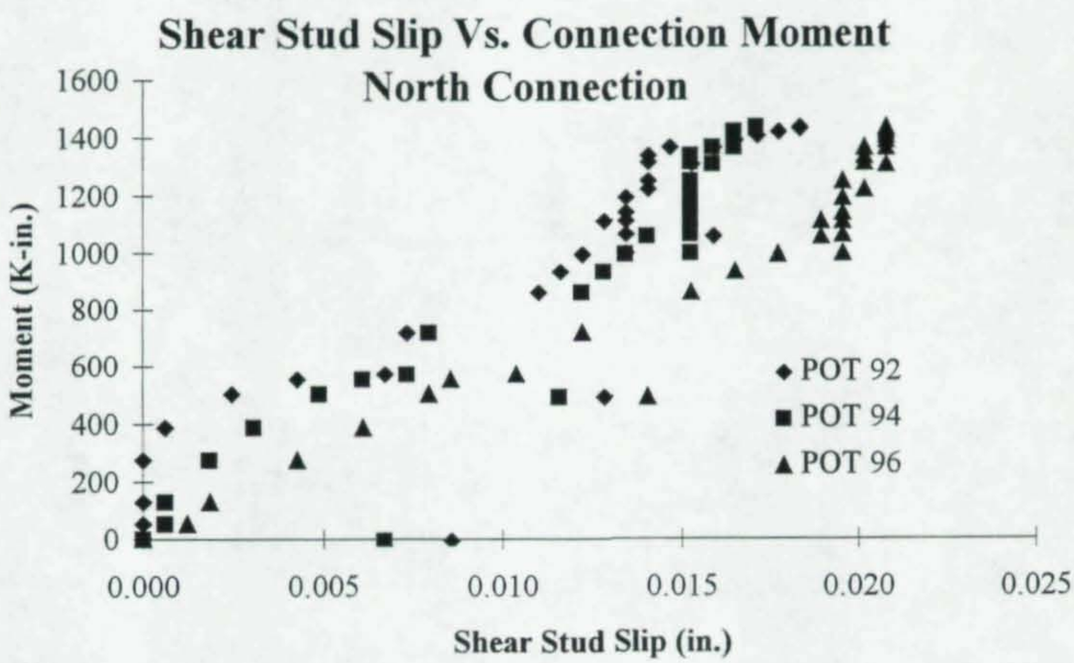
Shear Stud Slip Vs. Connection Moment
North Connection
Moment (K-in.)
POT 92
POT 94
POT 96
Shear Stud Slip (in.)
0
200
400
600
800
1000
1200
1400
1600
0.000
0.005
0.010
0.015
0.020
0.025

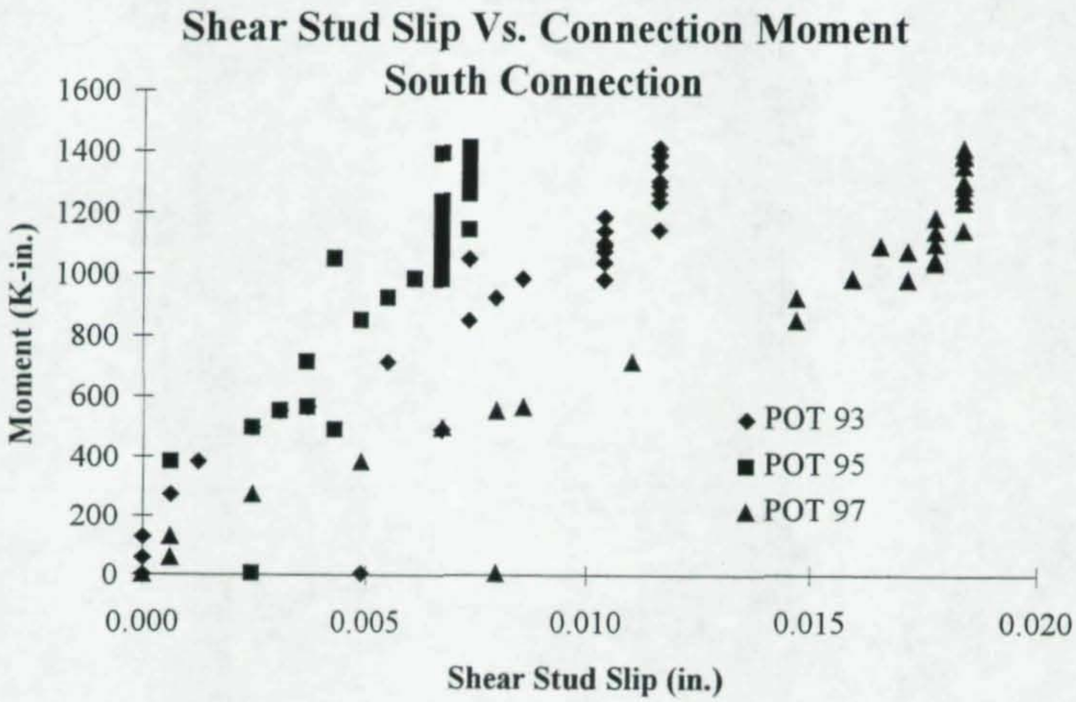
Shear Stud Slip Vs. Connection Moment
South Connection
Moment (K-in.)
1600
1400
1200
1000
800
600
400
200
0
0.000
0.005
0.010
0.015
0.020
Shear Stud Slip (in.)
POT 93
POT 95
POT 97